

THESIS ON MECHANICAL AND INSTRUMENTAL ENGINEERING E52

Vibration of Ladder Frames

ANDRES PETRITSHENKO

TUT
PRESS

Faculty of Mechanical Engineering
Department of Mechatronics
TALLINN UNIVERSITY OF TECHNOLOGY

Dissertation was accepted for the defense of the degree of Doctor of Philosophy in Engineering Sciences on April 26, 2010

Supervisor:

Gennadi Arjassov, Ass. Prof., PhD,
Department of Mechatronics,
Tallinn University of Technology

Opponents:

Musalimov, Viktor, Prof., D. Sc.
Sankt-Petersburg State University of Information Technologies,
Mechanics and Optics, Russia

Klauson, Aleksander, Prof., PhD,
Tallinn University of Technology, Estonia

Defense of the thesis: June 9, 2010

Declaration:

Hereby I declare that this doctoral thesis, my original investigation and achievement, submitted for the doctoral degree at Tallinn University of Technology has not been submitted for any academic degree.

Copyright: Andres Petritshenko, 2010
ISSN 1406-4758
ISBN 978-9985-59-995-2

MASINA- JA APARAADIEHITUS E52

**Risttaladest tasandraamide
võnkumised**

ANDRES PETRITSHENKO

Contents

INTRODUCTION	7
1. COUPLED FLEXURAL-TORSIONAL FREE VIBRATION OF LADDER FRAMES.....	13
1.1 Background	13
1.2 Basic parameters for slope-deflection method of continuous solid beams	15
1.2.1 Continuous solid beams with one axis of symmetry.....	18
1.2.2 Thin-walled open cross-section beams	27
1.2.3 Calculation of ladder frames by displacement method.....	32
1.2.4 Numerical results	35
1.3 Conclusions to the chapter	48
2. FORCED VIBRATION OF LADDER FRAMES UNDER THE ACTION OF REPEATED LOADING	50
2.1 Background	50
2.2 Differential equation of motion of discrete scheme of ladder frames.....	51
2.3 Calculation example.....	57
2.4 Steady-state forced vibration.....	60
2.5 Conclusion to the chapter.....	62
3. STUDY OF FREE VIBRATION OF LADDER FRAMES REINFORCED WITH PLATE.....	63
3.1 Background	63
3.2 Basic concept of the discrete scheme.....	64
3.3 Calculation of rib floors as an orthotropic plate.....	65
3.4 System of crossed beams (ladder frames).....	71
3.5 Calculation of continuous reinforced concrete floor of an industrial building	73
3.6 Conclusion to the chapter.....	75
GENERAL CONCLUSIONS	76
KOKKUVÕTE.....	78
REFERENCES.....	81
Paper I	87
Paper II.....	91
Paper III.....	99
ELULOOKIRJELDUS (CV)	107
CURRICULUM VITAE	108

INTRODUCTION

A structure is a combination of parts fastened together to create a supporting framework, which may be part of a building, ship, machine, space vehicle, road vehicle, engine or some other system. The vibration that occurs in most machines, structures and dynamic systems is undesirable, not only because of the resulting unpleasant motions, the noise and the dynamic stresses which may lead to fatigue and failure of the structure or machine, but also because of the energy losses and the reduction in performance that accompany the vibrations. It is therefore essential to carry out a vibration analysis of any proposed structure. Because of the very serious effects that unwanted vibrations can have on dynamic systems, it is essential that vibration analysis be carried out as an inherent part of their design; when necessary modifications can most easily be made to eliminate vibration or at least to reduce it as much as possible.

It is usually much easier to analyze and modify a structure at the design stage than it is to modify a structure with undesirable vibration characteristics after it has been built. However, it is sometimes necessary to be able to reduce the vibration of existing structures brought about by inadequate initial design, by changing the function of the structure or by changing the environmental conditions, and therefore techniques for the analysis of structural vibration should be applicable to existing structures as well as to those in the design stage. It is the solution to vibration problems that may be different depending on whether or not the structure exists.

There are two factors that control the amplitude and frequency of vibration in a structure: the excitation applied and the response of the structure to that particular excitation. Changing either the excitation or the dynamic characteristics of the structure will change the vibration stimulated.

The excitation arises from external sources such as ground or foundation vibration, cross winds, waves and currents, earthquakes and sources internal to the structure such as moving loads and rotating or reciprocating engines and machinery. These excitation forces and motions can be periodic or harmonic in time, due to shock or impulse loadings, or even random in nature.

The level of vibration in a structure can be attenuated by reducing either the excitation, or the response of the structure to that excitation or both. It is sometimes possible, at the design stage, to reduce the exciting force or motion by changing the equipment responsible, by relocating it within the structure or by isolating it from the structure so that the generated vibration is not transmitted to the supports. The structural response can be altered by changing the mass or stiffness of the structure, by moving the source of excitation to another location, or by increasing the damping in the structure. Naturally, careful analysis is necessary to predict all the effects of any such changes, whether at the design stage or as a modification to an existing structure.

It is necessary to analyze the vibration of structures in order to predict the natural frequencies and the response to the expected excitation. The natural frequencies of the structure must be found because if the structure is excited at one of these frequencies resonance occurs, with resulting high vibration amplitudes, dynamic stresses and noise levels. Accordingly resonance should be avoided and the structure designed so that it is not encountered during normal conditions; this often means that the structure need only be analyzed over the expected frequency range of excitation. Although it may be possible to analyze the complete structure, this often leads to a very complicated analysis and the production of much unwanted information. A simplified mathematical model of the structure is therefore usually sought that will, when analyzed, produce the desired information as economically as possible and with acceptable accuracy. The derivation of a simple mathematical model to represent the dynamics of a real structure is not easy, if the model is to produce useful and realistic information. It is often desirable for the model to predict the location of nodes in the structure. These are points of zero vibration amplitude and are thus useful locations for the assembly of particularly delicate equipment. Also, a particular mode of vibration cannot be excited by forces applied at one of its nodes.

Problem settings

A ladder frame is a combination of beams fastened together to create a supporting framework, which may be part of a building, ship, machine, space vehicle, road vehicle, engine or some other system. Ladder frames are composed mostly from beams of open cross-section, which generally have one or two axis of symmetry. There are many possibilities to form the layout of the ladder frames with same load carrying capacity sustained. It is possible to choose smaller cross-sectional dimensions of structural members and place them closer to each other or it is possible to choose larger cross-sectional dimensions and space them further from each other. Even load carrying capacity of ladder frames doesn't change; the dynamic behavior of ladder frames will change essentially. Cross-sectional dimensions of longitudinal members and cross-members and their corresponding mass influence directly the natural frequencies of whole ladder frame and corresponding modes of free vibration. It is important to choose stiffnesses and masses of structural members of ladder frames so that resonance or beating condition of structural members due to excitation cannot occur. In design layout of ladder frames it is desirable that cross-members and other parts are placed at the nodes of principal modes. It is possible, when reliable and easily used tool for the calculation of natural frequencies and corresponding modes is available, which assist a designer through design process. Final layout of ladder frames must be evaluated through the evaluation of forced response of ladder frames.

Forced response of ladder frames due to excitation is very important in final decision-making process of choosing the layout of ladder frames. Response of the ladder frames or another structure to some harmonic excitation without damping effect or in presence of viscous damping is well-studied. Response of ladder frames to another periodic loading of excitation in presence of hysteretic damping is considerably less dealt in scientific literature than in case of harmonic excitation.

In design stage of ladder frames, it is very important to design it to withstand the so-called extreme statical and dynamical conditions, which are imposed to it due to foundation vibration, moving loads, rotating engines and/or other operational conditions. From the point of view of dynamical response of ladder frames, it is quite a complex issue due to variety of ladder frames designs available. Frame members can be straight uniform beams or tapered. Depending on the purpose of ladder frames, the cross-members could be covered by some covering panels/materials (further floor components), which can be plywood or wooden slabs or thin metal sheets or concrete. Main purpose of floor components is to form a load carrying area and distribute it to the members of ladder frames uniformly. Depending on the fastening method, floor components might influence the rigidity of crossed beams completely or partly. In this case, the reinforcing effect of the covering panels due to simplification is usually ignored in dynamical analysis. Another situation is raised, when ladder frames are covered with panels of thin metal plates by means of welding or concrete panels, then relative displacement between panels and structural members of ladder frames is restrained and reinforcing effect of the plate cannot be ignored.

The study of free vibrational behavior of structural members of ladder frames is essential before study of forced response of structural members of ladder frames, because it gives a good reference to choose the right number and type of normal modes to be included in dynamic response analysis [1]. It is necessary to take into account that frequency spectrum of ladder frames is not continuous, but has isolated zones with highly packed frequencies. Also frequency values do not increase so quickly with the total number of frequencies. In ladder frames, the values of natural frequencies are close to each other and corresponding modes could have different values at the nodes. Evaluation of natural frequencies of ladder frames and corresponding modes gives the designer a possibility to choose a better layout of ladder frames.

Main objectives

The main objectives of the doctoral thesis are as follows:

1. To extend the theoretical analysis methods of free vibration of ladder frames that consists of uniform beams with one axis of symmetry and to study the

sensitivity of ladder frames by numerical examples. Main objective in case of thin-walled beams is to study the effect of warping onto the natural frequencies of ladder frames in two cases: I) when longitudinal members and cross-members of ladder frames are adjoined at the nodes in plane and II) when beam members of ladder frames are adjoined at the nodes on each other.

2. To extend a simplified alternative approach for calculation of forced vibration of ladder frames under the action of repeated loading in the presence of hysteretic damping.
3. To propose the alternative approach for calculation of natural frequencies and corresponding mode shape of ladder frames in case, when reinforcing effect of the covering plate cannot be excluded from the dynamic analysis.

To obtain the goal the following tasks have to be solved:

1. To solve the governing differential equation of motion of continuous beam element with one axis of symmetry by the theories of massive-profiled beams and thin-walled beams in closed form in frequency domain. Once a solution is found, it is possible to evaluate analytical nodal end forces and moments to calculate natural frequencies of ladder frames and the corresponding mode shapes. To obtain the goal in case of thin-walled beams, the different warping constraints corresponding to different position of beam members to each other has to be taken account in calculation of natural frequencies.
2. Repeated interrupted loading is discontinuous forcing function and thus a calculation of hysteretically damped response of structures to such kind of loading has to be performed taking into account loading time-history over the time of excitation. If the time interval to be analyzed is relatively long the analysis become laborious and time consuming. Analyses become more complex and laborious if structures with multi-degree-of-freedom have to be analyzed, because damping couples the system of differential of equations of MDOF systems and solution of system of differential equations is complicated. For practical use, it is possible to make some simplifications that lead to uncoupling of the system of differential equation of motion. Once system of differential equation of motion is uncoupled, the dynamic response of entire structure can be obtained by solving separately for response of each modal coordinate and then superposing these to obtain the total response in the original geometric coordinates.
3. When the reinforcing effect of covering plates of ladder frames cannot be excluded from the composition of differential equation of motion, the orthotropic plate theory or more refined thin plate theory is usually used. Due to its simplicity the orthotropic plate theory is widely used. The orthotropic

plate theory is not exact and depends on geometrical representation of ladder frames. The discrete model of ladder frames reinforced with plate for calculation of natural frequencies is proposed instead of the orthotropic model one and compared with results received by calculation of orthotropic plate model

Acknowledgement

This thesis would not exist if it wasn't for my supervisor *Dr Gennadi Arjassov*, who introduced me into this subject years ago; his expertise in this area and insightful comments throughout the course of this work have been of the utmost importance. I will always remember our numerous scientific discussions we had, which sometimes continued until late into the nights.

My greatest appreciation goes to my family for their support and understanding throughout the period of thesis compilation and my absence.

I gratefully acknowledge my colleagues from the Department of Mechatronics.

List of publications

The dissertation is based on the following publications, which are referred to in the text by using Roman numerals:

- Paper I. Aryassov, G., Petritshenko, A. 2007. Advanced dynamic models for analysis of ladder frames. *Annals of DAAAM for 2007 & Proceedings of the 18th International DAAAM Symposium*, Editor B. Katalinic, Published by DAAAM International, Vienna, Austria, pp. 565-566, ISBN 3-901509-58-5, ISSN 1726-9679
- Paper II. Aryassov, G., Petritshenko, A. 2008. Forced vibration under the action of repeated loading (2008). *Proceedings of 6th International Conference of DAAAM Baltic INDUSTRIAL ENGINEERING*, pp. 25-31, Editor R. Kyttner, Published by DAAAM International, Tallinn, Estonia, ISBN 978-9985-59-783-5
- Paper III. Aryassov, G.; Petritshenko, A. 2009. Study of free vibration of ladder frames reinforced with plate. *J. Solid State Phenomena*, Vols. 147-149, pp. 368-373, ISSN 1662-9779.

The personal contribution of the author

The contribution of the author to the papers included in the thesis is as follows:

- I. Andres Petritshenko is the main author of the paper. He is responsible for the literature overview, analysis, development of the theory and calculation. He had a major role in writing
- II. Andres Petritshenko participated in writing the paper. The author participated in development of the theory. The author has made calculations. He had major role in writing.
- III. Andres Petritshenko is the main author of the paper. He is responsible for literature overview, analysis and calculation. He had a major role in writing.

Other publications (not included in the thesis):

1. Aryassov, G., Baraskova, T. & Petritshenko, A. 2009. Symbolic solution algorithms of mechanic matrix equations. *Annals of DAAAM for 2009 & Proceedings of the 20th International DAAAM Symposium*, pp.0071-0072, Editor B. Katalinic, Published by DAAAM International, Vienna, Austria, ISBN 3-901509-68-1, ISSN 1726-9679
2. Aryassov, G., Petritshenko, A. 2008. Analysis of stress distribution in roots of bolt threads. *Annals of DAAAM for 2007 & Proceedings of the 18th International DAAAM Symposium*, pp. 0035-0036, Editor B. Katalinic, Published by DAAAM International, Vienna, Austria, ISBN 3-901509-68-1, ISSN 1726-9679
3. Aryassov, G., Petritshenko, A. 2008. Advanced determination of safety factor of fatigue strength of coiled springs. *Journal of Machine Engineering*, 8(4), pp. 111-121, Bialystoc Technical University , Bialystoc, Poland, ISSN 1895-7595
4. Aryassov, G., Petritshenko, A. 2006. Advanced dynamic models for analysis of vibrations of road train trailers with big loading capacity. *In: Proceedings of 8th International Conference on The Modern Information Technology in the Innovation Processes of the Industrial Enterprises*, pp.359-364, Hungarian Academy of Sciences, Budapest, Hungary, ISBN 963-86586-5-7

1 COUPLED FLEXURAL-TORSIONAL FREE VIBRATION OF LADDER FRAMES

1.1 Background

It is well known that when the cross-sections of the beam have two symmetrical axes, the shear center and centroid of the cross-section coincide, and all bending and torsional vibrations are independent of each other. This case represents no coupling at all. However, for large number of practical beams, the centroid and shear center of the cross-sections are non-coincident. When the cross-sections of beams have one symmetrical axis, the bending vibration in the direction of symmetrical axis is independent of the other vibrations. But the bending vibration in the perpendicular direction of the symmetrical axis is coupled with torsional vibration. In accordance with the Saint-Venant's theory of torsion, the warping displacement occurs in the cross-sections of the beams, except the beams with circular cross-sections [2]. For thick-walled or solid beams this warping influence is very small as a result of a fast diminishing of stress disturbances on the small parts of the beams that are close to their constrained sections. In thin-walled open section beams the warping effect considerably influence the warping displacements due to stresses produced by restrained warping with the self-equilibrating normal stress resultants that diminishes very slowly from their point of application.

Because of the practical importance of the bending-torsion coupled beams, a few investigators have made efforts to deal with coupled static and dynamic model of this problem. Various methods for analyzing natural frequencies and mode shapes of the thin-walled beam such as the so-called continuum method, the finite element method, the other approximate methods and the dynamic stiffness method have been attempted. A literature survey revealed a wealth of literature on the dynamic characteristics of the coupled flexural-torsional vibration of uniform thin-walled beams standalone, but so there is much smaller number of so-called exact solutions that are based on solving differential equations. Same can be applied for massive-profiled beams too. The theories for coupled bending-torsional vibration of the beams firstly have been developed by Timoshenko [3] and Vlasov [4] separately. Timoshenko in the [3] obtained the exact modal solutions using the classical continuum method, but only with simple boundary conditions and no allowance was made for shear deformation effect, rotatory inertia and warping. Vlasov in the [4] developed a new approach to thin-walled beams introducing a new concept of sectorial properties of cross-section and sectorial warping. No allowance was made for shear deformation. Hallau et al in the [5] used the dynamic stiffness method to compute exact natural frequencies, mode shapes, and generalized masses for coupled bending-torsional vibration of an aircraft

wing that was represented as an assemblage of three beams. However, the author gave no allowance for the warping, shear deformation and rotatory inertia. Friberg in the [6] presented a numerical procedure that generates an exact frequency dependent dynamic stiffness matrix (neglecting warping stiffness) and subsequently evaluated the natural frequencies and mode shapes for a simply supported and clamped beam. Shear deformation and rotatory inertia were neglected. Dokumaci in the [7] determined the coupled free vibration frequencies of a cantilever beam. But he neglected the effect of warping stiffness. Bishop et al in the [8] extended the theory of [7] by including the warping stiffness influence. Friberg in the [9] and Leung in the [10] presented a numerical procedure for developing the exact dynamic stiffness matrix of a thin-walled beam based on Vlasov beam theory. Banerjee et al in the [11] derived the analytical expressions for the coupled bending-torsional dynamic stiffness matrix elements of an axially loaded uniform beam element with non-coincident mass center and shear center. The influence of axial force on the coupled bending–torsional frequencies of a cantilever beam with thin-walled section was demonstrated by numerical results. However the warping stiffness was considered to be negligible and was not included in their theory. Banerjee et al in the [12] formulated an exact dynamic stiffness matrix for an axially loaded Timoshenko beam element from established theory and linking this to a new and convenient procedure that extended the well-known Wittrick–Williams algorithm [13] to ensure convergence upon any desired natural frequency. They considered the effect of the warping stiffness and the axial force was included in the analysis. Banerjee in the [14] derived explicit frequency equation and mode shapes for cantilever beam using the classical continuum approach. The warping stiffness, shear deformation and rotatory inertia effects were neglected from formulations. Li et al in the [15] derived the analytical expression for axially loaded thin-walled beam using the dynamic transfer matrix approach. Later they included the effect of warping stiffness, shear deformation and rotatory inertia in governing equations of motion [16]. Senjanovich et al in the [17] derived analytical expressions of coupled flexural and torsional vibrations and used them in the investigation of free vibration of flexible barges. The rotatory inertia was excluded from formulations.

In this thesis, the investigation of coupled flexural-torsional free vibration of ladder frames is based on Vlasov's formulated dynamic differential equation of motions of uniform massive-profiled and thin-walled beams [4]. The free vibration in longitudinal direction is independent of other vibration of beam element and is neglected from differential equation of motion of massive-profiled and thin-walled beams both, but all other transverse flexural-torsional and rotation vibrations sustained. In case of massive-profiled beams, the differential equation of motion includes secondary effects as rotatory inertia and shear deformation, but warping influence is neglected due to its local character [2]. Differential equation of motion by the theory of massive-profiled and thin-walled beams is solved in closed form; therefore the solutions can be

classified as so-called exact solutions. The solution of differential equation of motion represents the dynamic shape function and is used to evaluate dynamic nodal end moments and forces with proper end conditions and unit displacements. The slope-deflection method is then used to compose system of canonical equation regarding to chosen displacements. In case of thin-walled beams the torsional stiffness and sectorial rotatory inertia of cross-section has excluded as to investigate two cases of connections of longitudinal and cross-members at nodes. It is well known that torsional stiffness of thin-walled beams are relatively low [18] and exclusion of torsional stiffness from governing differential equation is justified. As the conditions of conjunction according to the warping at the nodes, two cases are considered: (I) cross-sections of beams adjoining to the nodes are being warped equally and (II) cross-sections of beams adjoining to the nodes are being warped independently from each other and have different mode. In the first case the warping of node can be determined by one unknown and in the second case warping at node can be determined by two unknowns. Dependence of natural frequencies of ladder frames due to changes in length and moment area of inertia of beams through numerical examples is given as well.

1.2 Basic parameters for slope-deflection method of continuous solid beams

As a basis, we use triply coupled differential equations of motion of uniform beam element given by [4], where effects of shear distortion, rotatory inertia, warping stiffness and warping inertia are taken into account. Beam element with arbitrary cross-section is depicted in Figure 1.1.

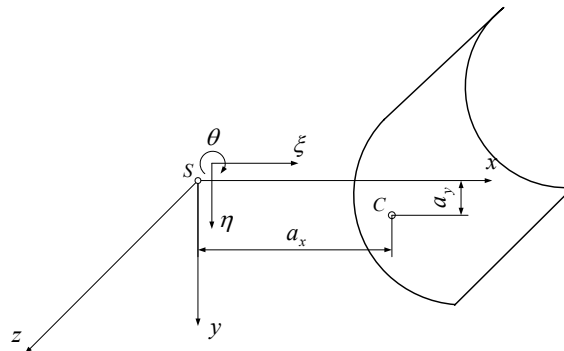


Figure 1.1. Coordinate system of beam element

A uniform straight beam element has length L . The shear center and centroid are denoted by S and C respectively, which are separated by distances a_x and a_y . In the left

handed Cartesian coordinate system used in Figure 1, the z axis is assumed to coincide with elastic axis (i.e. loci of the shear center of the cross-section). The bending translations of the centroid C are denoted by corresponding projections of $\xi(z,t)$ and $\eta(z,t)$ on the x and y axes respectively and the torsional rotation about z axis of shear center S is denoted by $\theta(z,t)$, where z and t denote distance from the origin and time respectively. The triply coupled differential equations of motion of uniform beam element are given then as follows [4]:

$$\begin{aligned}
& EI_y \frac{\partial^4 \xi(z,t)}{\partial z^4} + \frac{\gamma A}{g} \frac{\partial^2 \xi(z,t)}{\partial t^2} - \left(\frac{\gamma I_y}{g} + \frac{EI_y \gamma}{gk'_y G} \right) \frac{\partial^4 \xi(z,t)}{\partial z^2 \partial t^2} + \\
& + \frac{\gamma^2 I_y}{g^2 k'_y G} \frac{\partial^4 \xi(z,t)}{\partial t^4} + a_y \frac{\gamma A}{g} \frac{\partial^2 \theta(z,t)}{\partial t^2} = 0 \\
& EI_x \frac{\partial^4 \eta(z,t)}{\partial z^4} + \frac{\gamma A}{g} \frac{\partial^2 \eta(z,t)}{\partial t^2} - \left(\frac{\gamma I_x}{g} + \frac{EI_x \gamma}{gk'_x G} \right) \frac{\partial^4 \eta(z,t)}{\partial z^2 \partial t^2} + \\
& + \frac{\gamma^2 I_x}{g^2 k'_x G} \frac{\partial^4 \eta(z,t)}{\partial t^4} - a_x \frac{\gamma A}{g} \frac{\partial^2 \theta(z,t)}{\partial t^2} = 0 \\
& a_y \frac{\gamma A}{g} \frac{\partial^2 \xi(z,t)}{\partial t^2} - a_x \frac{\gamma A}{g} \frac{\partial^2 \eta(z,t)}{\partial t^2} + EI_\phi \frac{\partial^4 \theta(z,t)}{\partial z^4} - GI_d \frac{\partial^2 \theta(z,t)}{\partial z^2} - \\
& - \frac{\gamma I_\phi}{g} \frac{\partial^4 \theta(z,t)}{\partial z^2 \partial t^2} + r^2 \frac{\gamma A}{g} \frac{\partial^2 \theta(z,t)}{\partial t^2} = 0
\end{aligned} \tag{1.1}$$

where

- EI_x and EI_y - bending stiffnesses of beam,
- γ - specific weight of gravity,
- G - shear modulus of elasticity,
- EI_ϕ - warping stiffness,
- k'_x and k'_y - effective area coefficient in shear (shear coefficient or area reduction factor)
- A - area of cross-section of the beam element,
- GI_d - Saint-Venant torsional stiffness,
- a_x, a_y - coordinates of shear center of beam,

I_ϕ - geometrical parameter (bimoment of inertia),

r - geometrical parameter and defined as

$$r^2 = \frac{I_x + I_y}{A} + a_x^2 + a_y^2 \quad (1.2)$$

For free vibration of transversely loaded beam, a sinusoidal variation of $\xi(z,t), \eta(z,t), \theta(z,t)$ with circular frequency ω is assumed to be of forms

$$\begin{aligned} \xi(z,t) &= U(z) \sin \omega t \\ \eta(z,t) &= V(z) \sin \omega t \\ \theta(z,t) &= \Theta(z) \sin \omega t \end{aligned} \quad (1.3)$$

where $U(z), V(z)$ and $\Theta(z)$ are the amplitudes of the sinusoidally varying bending translations and torsional rotation, respectively. Substitution of Eq. (1.3) into Eq. (1.1) gives the three simultaneous differential equations for U, V and Θ

$$\begin{aligned} EI_x \frac{d^4 V(z)}{dz^4} - \frac{\gamma A \omega^2}{g} V(z) + \left(\frac{\gamma I_x}{g} + \frac{\gamma EI_x}{g k'_x G} \right) \omega^2 \frac{d^2 V(z)}{dz^2} + \frac{\gamma^2 I_x \omega^4}{g^2 k'_x G} V(z) + \\ + a_x \frac{\gamma A \omega^2}{g} \Theta(z) = 0 \\ EI_y \frac{d^4 U(z)}{dz^4} - \frac{\gamma A \omega^2}{g} U(z) + \left(\frac{\gamma I_y}{g} + \frac{EI_y \gamma}{g k'_y G} \right) \omega^2 \frac{d^2 U(z)}{dz^2} + \frac{\gamma^2 I_y \omega^4}{g^2 k'_y G} U(z) - \\ - a_y \frac{\gamma A \omega^2}{g} \Theta(z) = 0 \\ a_x \frac{\gamma A \omega^2}{g} V(z) - a_y \frac{\gamma A \omega^2}{g} U(z) + EI_\phi \frac{d^4 \Theta(z)}{dz^4} - GI_d \frac{d^2 \Theta(z)}{dz^2} + \frac{\gamma I_\phi \omega^2}{g} \frac{d^2 \Theta(z)}{dz^2} - \\ - r^2 \frac{\gamma A \omega^2}{g} \Theta(z) = 0 \end{aligned} \quad (1.4)$$

Using notations

$$\frac{d^i \eta(z)}{dz^i} = V^{(i)}, \frac{d^i \xi(z)}{dz^i} = U^{(i)}, \frac{d^i \theta(z)}{dz^i} = \Theta^{(i)} \quad (1.5)$$

where (i) denote the order of differentiation with respect to (z) , we can rewrite Eq. (1.4) in the following abbreviated form

$$\begin{aligned} EI_x V^{(4)} - \frac{\gamma A \omega^2}{g} V + \left(\frac{\gamma I_x}{g} + \frac{\gamma EI_x}{g k'_x G} \right) \omega^2 V^{(2)} + \frac{\gamma^2 I_x \omega^4}{g^2 k'_x G} V + a_x \frac{\gamma A \omega^2}{g} \Theta &= 0 \\ EI_y U^{(4)} - \frac{\gamma A \omega^2}{g} U + \left(\frac{\gamma I_y}{g} + \frac{EI_y \gamma}{g k'_y G} \right) \omega^2 U^{(2)} + \frac{\gamma^2 I_y \omega^4}{g^2 k'_y G} U - a_y \frac{\gamma A \omega^2}{g} \Theta &= 0 \\ a_x \frac{\gamma A \omega^2}{g} V - a_y \frac{\gamma A \omega^2}{g} U + EI_\phi \Theta^{(4)} - GI_d \Theta^{(2)} + \frac{\gamma I_\phi \omega^2}{g} \Theta^{(2)} - r^2 \frac{\gamma A \omega^2}{g} \Theta &= 0 \end{aligned} \quad (1.6)$$

Beams with one or two axis of symmetry are most widely used in design of ladder frames. Vibration of ladder frames, which consist of beams with two axis of symmetry, is considerably well known, so henceforth we are focusing on the study of vibration of ladder frames, which consists of beams with one axis of symmetry.

1.2.1 Continuous solid beams with one axis of symmetry

Let us suppose arbitrarily that axis of symmetry of cross-section is axis OY. Due to symmetry of cross-section, the axis OY is principal axis and shear coordinate a_x vanishes. System of ODE (ordinary differential equations) is then separated into two independent systems, one of which

$$EI_x V^{(4)} - \frac{\gamma A \omega^2}{g} V + \left(\frac{\gamma I_x}{g} + \frac{\gamma EI_x}{g k'_x G} \right) \omega^2 V^{(2)} + \frac{\gamma^2 I_x \omega^4}{g^2 k'_x G} V = 0 \quad (1.7)$$

describes transverse bending vibrations in the plane of symmetry and other ones

$$\begin{aligned}
EI_y U^{(4)} - \frac{\gamma A \omega^2}{g} U + \left(\frac{\gamma I_y}{g} + \frac{EI_y \gamma}{g k_y' G} \right) \omega^2 U^{(2)} + \frac{\gamma^2 I_y}{g^2 k_y' G} \omega^4 U - a_y \frac{\gamma A \omega^2}{g} \Theta = 0 \\
-a_y \frac{\gamma A \omega^2}{g} U + EI_\phi \Theta^{(4)} - GI_d \Theta^{(2)} + \frac{\gamma I_\phi \omega^2}{g} \Theta^{(2)} - r^2 \frac{\gamma A \omega^2}{g} \Theta = 0
\end{aligned} \tag{1.8}$$

describes coupled bending-torsional vibrations. Eq. (1.7) is well known in-plane free vibration differential equation of one parameter Timoshenko beam and is extensively studied in the [19], [20], [21]. Solution of Eq. (1.7) is given in standard text books [3]

and obtained by substitution of the trial solution $V(z) = Ce^{\frac{\lambda_\eta}{l} z}$ into the Eq. (1.7). Solution of Eq. (1.7) can be written (without proofing) in nondimensionalized form as follows

$$V(z) = C_1 \cosh \frac{\lambda_{1\eta}}{l} z + C_2 \sinh \frac{\lambda_{1\eta}}{l} z + C_3 \cos \frac{\lambda_{2\eta}}{l} z + C_4 \sin \frac{\lambda_{2\eta}}{l} z \tag{1.9}$$

where

C_1, C_2, C_3, C_4 - constants that are to be determined from boundary conditions,
 $\lambda_{1\eta}, \lambda_{2\eta}$ - frequency parameters and are calculated as

$$\begin{aligned}
\frac{\lambda_{1\eta}}{l} &= \sqrt{\sqrt{\left[\left(\frac{\gamma I_x}{g} + \frac{EI_x \gamma}{g k_x' G} \right) \frac{\omega^2}{2EI_x} \right]^2 + \left(\frac{\gamma A}{g} - \frac{\gamma^2 I_x \omega^2}{g^2 k_x' G} \right) \frac{\omega^2}{EI_x} - \left(\frac{\gamma I_x}{g} + \frac{EI_x \gamma}{g k_x' G} \right) \frac{\omega^2}{2EI_x}} \\
\frac{\lambda_{2\eta}}{l} &= \sqrt{\left(\frac{\gamma I_x}{g} + \frac{EI_x \gamma}{g k_x' G} \right) \frac{\omega^2}{2EI_x} - \sqrt{\left[\left(\frac{\gamma I_x}{g} + \frac{EI_x \gamma}{g k_x' G} \right) \frac{\omega^2}{2EI_x} \right]^2 + \left(\frac{\gamma A}{g} - \frac{\gamma^2 I_x \omega^2}{g^2 k_x' G} \right) \frac{\omega^2}{EI_x}}}
\end{aligned} \tag{1.10}$$

where

ω - circular natural frequency of vibration

Leaving the problem of uncoupled vibration, which is considerably well known, we turn our attention to the coupled bending-torsional behavior of beam element.

Eq. (1.8) can be combined into one equation by eliminating either U or Θ . Neglecting warping effect from Eq. (1.9), which for thick-walled beams is considerably small comparing to other parameters [2], we can rewrite Eq. (1.8) and Eq. (1.9) as follows

$$EI_y U^{(4)} - \frac{\gamma A \omega^2}{g} U + \left(\frac{\gamma I_y}{g} + \frac{EI_y \gamma}{g k_y' G} \right) \omega^2 U^{(2)} + \frac{\gamma^2 I_y}{g^2 k_y' G} \omega^4 U - a_y \frac{\gamma A \omega^2}{g} \Theta = 0 \quad (1.11)$$

$$-a_y \frac{\gamma A \omega^2}{g} U - GI_d \Theta^{(2)} - r^2 \frac{\gamma A \omega^2}{g} \Theta = 0 \quad (1.12)$$

From Eq.(1.12)

$$a_y \frac{\gamma A \omega^2}{g} U = -GI_d \Theta^{(2)} - r^2 \frac{\gamma A \omega^2}{g} \Theta \quad (1.13)$$

Using notations

$$a_y \frac{\gamma A \omega^2}{g} = m, \quad GI_d = n, \quad r^2 \frac{\gamma A \omega^2}{g} = p \quad (1.14)$$

we receive

$$U = -\frac{n}{m} \Theta^{(2)} - \frac{p}{m} \Theta \quad (1.15)$$

Differentiating Eq. (1.15) with respect to (z) , we receive

$$\begin{aligned} U^{(2)} &= -\frac{n}{m} \Theta^{(4)} - \frac{p}{m} \Theta^{(2)} \\ U^{(4)} &= -\frac{n}{m} \Theta^{(6)} - \frac{p}{m} \Theta^{(4)} \end{aligned} \quad (1.16)$$

Substituting Eq. (1.16) in Eq. (1.11) we receive sixth order differential equation

$$\begin{aligned}
& EI_y \left(-\frac{n}{m} \Theta^{(6)} - \frac{p}{m} \Theta^{(4)} \right) - \frac{\gamma A \omega^2}{g} \left(-\frac{n}{m} \Theta^{(2)} - \frac{p}{m} \Theta \right) + \\
& + \left(\frac{\gamma I_y}{g} + \frac{EI_y \gamma}{g k'_y G} \right) \omega^2 \left(-\frac{n}{m} \Theta^{(4)} - \frac{p}{m} \Theta^{(2)} \right) + \frac{\gamma^2 I_y}{g^2 k'_y G} \omega^4 \left(-\frac{n}{m} \Theta^{(2)} - \frac{p}{m} \Theta \right) - a_y \frac{\gamma A \omega^2}{g} \Theta = 0
\end{aligned} \tag{1.17}$$

Substituting trial solution of $\Theta(z) = e^{\frac{\lambda z}{l}}$ into the Eq. (1.17) and after manipulation we can rewrite the Eq. (1.17) in abbreviated form as follows

$$aW^{(6)} + bW^{(4)} + cW^{(2)} - d = 0 \tag{1.18}$$

where by use of Eq.(1.14)

$W = U$ or Θ - differential operator

$$a = 1 \tag{1.19}$$

$$b = \frac{\omega^2 \gamma l^2}{g EI_y} \left(\frac{1}{E} + \frac{1}{k'_y G} - \frac{r^2 A}{G I_d} \right) \tag{1.20}$$

$$c = \frac{\omega^2 l^4 \gamma}{g EI_y} \left[\frac{\gamma I_y \omega^2}{g k'_y G} - A - \left(\frac{\gamma I_y}{g} + \frac{EI_y \gamma}{g k'_y G} \right) \frac{r^2 A \omega^2}{G I_d} \right] \tag{1.21}$$

$$d = -\frac{\omega^4 \gamma^2 A^2 l^6}{g EI_y} \left[\left(\frac{\gamma I_y \omega^2}{g k'_y G} - 1 \right) r^2 - a_y^2 \right] \tag{1.22}$$

From Eq. (1.18) we get characteristic equation as

$$\lambda^6 + b\lambda^4 + c\lambda^2 - d = 0 \tag{1.23}$$

Transforming Eq. (1.23) by substitution

$$k = \lambda^2 - b/3 \tag{1.24}$$

we receive it in condensed form as

$$k^3 + 3pk - 2q = 0 \quad (1.25)$$

where

$$p = \frac{(3ac - b^2)}{9a^2} \text{ and } q = \left(-\frac{b^3}{27a^3} + \frac{bc}{6a^2} + \frac{d}{2a} \right) \quad (1.26)$$

Roots of third order polynomial can be determined using Cardano's method. Three different types of solution of Eq. (1.24) are possible, depending on the sign of parameters p and $D=q^2+p^3$. In the considered case we assume that $p < 0$. In that case roots of Eq. (1.25) read

$$\begin{aligned} k_1 &= 2R \cos\left(\frac{\varphi}{3}\right) \\ k_2 &= 2R \cos\left(\frac{\pi - \varphi}{3}\right) \\ k_3 &= 2R \cos\left(\frac{\pi + \varphi}{3}\right) \end{aligned} \quad (1.27)$$

where

$$\begin{aligned} R &= \pm \sqrt{|p|} \\ \varphi &= \cos^{-1} \frac{q}{R^3} \end{aligned} \quad (1.28)$$

The sign of R can be chosen so that $k_1 > 0$. Numerical examples show that in that case $k_2 < 0$ and $k_3 < 0$ [22].

Substituting Eq. (1.28) into Eq. (1.27) and then into Eq. (1.24), we receive the roots of characteristic equation as follows

$$\lambda_{1\xi}^2 = 2 \sqrt{\left| c^2 - \frac{b^2}{3} \right|} \cos \frac{\phi}{3} - \frac{b}{3}, \quad (1.29)$$

$$\lambda_{2\xi}^2 = 2 \sqrt{\left| c^2 - \frac{b^2}{3} \right|} \cos \left(\frac{\pi}{3} - \frac{\phi}{3} \right) + \frac{b}{3}, \quad (1.30)$$

$$\lambda_{3\xi}^2 = 2\sqrt{\left|c^2 - \frac{b^2}{3}\right|} \cos\left(\frac{\pi}{3} + \frac{\phi}{3}\right) + \frac{b}{3} \quad (1.31)$$

Then the six roots of characteristic equation (1.23) are

$$\lambda_{1\xi}; -\lambda_{1\xi}; i\lambda_{2\xi}; -i\lambda_{2\xi}; i\lambda_{3\xi}; -i\lambda_{3\xi} \quad (1.32)$$

where $i = \sqrt{-1}$.

Using hyperbolic and trigonometric identities, it follows that solution of Eq. (1.18) is of following form

$$\begin{aligned} W(z) = & C_1 \sinh \frac{\lambda_{1\xi}}{l} z + C_2 \cosh \frac{\lambda_{1\xi}}{l} z + C_3 \sin \frac{\lambda_{2\xi}}{l} z + C_4 \cos \frac{\lambda_{2\xi}}{l} z + \\ & + C_5 \sin \frac{\lambda_{3\xi}}{l} z + C_6 \cos \frac{\lambda_{3\xi}}{l} z \end{aligned} \quad (1.33)$$

$W(z)$ in Eq. (1.33) represents the solution for both the transverse displacement U and the torsional rotation Θ with different constant values. Thus

$$\begin{aligned} U(z) = & C_1 \sinh \frac{\lambda_{1\xi}}{l} z + C_2 \cosh \frac{\lambda_{1\xi}}{l} z + C_3 \sin \frac{\lambda_{2\xi}}{l} z + C_4 \cos \frac{\lambda_{2\xi}}{l} z + \\ & + C_5 \sin \frac{\lambda_{3\xi}}{l} z + C_6 \cos \frac{\lambda_{3\xi}}{l} z \end{aligned} \quad (1.34)$$

$$\begin{aligned} \Theta(z) = & A_1 \sinh \frac{\lambda_{1\xi}}{l} z + A_2 \cosh \frac{\lambda_{1\xi}}{l} z + A_3 \sin \frac{\lambda_{2\xi}}{l} z + A_4 \cos \frac{\lambda_{2\xi}}{l} z + \\ & + A_5 \sin \frac{\lambda_{3\xi}}{l} z + A_6 \cos \frac{\lambda_{3\xi}}{l} z \end{aligned} \quad (1.35)$$

where C_1 - C_6 and A_1 - A_6 are two different sets of constants. It can be readily verified by substituting Eq. (1.34) and (1.35) into Eq. (1.11) and (1.12) respectively, that constants C_1 - C_6 and A_1 - A_6 are related in the following way:

$$\begin{aligned} A_1 = \rho_1 C_1 \quad A_3 = \rho_2 C_3 \quad A_5 = \rho_3 C_5 \\ A_2 = \rho_1 C_2 \quad A_4 = \rho_2 C_4 \quad A_6 = \rho_3 C_6 \end{aligned} \quad (1.36)$$

where ρ_i is a characteristic of principal modes of vibration and is expressed in form as

$$\rho_i = a_y \omega^2 \gamma A / g \left(GI_d \frac{\lambda_{i\xi}^2}{l^2} + \frac{r^2 \gamma \omega^2}{g} \right), \quad (i=1,2,3) \quad (1.37)$$

The expressions for rotation of cross-section $\psi(z)$, bending moment $M(z)$, shear force $Q(z)$ and the torque $T(z)$ in terms of transverse displacement are depicted in Figure 1.2 and are as follows:

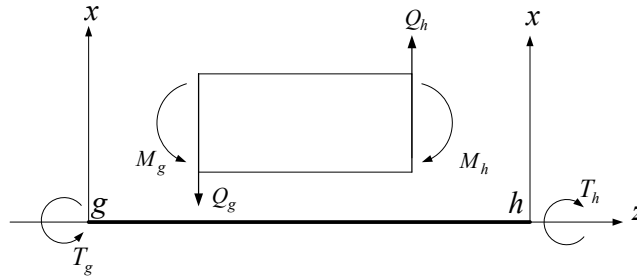


Figure 1.2. Sign convention for positive internal forces and moments

Rotation of cross-section $\psi(z)$

$$\psi(z) = \frac{dU}{dz} \quad (1.38)$$

Bending moment $M(z)$

$$-\frac{M^\eta(z)}{EI_y} = \frac{d^2U(z)}{dz^2} \quad (1.39)$$

Shear force $Q(z)$

$$-\frac{Q^\xi(z)}{EI_y} = \frac{d^3U(z)}{dz^3} \quad (1.40)$$

Torsion moment $T(z)$

$$\frac{T(z)}{GJ_d} = \frac{d\Theta(z)}{dz} \quad (1.41)$$

1.2.1.1 Boundary conditions and nodal end forces

For evaluation of nodal end forces regarding to different boundary conditions, the sign convention given in Figure 1.3 is used.

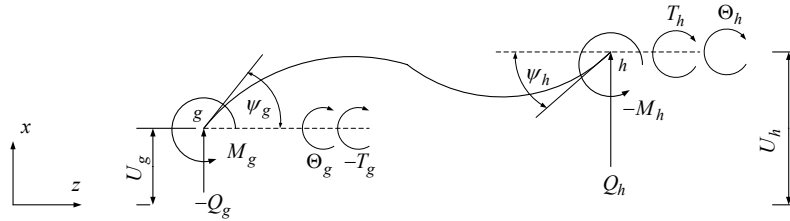


Figure 1.3. End conditions for displacements and forces

The nodal end forces are the holding actions at the end of the beam element when the beam is deformed as to have unit displacement with proper boundary conditions considered. The most common boundary conditions for planar structure are *clamped-hinged*, *clamped-free* and *clamped-clamped* end conditions

Clamped-hinged boundary conditions

The clamped-hinged end conditions imply restraint against translation and torsional rotation at the hinged end, while bending moment is zero. The boundary conditions in this case are

$$U_g = \Theta_g = U_g^{(2)} = U_h = \psi_h = \Theta_h = 0 \quad (1.42)$$

where superscript indicates the order of differentiation with respect to z and hinged end was taken at the left end of the beam arbitrarily. Substituting the Eq. (1.34), (1.35) and (1.38) into the Eq. (1.42), we receive the system of equations, which can be written in abbreviated form as

$$\{\delta\} = [H]\{C\} \quad (1.43)$$

where

$\{\delta\}$ - column vector of end displacements,

$[H]$ - matrix 6x6 of hyperbolic and trigonometric terms in system of Eq. (1.42),

$\{C\}$ - column vector of integration constants C_i

From Eq. (1.43) it is possible to express unknown integration constants C_i as

$$\{C\} = [H]^{-1} \{\delta\} \quad (1.44)$$

Introducing unit displacements at once into the column vector of $\{\delta\}$, we can find sets of integration constants C_i due to the unit displacement at the ends of the beam in each particular case. Substituting the integration constants C_i into the Eq. (1.34) and (1.35), we receive the dynamic displacement functions. Finally, the nodal end forces and moments can be found by substitution of sets of dynamic displacement functions into the Eq. (1.39)-(1.41) and following sign convention given in Figure 1.3.

Clamped-free boundary conditions

The end condition for the clamped-free beam at the built-in end implies that translations and rotations are zero. At the free end the shear force, bending moment and torsion are zero (free end of the beam is chosen at the right side of the beam arbitrarily)

$$U_g = \psi_g = \Theta_g = Q_h = M_h = T_h = 0 \quad (1.45)$$

Analogously, following the procedure for *clamped-hinged* boundary conditions from Eq. (1.43)-(1.44), the sets of dynamic displacements functions and corresponding nodal end forces and moments can be evaluated.

Clamped-clamped boundary conditions

A hinged ends implies restraint against translations and rotations. The boundary conditions are as follows

$$U_g = \psi_g = \Theta_g = U_h = \psi_h = \Theta_h = 0 \quad (1.46)$$

Analogously, as in previous sections, the sets of dynamic displacement functions and corresponding nodal end forces and moments can be found.

1.2.2 Thin-walled open cross-section beams

System of governing differential equation of motion has the same structure for thin-walled open cross-section beams as it was given for solid beams of Eq. (1.1). Neglecting from Eq. (1) a terms consisting of shear coefficient and changing term EI_ϕ for EI_ω (sectorial stiffness), we receive triply coupled system of differential equation of motion for thin-walled open-cross-section beams [4]. Using assumption of sinusoidal variation and procedure from Eq. (1.3)-(1.6) and using previously mentioned notices we receive a triply coupled system of DE of motion for twin-walled beams with separated variables.

1.2.2.1 Thin-walled open cross-section beams with single axis of symmetry

Let us suppose arbitrarily that axis of symmetry of cross-section is axis OY. Due to symmetry of cross-section, the axis OY is the principal axis and the shear coordinate a_x vanishes. The system of ODF (ordinary differential equations) is then separated into two independent systems, one of which

$$EI_x \frac{d^4 \eta(z)}{dz^4} - \frac{\gamma A \omega^2}{g} \eta(z) + \frac{\gamma I_x \omega^2}{g} \frac{d^2 \eta(z)}{dz^2} = 0 \quad (1.47)$$

describes bending vibration in the plane of symmetry and another one

$$\begin{aligned} EI_y \frac{d^4 \xi(z)}{dz^4} - \frac{\gamma A \omega^2}{g} \xi(z) + \frac{\gamma I_y \omega^2}{g} \frac{d^2 \xi(z)}{dz^2} - \frac{a_y \gamma A \omega^2}{g} \theta(z) &= 0 \\ EI_\omega \frac{d^4 \theta(z)}{dz^4} - GI_d \omega^2 \frac{d^2 \theta(z)}{dz^2} + \frac{\gamma I_\omega \omega^2}{g} \frac{d^2 \theta(z)}{dz^2} - \frac{a_y \gamma A \omega^2}{g} \xi(z) - \frac{r^2 \gamma A \omega^2}{g} \theta(z) &= 0 \end{aligned} \quad (1.48)$$

describes joint bending-torsional vibration at condition of restrained warping of cross-section. New term entered in Eq. (1.48) is

EI_{ϖ} - sectorial stiffness,

Neglecting sectorial rotatory inertia of cross-section from Eq. (1.47), we receive the Euler-Bernoulli beam element in standard form. Then, solution of Eq. (1.47) is given in standard text books [3] and obtained by substitution of the trial solution

$V(z) = Ce^{\frac{\lambda}{l}z}$ into the Eq. (1.47). Solution of Eq. (1.47) can be written (without proofing) in nondimensionalized form as follows

$$\eta(z) = C_1 ch\lambda_{\eta} \frac{z}{l} + C_2 sh\lambda_{\eta} \frac{z}{l} + C_3 \cos\lambda_{\eta} \frac{z}{l} + C_4 \sin\lambda_{\eta} \frac{z}{l} \quad (1.49)$$

where frequency parameter is expressed as

$$\lambda_{\eta} = l^4 \sqrt{\frac{\gamma A \omega^2}{g E I_x}} \quad (1.50)$$

Constants C_1, C_2, C_3, C_4 can be found from boundary conditions in the usual way or from standard textbooks [23], [24].

Neglecting a torsional stiffness GI_d and rotatory inertia of cross-section from Eq. (1.48) and following the procedure in the same manner as it was made through Eq. (1.13)-(1.22), we receive a characteristic equation in the following form

$$\lambda^{*8} - \frac{r^2 \gamma A \omega^2 l^4}{g E I_{\varpi}} \lambda^{*4} + \frac{(r^2 - a_y^2)}{E I_{\varpi} E I_y} \left(\frac{\gamma A \omega^2 l^4}{g} \right)^2 = 0 \quad (1.51)$$

where frequency parameters (roots) are expressed as

$$\lambda_1^{*4} = \frac{2\gamma A\omega^2 l^4}{g} \left[\frac{r^2}{EI_\sigma} - \frac{(1 - a_y^2/r^2)}{EI_y} \right], \quad (1.52)$$

$$\lambda_2^{*4} = \frac{2\gamma A\omega^2 l^4}{gEI_y} \left[1 - \frac{a_y^2}{r^2} \right]$$

The roots of the Eq. (1.52) are real and are

$$i\lambda_{1\xi}; -i\lambda_{1\xi}; \lambda_{1\xi}; -\lambda_{1\xi}; i\lambda_{2\xi}; -i\lambda_{2\xi}; \lambda_{2\xi}; -\lambda_{2\xi} \quad (1.53)$$

where $i = \sqrt{-1}$.

Using hyperbolic and trigonometric identities, it follows that solution of Eq. (1.48) is of the following form

$$U(z) = C_1^* \cos \lambda_1^* \frac{z}{l} + C_2^* \sin \lambda_1^* \frac{z}{l} + C_3^* \cosh \lambda_1^* \frac{z}{l} + C_4^* \sinh \lambda_1^* \frac{z}{l} + \quad (1.54)$$

$$+ C_5^* \cos \lambda_2^* \frac{z}{l} + C_6^* \sin \lambda_2^* \frac{z}{l} + C_7^* \cosh \lambda_2^* \frac{z}{l} + C_8^* \sinh \lambda_2^* \frac{z}{l}$$

$$\Theta(z) = A_1 \cos \lambda_1^* \frac{z}{l} + A_2 \sin \lambda_1^* \frac{z}{l} + A_3 \cosh \lambda_1^* \frac{z}{l} + A_4 \sinh \lambda_1^* \frac{z}{l} + \quad (1.55)$$

$$A_5 \cos \lambda_2^* \frac{z}{l} + A_6 \sin \lambda_2^* \frac{z}{l} + A_7 \cosh \lambda_2^* \frac{z}{l} + A_8 \sinh \lambda_2^* \frac{z}{l}$$

where C_1 - C_8 and A_1 - A_8 are two different sets of constants. It can be readily verified by substituting Eq. (1.54) and (1.55) into Eq. (1.48), those constants C_1 - C_8 and A_1 - A_8 are related in the following way:

$$\begin{aligned} A_1 &= \rho_1 C_1 & A_3 &= \rho_1 C_3 & A_5 &= \rho_2 C_5 & A_7 &= \rho_2 C_7 \\ A_2 &= \rho_1 C_2 & A_4 &= \rho_1 C_4 & A_6 &= \rho_2 C_6 & A_8 &= \rho_2 C_8 \end{aligned} \quad (1.56)$$

where characteristics of principal modes are expressed as

$$\rho_1^* = \frac{I_y r^2 / I_{\omega} + a_y^2 / r^2 - 2}{a_y}, \quad (1.57)$$

$$\rho_2^* = -\frac{a_y}{r^2}$$

Expressions for rotation of cross-section $\psi(z)$, bending moment $M(z)$, shear force $Q(z)$ and the bimoment $B(z)$ in terms of transverse displacement using sign convention given in Figure 1.4, where subscript denotes the end of beam element.

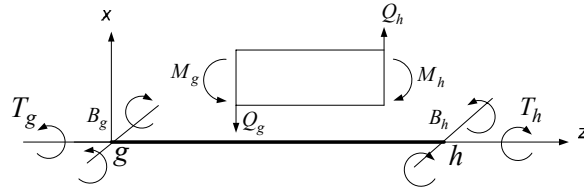


Figure 1.4. Sign convention for positive internal forces and moments of thin-walled beam

Rotation of cross-section $\psi(z)$

$$\psi(z) = \frac{dU(z)}{dz} \quad (1.58)$$

Bending moment $M(z)$

$$-\frac{M(z)}{EI_y} = \frac{d^2U(z)}{dz^2} \quad (1.59)$$

Shear force $Q(z)$

$$-\frac{Q(z)}{EI_y} = \frac{d^3U(z)}{dz^3} \quad (1.60)$$

Flexural-torsional moment $M_{\omega}(z)$

$$-M_{\omega} = \frac{EI_{\omega}}{l^3} \frac{d^3\Theta(z)}{dz^3} - \frac{\gamma I_{\omega}}{gl} \frac{d\Theta(z)}{dz} \quad (1.61)$$

Bimoment $B(z)$

$$-B_{\omega} = \frac{EI_{\omega}}{l^2} \frac{d^2\Theta(z)}{dz^2} \quad (1.62)$$

Saint-Venant' torsion moment $T(z)$

$$\frac{T(z)}{GJ_d} = \frac{d\Theta(z)}{dz} \quad (1.63)$$

Total torsional moment

$$M_T = M_{\omega} + T \quad (1.64)$$

1.2.2.2 Boundary conditions and nodal end forces

For evaluation of nodal end forces regarding to different boundary conditions, the sign convention given in Figure 1.5 is used.

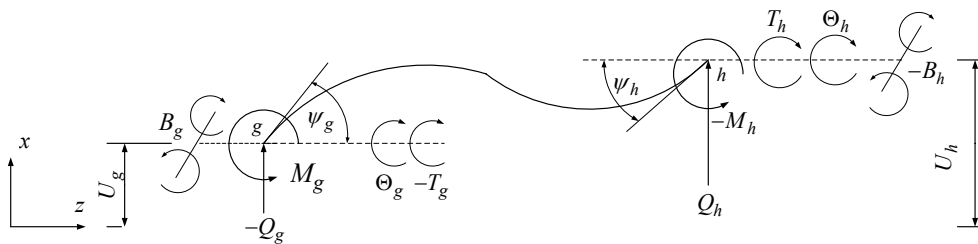


Figure 1.5. Nodal end forces of thin-walled beams

Clamped-hinged boundary conditions

The clamped-hinged end conditions imply restraint against translation and torsional rotation at the hinged end, but not against warping. The boundary conditions in this case are (hinged end taken arbitrarily at the left side of the beam element)

$$U_g = \Theta_g = U_g^{(2)} = \Theta_g^{(2)} = U_h = \psi_h = \Theta_h = \Theta_h^{(1)} = 0 \quad (1.65)$$

where superscript indicates the order of differentiation with respect to z . The procedure for evaluation of integration constants C_i , dynamic displacement functions and nodal end moments and forces is similar to the procedure given in section 1.2.1.1

Clamped-free boundary conditions

The end condition for the clamped-free beam at the built-in end implies that translations and slopes are zero. At the free end the shear force, bending moment, bimoment and torsion are zero (free end of the beam is chosen at the right side of the beam arbitrarily)

$$U_g = \psi_g = \Theta_g = \Theta_g^{(1)} = Q_h = M_h = B_h = T_h = 0 \quad (1.66)$$

Clamped-clamped boundary conditions

A hinged ends imply restraint against translations and rotations. The boundary conditions are as follows

$$U_g = \psi_g = \Theta_g = \Theta_g^{(1)} = U_h = \psi_h = \Theta_h = \Theta_h^{(1)} = 0 \quad (1.67)$$

The procedure for evaluation of integration constants C_i , the dynamic displacement functions and nodal end moments and forces is similar to procedure given in section 1.2.1.1, keeping in mind the boundary conditions given in Eq. (1.65)-(1.67) and using sign convention depicted in Figure 1.4.

1.2.3 Calculation of ladder frames by displacement method

For calculation of free vibration of ladder frames made up from uniform shapes of beams the scheme depicted in Figure 1.6 is used. Let us suppose that the ladder frame under consideration consists of m longitudinal members and n cross-members, which

are placed at right angle to each other. The coordinate axis is placed at the first chosen node. Coordinate axis z is directed along the longitudinal member and x coordinate axis is directed along the cross-member of ladder frame. In this case, every node can be marked symbolically as (z,x) , where x indicates the number of longitudinal member and z indicates the number of cross-member at the node.

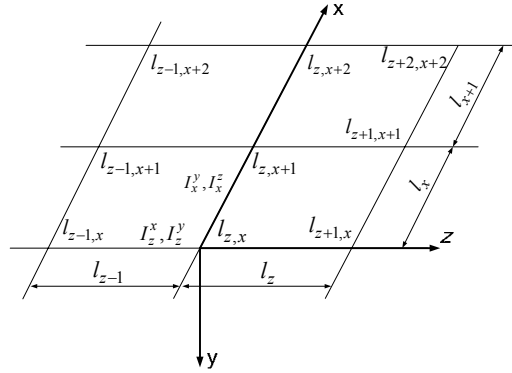


Figure 1.6. Part of ladder frames in general

Displacements due to deformations of node (z,x) according Figure 1.6 can be divided into the two groups:

1. In plane displacements – $U_{z,x}, W_{z,x}$ and $\gamma_{z,x}^y$, in direction of x and z coordinate axis respectively and angular displacement about y coordinate axis (superscript indicates the rotation axis)
2. Out of plane displacements - $V_{z,x}, \gamma_{z,x}^x, \gamma_{z,x}^z, \Theta_{z,x}^x$ and $\Theta_{z,x}^z$, in transversal direction of y coordinate axis, angular and torsional angular displacements about x and z axis respectively (the last two one for thin-walled beams).

In this thesis, the out of plane displacements will be considered only. According to the theory developed for uniform massive-profiled beams in section 1.2.1 we can compose for each node (x,z) of ladder frames three equations of equilibrium of dynamic end moments and forces

$$\sum_{i,j} M_{i,j}^x = 0; \quad \sum_{i,j} M_{i,j}^z = 0; \quad \sum_{i,j} Q_{i,j} = 0 \quad (1.68)$$

where superscript indicates the axis of rotation and subscript indicates the node. In case of thin-walled beams there exist two not well-defined antipodal cases for equilibrium equations:

1. Cross-sections of beams adjoining to the nodes are being warped equally
2. Cross-sections of beams adjoining to the nodes are being warped independently to each other and have different mode. This kind of connection can be described as hinged connection between the crossing members, where warping deflection is not restrained.

In the first case the warping of node can be determined by one unknown. For each node (z,x) of a ladder frame it is possible to obtain four equations of equilibrium

$$\sum_{i,j} M_{i,j}^x = 0; \quad \sum_{i,j} M_{i,j}^z = 0; \quad \sum_{i,j} Q_{i,j} = 0; \quad \sum_{i,j} B_{i,j} = 0 \quad (1.69)$$

In the second case, the warping of the nodes can be determined by two unknowns. Then five equations of equilibrium can be obtained for each node (z,x) of a ladder frame

$$\sum_{i,j} M_{i,j}^x = 0; \quad \sum_{i,j} M_{i,j}^z = 0; \quad \sum_{i,j} Q_{i,j} = 0; \quad \sum_{i,j} B_{i,j}^x = 0; \quad \sum_{i,j} B_{i,j}^z = 0 \quad (1.70)$$

The systems of Eq. (1.68), (1.69) and (1.70) are functions of out of plane displacements, which depend on boundary conditions of node equilibrium to be evaluated and boundary conditions of nodes it linked to. After evaluation of equilibrium conditions for every node in planar frame we receive a global system of equation, which can be written in abbreviate form as follows

$$\{M\} = [F]\{\delta\} \quad (1.71)$$

where

$\{M\}$ - zero column vector,

$[F]$ - functions of dynamic nodal end moments and forces,

$\{\delta\}$ - column vector of unknown out of plane displacements

The necessary and sufficient condition for non-zero elements in the column vector of $\{\delta\}$ in Eq. (1.71) is that $\det(F)=0$, and the vanishing of $\det(F)$ determines the natural frequencies of the system

$$\det(F) = 0 \quad (1.72)$$

The Eq. (1.72) is a transcendental equation of trigonometric and hyperbolic functions which contains the natural frequencies of ω of ladder frames. The roots of Eq. (1.72) may be obtained numerically by applying the standard iterative methods.

For checking the correctness of the expansion of $\det(F)$ and to avoid any numerical problem in evaluation of $\det(F)$, the expression $\det(F)=0$ at $\omega=0$ can be used.

Corresponding to particular value of natural frequency ω_n the mode shapes can be found. For calculation of mode shapes it is necessary to substitute arbitrarily chosen displacement equal to unity in column vector of Eq. (1.71) and express all other displacement through it.

1.2.4 Numerical results

Let us consider for simplicity calculation examples of ladder frame consisting of two longitudinal $n=2$ and two cross girders $m=2$ made up of channel section beams. The system of ladder frames is given in Figure 1.7.

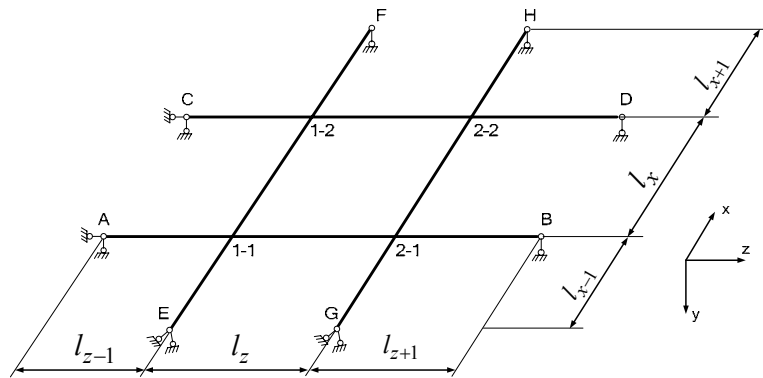


Figure 1.7. Dimensions and end conditions of ladder frame of 2x2

The properties of channel sections used for calculation are given in Table 1.1. For simplicity, ladder frames with hinged ends are considered, but can be extended to other end conditions.

The calculations are executed according to two theories: the theory of thin-walled beams and the theory of massive-profiled beams

Table 1.1. Basic properties of ladder frame of 2x2

	Channel section beams			
	Beam AB	Beam CD	Beam EF	Beam GH
Modulus of elasticity E , GPa	$2,0 \cdot 10^{11}$			
Shear modulus of elasticity G , GPa	$7,7 \cdot 10^{10}$			
Moment of inertia, I_z, I_x , m^4	$206,9 \cdot 10^{-8}$	$206,9 \cdot 10^{-8}$	$206,9 \cdot 10^{-8}$	$206,9 \cdot 10^{-8}$
Moment of inertia, I_y , m^4	$38,2 \cdot 10^{-8}$	$38,2 \cdot 10^{-8}$	$38,2 \cdot 10^{-8}$	$38,2 \cdot 10^{-8}$
Torsion moment of inertia I_d , m^4	$2,727 \cdot 10^{-8}$	$2,727 \cdot 10^{-8}$	$2,727 \cdot 10^{-8}$	$2,727 \cdot 10^{-8}$
Sectorial moment of inertia I_ω , m^6	$354,8 \cdot 10^{-12}$	$354,8 \cdot 10^{-12}$	$354,8 \cdot 10^{-12}$	$354,8 \cdot 10^{-12}$
Area of cross-section A , m^2	$12,5 \cdot 10^{-4}$	$12,5 \cdot 10^{-4}$	$12,5 \cdot 10^{-4}$	$12,5 \cdot 10^{-4}$
Mass per unit length m , kg/m	9,82	9,82	9,82	9,82
Length of beams l , m	$l_{z-1}=l_z=l_{z+1}=1$		$l_{x-1}=l_x=l_{x+1}=1$	

In case of thin-walled beams, two extreme cases are considered: (I) cross-sections of beams adjoining to the nodes are being warped equally; (II) cross-sections of beams adjoining to the nodes are being warped independently to each other and have different mode. For clarity the position of beams to each other in both cases is given in Figure 1.8.

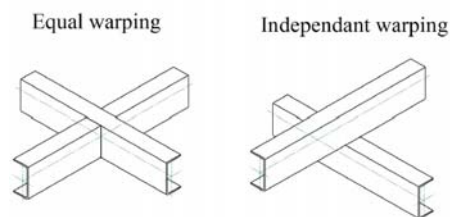


Figure 1.8. Node conditions for warping

The results of calculations of natural frequencies are shown in Figure 1.10. Calculated natural frequencies with different mode shapes are given in Table 1.2. For notation of mode shapes corresponding to particular natural frequencies ω_{ij} , the two-index numbering is used. Here first index i means that longitudinal beams oscillate in the normal mode of vibration having $(i-1)$ nodes, the second index j means that cross girder beams vibrate in the normal mode with $(j-1)$ nodes.

Table 1.2. Natural frequencies of ladder frame (2x2)

Modes of vibration		Natural frequencies by theory of massive beams in rad/s	Natural frequencies by theory of thin-walled beams in rad/s	
i	j	maximum moment of inertia	maximum moment of inertia	
			warping with one unknown	warping with two unknowns
1	1	714,08	728,14	723,02
1	2	2792,05	2887,09	2854,36
2	1	1442,41	1481,31	1469,27
2	2	2963,43	3069,78	3033,07
3	1	3706,07	3851,93	3825,43
3	2	3663,23	3798,45	3766,31
4	1	8640,37	9113,56	9051,12
4	2	5605,53	5883,24	5830,39

The first four fundamental modes of vibrations are depicted in Figure 1.9.

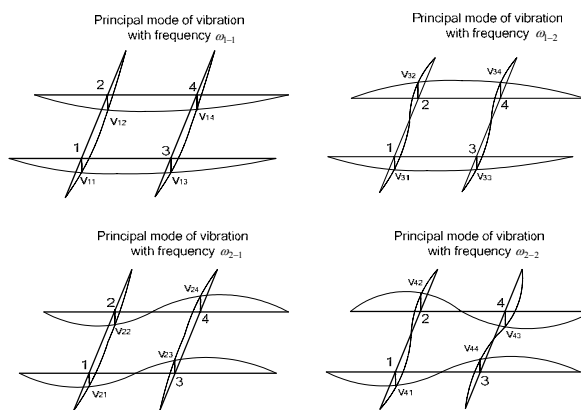


Figure 1.9. Fundamental mode shapes corresponding to the first four natural frequencies

From the Table 1.2 it is seen that difference between the values of natural frequencies grows at higher frequency range. In case of thin-walled beams it is interesting to note that values of natural frequencies depend on the position of structural members to each other. According to Figure 1.10, the values of natural frequencies are higher when members of ladder frame are in plane as it is shown in the left part of the Figure 1.8 and lower when members are assembled as it is shown in the right part of Figure 1.8. The difference between natural frequencies is higher at higher frequencies. Thus, from the point of view of free vibration analysis of ladder frames it is important to consider the position of thin-walled structural members of ladder frames to each other at the nodes and take it into account in calculation of natural frequencies.

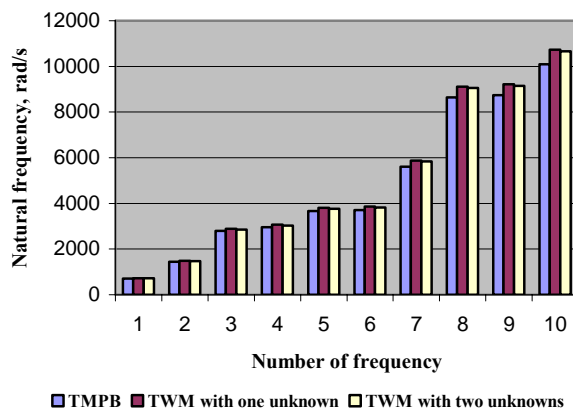


Figure 1.10. Natural frequencies of ladder frame made up of channel section beams (data Table 1.1)

To explore free vibrational behavior of ladder frame of 2x2 by the theory of massive profiled beams and thin-walled beams, the natural frequencies are calculated with different lengths and moment area of inertias of the longitudinal and lateral beams (other properties as given in Table 1.2 are changed accordingly). For comparison first four values of natural frequencies are given. Calculation results by TMPB (theory of massive profiled beams) are depicted through Figure 1.11 to Figure 1.18. Notations used in Figure 1.11...1.18 according to Figure 1.8 are as follows: $L11=l_z$; $L22=l_x$; $L01=l_{z-1}+l_z+l_{z+1}$; $L02=l_{x-1}+l_x+l_{x+1}$; $I1$ – moment area of inertia of longitudinal beam; $I2$ – moment are of inertia of lateral beam. As reference, the lengths of the longitudinal and lateral beam are taken $L01 = 3 m$ and $L02 = 2,55 m$ accordingly. Calculations of natural frequencies of ladder frame are performed at different values of moment area of

inertia and lengths of the middle parts of longitudinal and lateral beams. Results of calculation are depicted from Figure 1.11 to Figure 1.18. Two sets of lengths of middle part of lateral beams are used in calculations- 1 m and $1,3\text{ m}$. The even number in figure indication represents the lengths of the middle part of lateral beams with length 1 m and odd number represents the length of the middle part of lateral beams with length $1,3\text{ m}$. Varying lengths of the middle part of longitudinal beams are the same for all figures and are depicted on them.

As it is seen from Figure 1.11 to Figure 1.18 the values of natural frequencies are greatly affected by changes in length of the middle part of the lateral beams. Anyway, with decrease of the middle part of longitudinal beams, the difference between natural frequencies increases accordingly. Based on the comparison of results given from Figure 1.11 to Figure 1.18, it can be concluded that changes of natural frequencies are more affected by decreasing of lengths of the middle parts of lateral and longitudinal beams than their increasing moment area of inertia.

The spectrum of natural frequencies has highly packed zones, where magnitudes of frequencies are close on their values. The changes in lengths of middle part of longitudinal and lateral beams and moment area of inertia of beams affect greatly the packaged zones of the spectrum of natural frequencies. With decreasing the lengths of middle part of beams and increasing the moment area of inertia of beams, the spectrum of natural frequencies becomes more packaged to the zones compared to the cases, when the lengths of middle parts of beams increase and their moment area of inertia decrease accordingly.

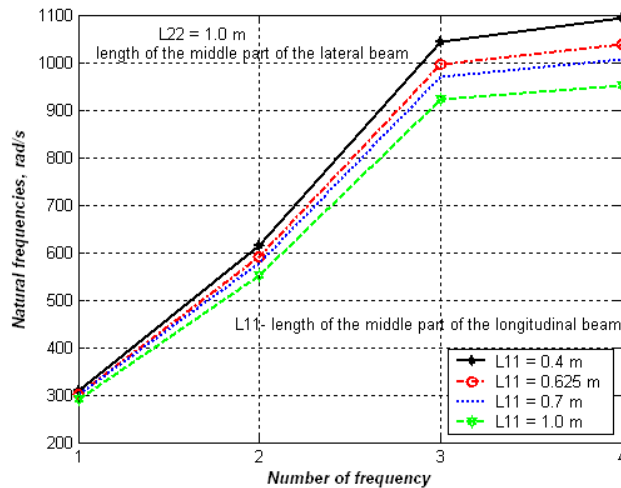


Figure 1.11. NF of ladder frame due to changes in lengths of middle part of longitudinal beams; $I_1=1063\text{ cm}^4$, $I_2=171\text{ cm}^4$, $L22=1,0\text{ m}$

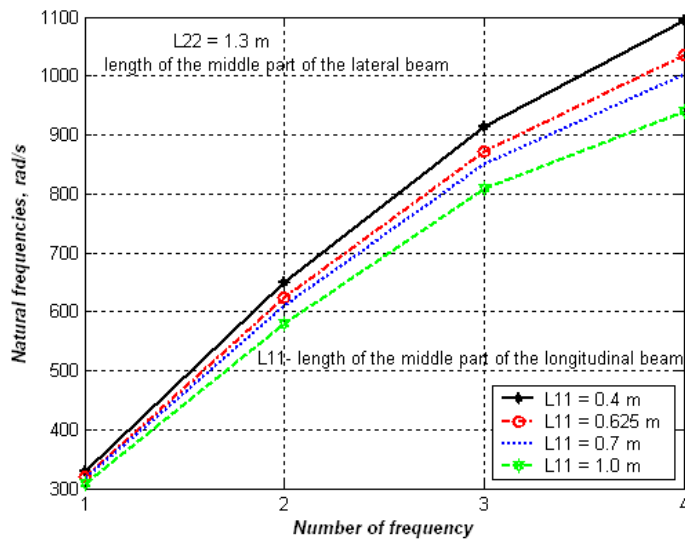


Figure 1.12. NF of ladder frame due to changes in length of the middle part of longitudinal beams, $I_1=1063 \text{ cm}^4$, $I_2=171 \text{ cm}^4$, $L_{22}=1,3 \text{ m}$

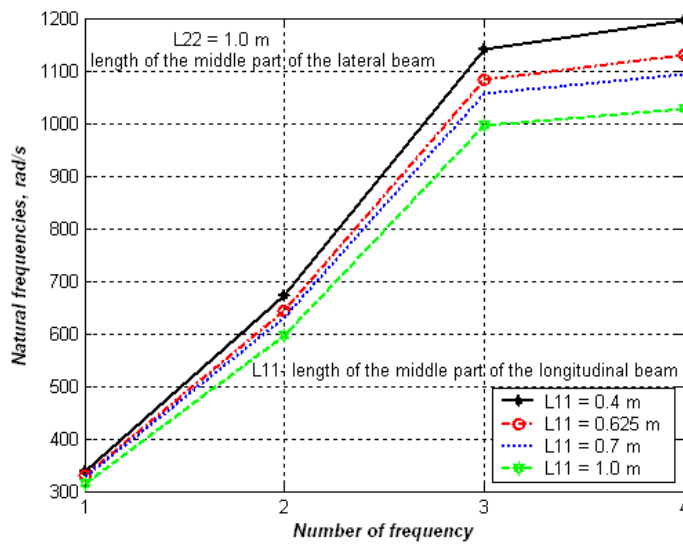


Figure 1.13. NF of ladder frame due to changes in lengths of middle part of longitudinal beams; $I_1=1505 \text{ cm}^4$, $I_2=318 \text{ cm}^4$, $L_{22} = 1,0 \text{ m}$

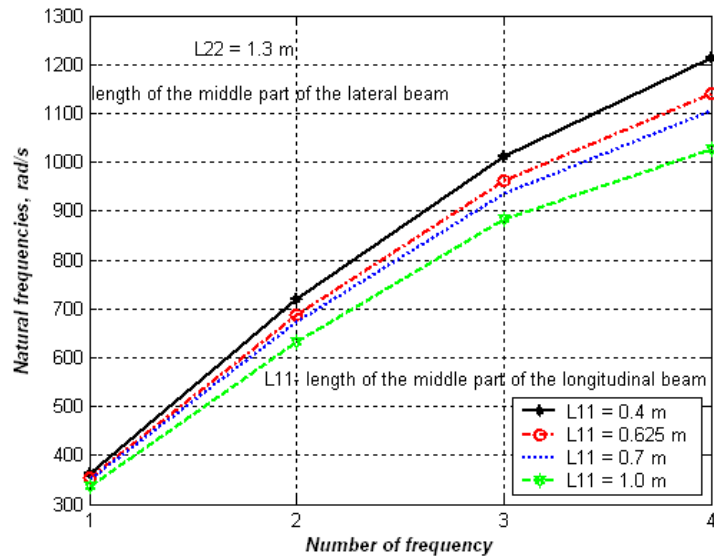


Figure 1.14. NF of ladder frame due to changes in lengths of middle part of longitudinal beams, $I_1=1505$ cm⁴, $I_2=318$ cm⁴, $L_{22}=1,3$ m

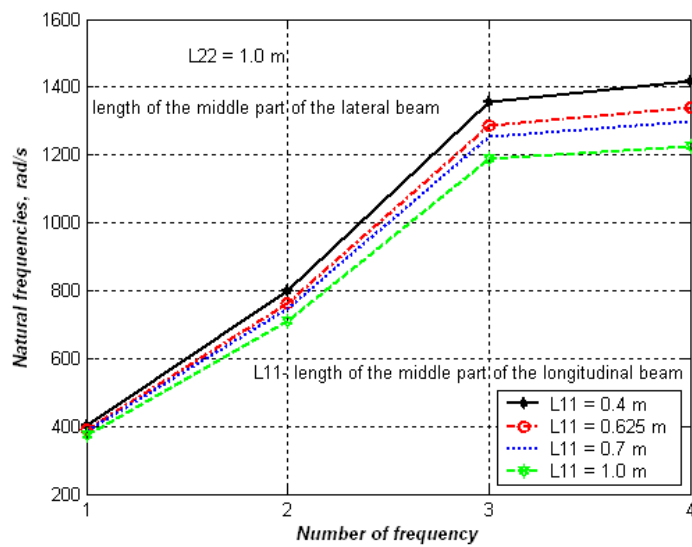


Figure 1.15. NF of ladder frame due to changes in lengths of middle part of longitudinal beams; $I_1=2792$ cm⁴, $I_2=435$ cm⁴, $L_{22} = 1,0$ m

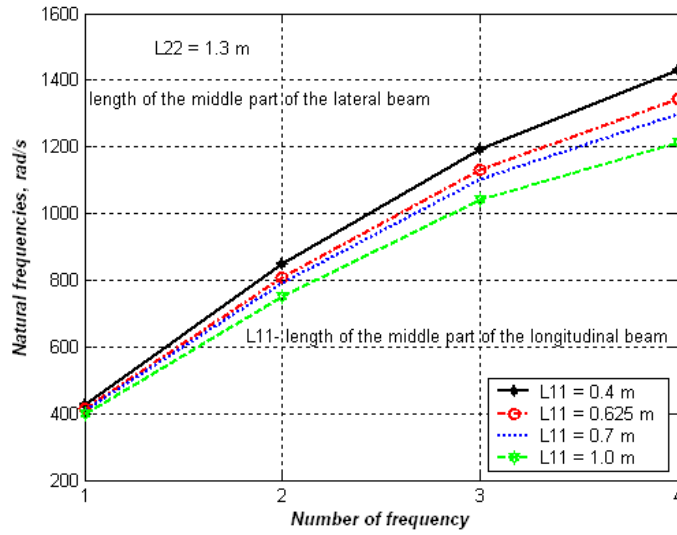


Figure 1.16. NF of ladder frame due to changes in lengths of middle part of longitudinal beams, $I_1=2792 \text{ cm}^4$, $I_2=435 \text{ cm}^4$, $L_{22}=1,3 \text{ m}$

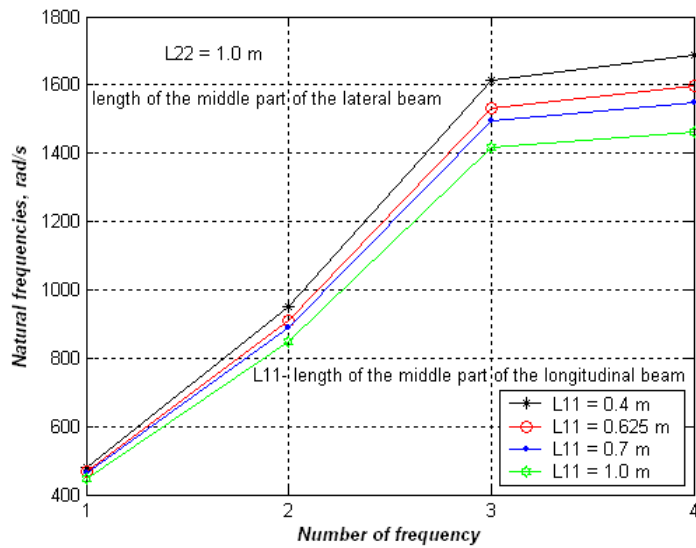


Figure 1.17. NF of ladder frame due to changes of lengths of middle part of longitudinal beams; $I_1=5790 \text{ cm}^4$, $I_2=689 \text{ cm}^4$, $L_{22} = 1,0 \text{ m}$

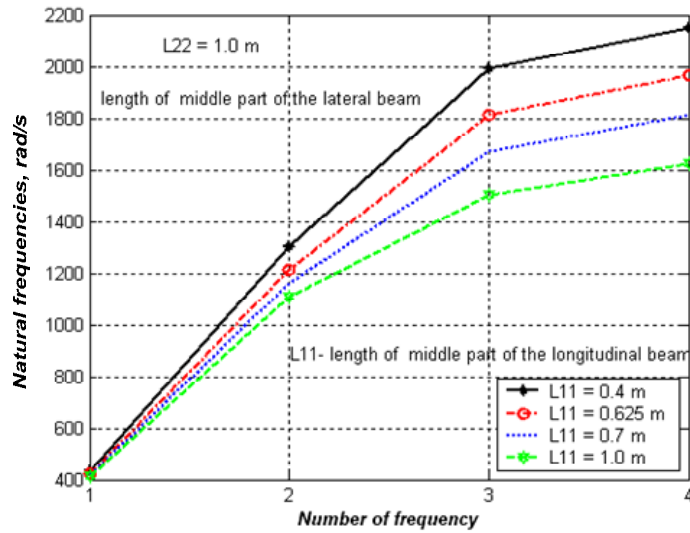


Figure 1.18. NF of ladder frame due to changes of lengths of middle part of longitudinal beams, $I_1=5790 \text{ cm}^4$, $I_2=689 \text{ cm}^4$, $L_{22}=1,3 \text{ m}$

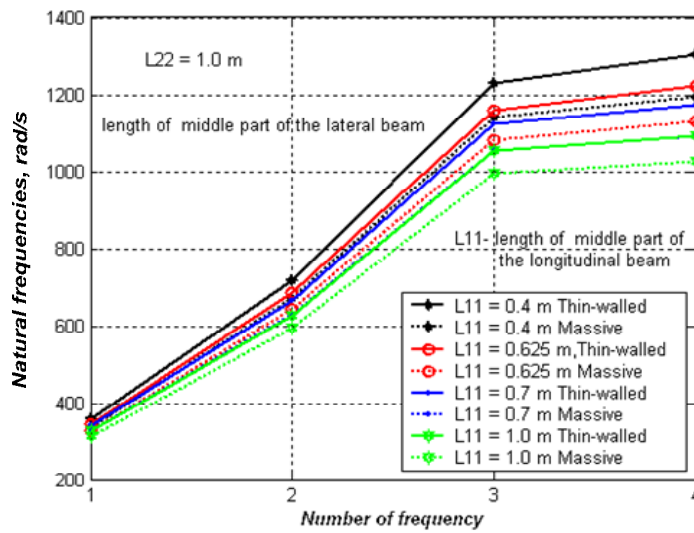


Figure 1.19. Comparison of NF calculated by TMPB and TWB with identical properties of ladder frame, $I_1=1505 \text{ cm}^4$, $I_2=318 \text{ cm}^4$, $L_{22}=1,0 \text{ m}$

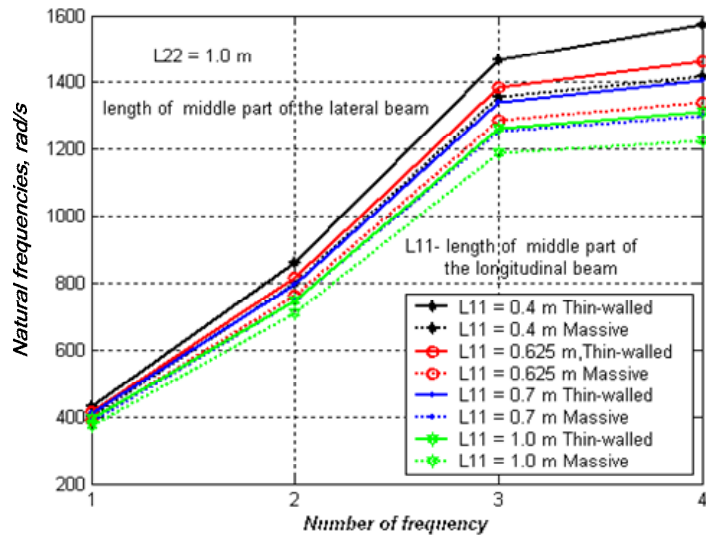


Figure 1.20. Comparison of NF calculated by TMPB and TWB with identical properties of ladder frame, $I_1=2792 \text{ cm}^4$, $I_2=495 \text{ cm}^4$, $L22=1,0 \text{ m}$

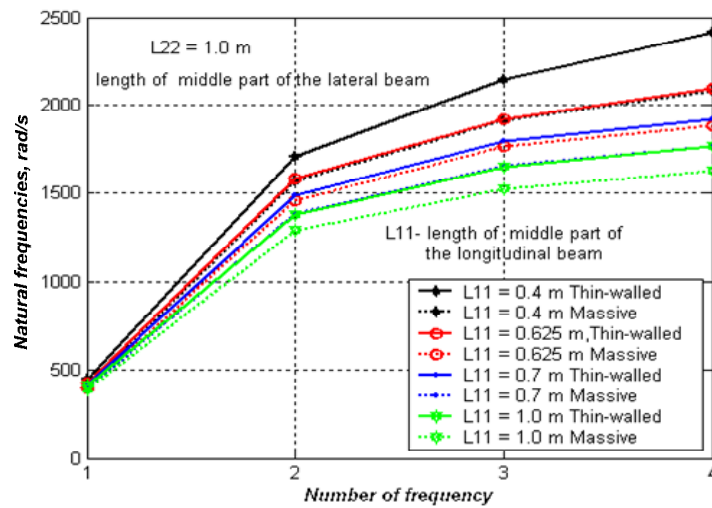


Figure 1.21. Comparison of NF calculated by TMPB and TWB with identical properties of ladder frame, $I_1=5790 \text{ cm}^4$, $I_2=689 \text{ cm}^4$, $L22=1,0 \text{ m}$

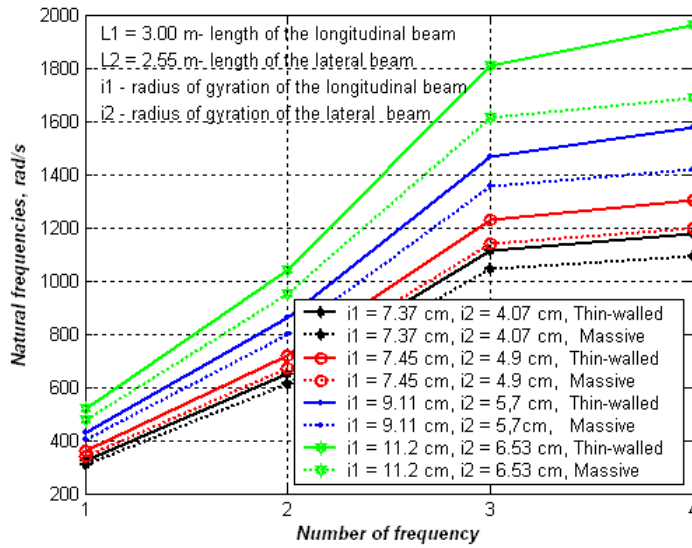


Figure 1.22. Comparison of NF calculated by TMPB and TWB with different radius of gyration of the beams, $L22 = 1,0\text{ m}$, $L22 = 0,4\text{ m}$

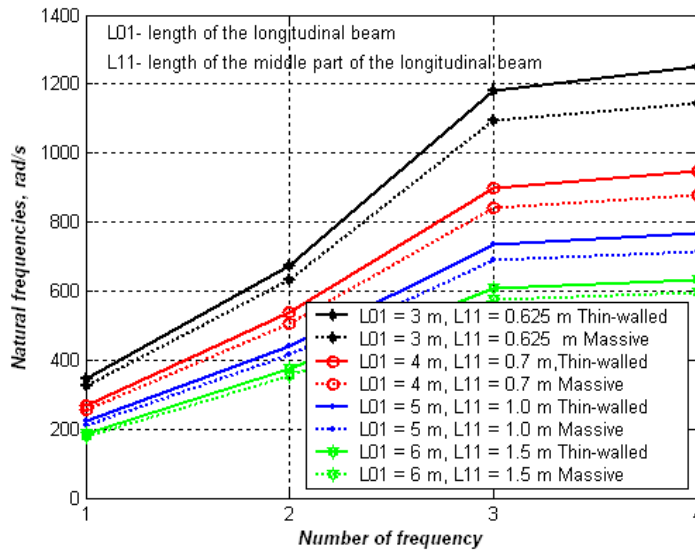


Figure 1.23. Comparison of NF calculated by TMPB and TWB with different lengths of the longitudinal beams LO1 and middle parts L11, $I_1 = 1505\text{ cm}^4 = \text{const}$, $I_2 = 318\text{ cm}^4 = \text{const}$, $LO2 = 2,55\text{ m} = \text{const}$, $L11 = 1,0\text{ m} = \text{const}$

In the Figure 1.19 to 1.23 are depicted the values of natural frequencies calculated by TMPB and TWB (theory of thin-walled beams) at identical cross-sectional properties and lengths of the middle parts of beams. In case of calculations by TWB, the warping effect with one unknown was considered. As it is seen from depicted graphs in Figure 1.19 to Figure 1.23 the values of natural frequencies are higher at identical parameters of the beams and the difference between natural frequencies increases with number of frequency.

For comparison of natural frequencies (NF) in case of beams with two axis of symmetry, the calculations are performed by theories of massive-profiled beams and thin-walled beams both. For calculation of NF of ladder frames by theory of massive profiled beams, the dynamic end forces and moments provided by [32] were used. In case of thin-walled beams the dynamic end forces and moments were derived from Eq. (1.47) and Eq. 1.48) taking into account that in case of beams with two axis of symmetry there are three independent differential equation of motion. Solutions of independent differential equations of motions for thin-walled beams with two axis of symmetry can be found from [4] and the derivation of dynamical end forces and moments doesn't differ from procedure given above, so it is not repeated here. Especially, it was interest to check the natural frequencies of ladder frames made up from thin-walled beams, when longitudinal and lateral beams are in plane and out of plane as it has been shown in Figure 1.8.

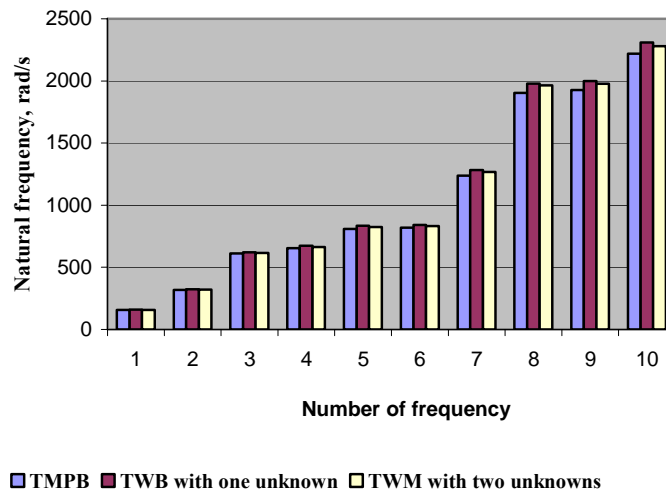


Figure 1.24. NF of ladder frame made up from rectangular cross-section

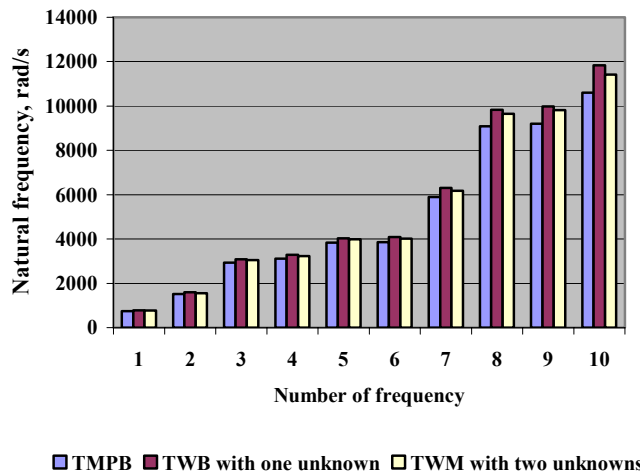


Figure 1.25. NF of ladder frame made up from I-beams

Calculations of natural frequencies by TMPB and TWB were executed with identical lengths of longitudinal and lateral beams of ladder frame given in Table 1.1. As an example, the rectangular cross-section beams and I-beams have been chosen. The cross-sectional properties of chosen beams are given in Table 1.3.

Table 1.3. Cross-sectional properties of beams with two axis of symmetry

	Rectangular cross-section beam	I-beam
Moment of inertia, I_z, I_x, m^4	$1,125 \cdot 10^{-8}$	$317,8 \cdot 10^{-8}$
Moment of inertia, I_y, m^4	$0,03125 \cdot 10^{-8}$	$15,9 \cdot 10^{-8}$
Torsion moment of inertia I_d, m^4	$0,1125 \cdot 10^{-8}$	$1,74 \cdot 10^{-8}$
Sectorial moment of inertia I_{ω}, m^4	$0,0209 \cdot 10^{-12}$	$890,1 \cdot 10^{-12}$
Area of cross-section A, m^2	$1,5 \cdot 10^{-4}$	$13,2 \cdot 10^{-4}$
Mass per unit length $m, kg/m$	1,18	10,4

The calculated NF of ladder frame made up from rectangular cross-section and I-beams are depicted in Figure 1.24 and Figure 1.25. As it was assumed that, in case of

ladder frame made up from TW beams with two axis of symmetry, there is difference between the values of NF calculated for beams assembled in plane and on each other. The difference grows with growth of frequencies.

1.3 Conclusions to the chapter

The present chapter of this thesis presents derivation of dynamic displacement functions for beams with one axis of symmetry according to the massive-profiled and thin-walled beam theory for the slope-deflection method that was used for computation of natural frequencies and corresponding mode shapes of ladder frames in numerical examples. While the derivation of dynamic displacement function is based on the solution of governing differential equation of motion in closed form, it belongs to the so-called “exact” methods and can be used for validation of approximate methods.

In case of massive-profiled beams the effect of shear force and rotatory inertia was included, but the effect of warping was excluded due to its negligible effect [2]. In case of thin-walled beams, the effect of rotatory inertia and torsional stiffness was excluded to show the difference between values of natural frequencies when I) longitudinal and lateral beams of ladder frames are joined to each other in plane and II) beams are assembled to each other. Numerical examples are provided and sensitivity of natural frequencies of ladder frames is discussed.

Numerical results calculated by both theories have shown that natural frequencies of ladder frames are more sensitive to changes of middle parts of the beams than to changes in the moment area of inertia. Differences between natural frequencies grow with the increase in the number of natural frequencies.

The spectrum of natural frequencies of ladder frames has highly packaged zones, where magnitudes of natural frequencies are close in their values. With decrease of lengths of longitudinal and lateral beams and with increase of moment area of inertia of beams the spectrum of natural frequencies becomes more packaged to the zones, where magnitudes of natural frequencies are close in their values. Condensation of natural frequencies to the zones is more affected by decrease of the lengths of longitudinal and lateral beam members, rather than their increasing moment area of inertia.

The provided numerical results show that natural frequencies of the ladder frames consisting of thin-walled beams differ from appropriate frequencies of the system with massive-profiled beams at identical bending-torsion characteristics of cross-section and lengths. The maximum difference of the values of frequencies takes place, when calculations by the theory of thin-walled beams have been executed taking into account of one constraint imposed on the warping of a node. Calculations were performed when two constraints are applied on the warping of a node and results are compared with that of one constraint are applied on the warping. It was defined that with the

growth of the frequency number the difference between the values of frequencies is increased and can achieve 12...16 %.

Investigation of the free vibrations of the systems consisting of thin-walled beams with one and two axis of symmetry has shown that for nodal conjunctions where longitudinal members and cross-members of ladder frames are in the same plane of the system, the one constraint on the warping by calculation of the displacement method must be imposed. However in the case of nodal conjunctions, when beams are in different planes of the system, two constraints on the warping must be applied.

2 FORCED VIBRATION OF LADDER FRAMES UNDER THE ACTION OF REPEATED LOADING

2.1 Background

Response of the structures to the action of repeated interrupted loading is considerably less covered in scientific literature compared to analysis of response of structures due to instant impulses or due to periodic harmonic excitations. Repeated interrupted loading differ from instant impulses due to its relatively long lasting action of structure and it is mathematically discontinuous function. Due to the long lasting action of loading, the maximum response of ladder frames or resonance condition may occur during or after the excitation has ceased. Thus the forced response of ladder frames to the repeated interrupted loading is of practical interest.

In this thesis the response of ladder frames under the action of repeated (periodic) interrupted loading in the presence of structural damping is considered. This kind of loading can be used for analysis of skeletal structures (ladder frames, grillages etc.) as machine foundation, vehicles and trailers frames, ship hulls etc. For formulation of the problem, a discrete scheme of ladder frames is used. Use of discrete schemes in analysis of response of structures has been widely used in seismological applications and it has been found that they give adequate accuracy for practical use. It is well known, that structural damping is an inherent property of structures and consists of energy losses due to friction in structural joints and hysteretic damping or material damping of structural members. Consideration of structural damping in response analysis of structures is not so straightforward due to complexity of mathematical modeling of energy losses in joints and due to variety of structural joints available [51]. It is therefore often general practice to test complicated and expensive specimens to measure structural damping properties and incorporate them into the model of differential equations, but measured damping properties will be usable only for particular type of structures and expansion of test data to other structures is limited [23].

Over the last decades many of hysteretic damping models have been developed [25], [26]. The most attractive due to its simplicity is the linear hysteretic damping model or the so-called complex stiffness model. It is easy to incorporate it to the equation of motion and to get solution in closed form. Anyway, as it was pointed out by many authors [25], [27], [28] and [29] that use of the linear hysteretic damping model or the complex stiffness model in transient response analysis violates the requirement of causality: the system responses before exciting. To overcome this difficulty and investigate a transient response of structures it is accepted that the model of equivalent viscous damping can be used if the system with one-degree-of-freedom is

dealt with [25]. As to multi-degree-of-freedom systems, this model can be exploited for separate undamped modes of vibration, i.e., it is assumed that damping forces do not change the modes of vibration [30], [31]. Another widely used approach is to applying the Fourier transform or series to frequency domain response to obtain a time-domain behavior of a system, which is an application of the superposition principle.

In this thesis, for derivation of forced response of ladder frames under the action of periodic interrupted loading, the Sorokin's complex internal friction theory is used [35]. The Sorokin's internal friction theory is based on the assumption that hysteresis loop has a form of ellipsis and internal friction coefficient is independent of frequency and is constant over the period of loading. Response of a system under the action of periodic interrupted loading is derived in time-domain using "step-by-step" method for SDOF (single-degree-of-freedom). The response during each step then is calculated from the initial conditions (displacement and velocity) existing at the beginning of the step and from the history of loading during the step. Thus the response for each step is an independent analysis problem, and there is no need to combine response contributions within the step. Response of system with SDOF to periodic repeated loading is extended to discrete MDOF (multiple-degree-of-freedom) system using the free vibration normal mode approach. The normal mode approach allows to represent free-vibration mode shapes as independent displacement patterns, the amplitudes of which serve as generalized coordinates to express any set of displacements. The mode shapes thus serve the same purpose as the trigonometric functions in a Fourier series and they possess orthogonality properties.

The use of mode shapes as generalized coordinates serves to transform the equations of motion from a set of simultaneous differential equations, which are coupled by the off-diagonal terms in the mass and stiffness matrices, to a set of independent geometric normal-coordinate equations. Therefore, the total displacements (in original geometric coordinates) of the system can be developed by superposing suitable amplitudes of the normal modes.

For validation of approximate method resolving periodic interrupted loading onto the mode shapes of vibration the numerical calculation and results are provided.

2.2 Differential equation of motion of discrete scheme of ladder frames

Discrete scheme of ladder frame is represented in Figure 2.1 and for simplicity of system it consists of four masses concentrated at the nodes of lateral and longitudinal crossing beams with $r = n \cdot m$ degrees of freedom, where n – number of lateral beams, m – number of longitudinal beams. From Figure 2.1, $n = m = 2$.

It is assumed that loads are applied to these concentrated masses. Such formulation of the problem does not change the general solution, because any load can be reduced to the points of concentration of the masses [32], [33]. Latest holds even in conditions,

when real disturbing forces are absent and support excitations occur. Structural damping and internal friction due to imperfect elasticity of vibrating bodies are the main factors of damping in the ladder frames. In general, structural damping depends on the definite type of construction and must be determined for every case separately.

In this paper, it is assumed that structural damping and internal friction due the imperfect elasticity are linear. Therefore, for simplification of calculations it is accepted that the viscous damping factor γ is independent of frequency of cyclical strains, and includes the losses of structural damping [31].

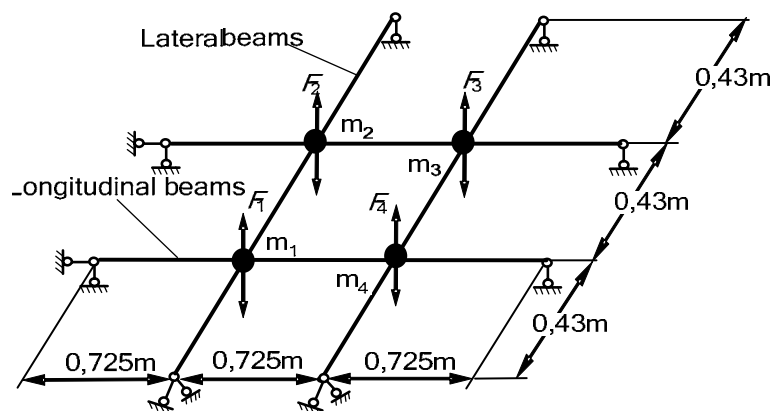


Figure 2.1. Scheme of loading of ladder frame

In Figure 2.2 the schedules of periodical repeated loadings which are acting on the ladder frame are shown.

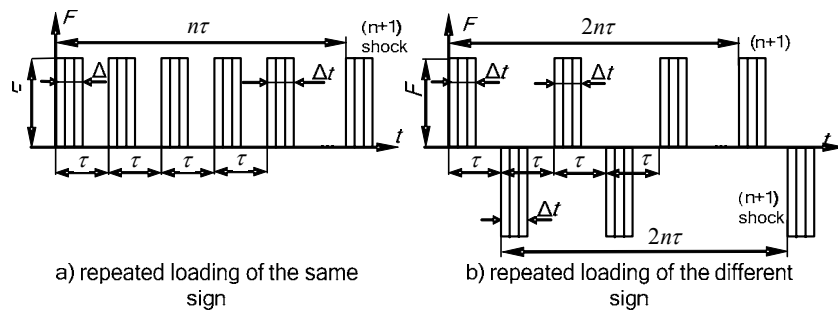


Figure 2.2. Function of periodic loading

Differential equations of forced vibrations taking into account resisting forces according to Sorokin's complex internal friction theory [32] are given as

$$m_k \ddot{y}_k^*(t) + (u + iv) \sum_{j=1}^r C_{kj} y_k^*(t) = F_k(t) \quad (2.1)$$

$(k=1, 2, 3, \dots, r)$

where

$$u = \frac{1 - \gamma^2/4}{1 + \gamma^2/4}, \quad v = \frac{\gamma}{1 + \gamma^2/4} \quad (2.2)$$

y_k^* – complex displacement of k^{th} mass,

C_{kj} – stiffness coefficient of system,

γ – internal friction coefficient,

F_k – forcing function.

Solution of Eq. (2.1) for SDOF system consists of two parts

$$y(t) = y_c(t) + y_s(t) \quad (2.3)$$

in which $y_s(t)$ represents a steady-state response and $y_c(t)$ is a transient response of free vibration. Solution of transient response of free vibration can be found in the textbook [50] and taking into account that initial displacements are zero, it is represented as follows

$$\text{Re}(y^*) = y_c = e^{-\frac{\gamma}{2}\omega t} \left(y_0 \cos \omega t + \frac{y_0 + \frac{\gamma}{2}\omega y_0}{\omega} \sin \omega t \right) \quad (2.4)$$

where

$\text{Re}(y^*)$ - real part of complex displacement,

ω - undamped natural frequency.

Particular solution of Eq. (2.1) is found by using time-history of repeated loading represented in Figure 2.1 “step-by-step” method. In time step $0 \leq \Delta t \leq t$, the forcing function is constant over the step and general solution of Eq. (2.1) can be written as

$$y_k(t) = \frac{F}{m\omega^2} \left[1 - e^{-\frac{\gamma}{2}\omega t} \left(\cos \omega t + \frac{\gamma}{2} \sin \omega t \right) \right] \quad (2.5)$$

In time step $\Delta t \leq t \leq \tau$ the SDOF system performs free vibration with initial conditions given at the end of the last step. So for this time step solution of Eq. (2.1) is

$$y_k(t) = \frac{F}{m\omega^2} \left\{ e^{-\frac{\gamma}{2}\omega(t-\Delta t)} \left[\cos \omega(t-\Delta t) + \frac{\gamma}{2} \sin \omega(t-\Delta t) \right] - e^{-\frac{\gamma}{2}\omega t} \left(\cos \omega t + \frac{\gamma}{2} \sin \omega t \right) \right\} \quad (2.6)$$

Following the procedure given in Eq. (2.4)-(2.6) we can write solution of Eq. (2.1) for any time step. The same procedure is applied to the solution of Eq. (2.1) when loading function with opposite sign is considered. Finally, due to the periodicity of the given excitation loadings, we obtain the expression for determining the displacements after $(n+1)^{\text{th}}$ load application

$$y(t) = \frac{F}{m\omega^2} (A^* - B^*) \quad (2.7)$$

where A^* and B^* are trigonometric functions and can be written as follows

$$A^* = \sum_{\nu=0}^n \exp \left[-\frac{\gamma}{2} \omega(t - \nu\tau - \Delta t) \right] (-1)^\nu \cdot \left\{ \cos \omega(t - \nu\tau - \Delta t) + \frac{\gamma}{2} \sin \omega(t - \nu\tau - \Delta t) \right\} \quad (2.8)$$

$$B^* = \sum_{\nu=0}^n \exp \left[-\frac{\gamma}{2} \omega(t - \nu\tau) \right] (-1)^{\nu+1} \cdot \left[\cos \omega(t - \nu\tau) + \frac{\gamma}{2} \sin \omega(t - \nu\tau) \right] \quad (2.9)$$

Multipliers $(-1)^\nu$ and $(-1)^{\nu+1}$ in A^* and B^* of Eq. (2.8) and Eq. (2.9) in case of repeated loading of the same sign are always equal to one.

Previously given procedure for calculation of SDOF system response to repeated loading of the same sign and opposite sign can be extended to MDOF systems. The free vibration normal mode shapes constitute independent displacement patterns, the amplitudes of which may serve as generalized coordinates to express any set of displacements. It is well known that free vibrational mode shapes possess the orthogonality properties and they are efficient in the sense that they can describe all

displacements with sufficient accuracy employing only few shapes. Moreover, in practical problems, it can be assumed with sufficient accuracy that small resisting forces do not affect the frequencies and the modes of vibration. In this case, the load can be resolved into components of normal modes of vibrations [30]. Thus by use of normal modes it is possible to reduce the coupled equations of forced vibrations of a MDOF systems to a set of uncoupled equations, each involving just a single degree of freedom. Moreover, for sufficiently small damping and the region far from resonance we can neglect the phase difference between the separate vibrating masses of system and their normal modes. Such an approach gives the possibility to get convenient expressions for computer calculation.

Eq. (2.1) written for MDOF systems in matrix form as

$$\mathbf{m}\ddot{\mathbf{y}}(t) + (u + iv)\mathbf{C}\mathbf{y}(t) = \mathbf{F}(t) \quad (2.10)$$

where bold letters represents system with r -degrees of freedom.

Undamped natural frequencies can be found by substitution of trial solution $\mathbf{y} = \mathbf{\Phi}e^{i\omega t}$ into the Eq. (2.10), which leads to

$$-\omega^2\mathbf{m}\mathbf{\Phi} + \mathbf{C}\mathbf{\Phi} = \mathbf{0} \quad (2.11)$$

Premultiplying Eq. (2.11) by inverse of mass matrix, we receive the eigenvalue and eigenvector problem in standard form as

$$\left(\mathbf{m}^{-1}\mathbf{C} - \omega\mathbf{I}\right)\mathbf{\Phi} = \mathbf{0} \quad (2.12)$$

Nontrivial solution of Eq. (2.12) is obtained by setting the determinant of Eq. (2.12) to zero

$$\det\left|\mathbf{m}^{-1}\mathbf{C} - \omega\mathbf{I}\right| = 0 \quad (2.13)$$

For each eigenvalue corresponds the nontrivial eigenvector. Since the system is homogeneous and mode shapes are not unique, it is necessary to substitute arbitrarily chosen displacement equal to unity in column vector $\mathbf{\Phi}$ of Eq. (2.12) and express all other displacement through it. The resulting matrix $\mathbf{\Phi}$ of mode shapes is a square matrix made up from r mode shapes ($r \times r$).

Displacement vector \mathbf{y} can be developed by superposing suitable amplitudes of the normal modes [34] as

$$\mathbf{y} = \Phi \mathbf{Y} \quad (2.14)$$

where

\mathbf{Y} – column matrix of principal coordinates (modal amplitude)

Total displacement vector \mathbf{y} is obtained by summing the modal vectors as expressed by

$$\mathbf{y} = \phi_1 Y_1 + \phi_2 Y_2 + \dots + \phi_r Y_r = \sum_{i=1}^r \phi_i Y_i \quad (2.15)$$

Thus, from Eq. (2.14) it is possible to evaluate the generalized principal coordinates as follows

$$\Phi^{-1} \mathbf{y} = \mathbf{Y} \quad (2.16)$$

Introducing Eq. (2.14) and its second time derivative of $\ddot{\mathbf{y}} = \Phi \ddot{\mathbf{Y}}$ to Eq. (2.10) leads to

$$\mathbf{m} \Phi \ddot{\mathbf{Y}}(t) + (u + iv) \mathbf{C} \Phi \mathbf{Y}(t) = \mathbf{F}(t) \quad (2.17)$$

Premultiplying Eq. (2.17) by transpose of the i^{th} mode-shape vector ϕ_i^T , it becomes

$$\phi_i^T \mathbf{m} \Phi \ddot{\mathbf{Y}}(t) + (u + iv) \phi_i^T \mathbf{C} \Phi \mathbf{Y}(t) = \phi_i^T \mathbf{F}(t) \quad (2.18)$$

Expanding the left terms in Eq. (2.18) as shown in Eq. (2.15), the all terms except the i^{th} vanishes due to assumed orthogonality properties of mode shapes; hence the result is

$$\phi_i^T \mathbf{m} \phi_i \ddot{Y}_i(t) + (u + iv) \phi_i^T \mathbf{C} \phi_i Y_i(t) = \phi_i^T \mathbf{F}(t) \quad (2.19)$$

The terms in left side of Eq. (2.19) are generalized mass and generalized complex stiffness for mode i respectively. The term in the right side is generalized force for mode i accordingly. Eq. (2.19) rewritten in generalized terms is

$$M_i \ddot{Y}_i(t) + (u + iv) C_i Y_i(t) = F_i(t), \quad (i=1, 2, \dots, r) \quad (2.20)$$

which is a differential equation describing the motion of SDOF equation for mode i . Thus, by use of procedure from Eq. (2.11) to (2.20) the system of differential equation of motion of MDOF system is reduced to the generalized system with SDOF. Thus, the solution of Eq. (2.20) for one discrete mass in r -degrees of freedom system is same as it was given in Eq. (2.7), (2.8) and (2.9) for SDOF. Solution of Eq. (2.20) for single discrete mass m_k in r -degrees of freedom system after $(n+1)^{\text{th}}$ load application can be written in terms of matrix elements as follows

$$y_k(t) = \sum_{i=1}^r \frac{y_{ki} \sum_{j=1}^r F_j y_{ji}}{\omega_i^2 \sum_{j=1}^r m_j y_{ji}^2} (A_i^* - B_i^*), \quad (k=1,2,\dots,r) \quad (2.21)$$

where

ω_i - undamped natural frequencies of r - degree of freedom system,

A_i^* and B_i^* - are trigonometric functions and can be written as follows

$$A_i^* = \sum_{\nu=0}^n \exp\left[-\frac{\gamma}{2}\omega_i(t-\nu\tau-\Delta t)\right] (-1)^\nu \cdot \left[\cos\omega_i(t-\nu\tau-\Delta t) + \frac{\gamma}{2}\sin\omega_i(t-\nu\tau-\Delta t)\right]$$

$$B_i^* = \sum_{\nu=0}^n \exp\left[-\frac{\gamma}{2}\omega_i(t-\nu\tau)\right] (-1)^{\nu+1} \cdot \left[\cos\omega_i(t-\nu\tau) + \frac{\gamma}{2}\sin\omega_i(t-\nu\tau)\right] \quad (2.22)$$

Thus, by use of assumptions given before, the displacement of each discrete mass in r -degrees of freedom system can be described by Eq. (2.21) and (2.22).

2.3 Calculation example

Consider the calculation example of the of ladder frame of 2x2 given in Figure 2.1, where force F_1 is applied to mass m_1 only. The masses of longitudinal and lateral beams per unit length are $\bar{m}_x = \bar{m}_y = 1,1927$ kg/m, moments of inertia of the beams are $I_x = I_y = 0,03125 \cdot 10^{-8}$ m⁴, four equal masses $m_1 = m_2 = m_3 = m_4 = 1,3775$ kg concentrated in the crossing nodes of the beams. The periodical repeated load $F_1=29,7$ N was applied to mass m_1 (Figure 2.1), the duration of loading was $\Delta t = 0,08$ s, the interval between the repeated loading was $\tau = 0,5$ s. The normal mode method

requires the natural frequencies and modes of free vibrations to be known. Taking into consideration the discrete scheme with four degrees of freedom, we received the following natural frequencies of the ladder frame: $\omega_1 = 28,6$ rad/s, $\omega_2 = 53,3$ rad/s, $\omega_3 = 104,0$ rad/s, $\omega_4 = 112,0$ rad/s and normal mode characteristics of vibrations are given in Table 2.1

Table 2.1. Normal mode characteristics of vibrations

$y_{11} = 1$	$y_{21} = 1$	$y_{31} = 1$	$y_{41} = 1$
$y_{12} = 1$	$y_{22} = 1$	$y_{32} = -1$	$y_{42} = -1$
$y_{13} = 1$	$y_{23} = -1$	$y_{33} = 1$	$y_{43} = -1$
$y_{14} = 1$	$y_{24} = -1$	$y_{34} = -1$	$y_{44} = 1$

Substituting these values into the Eq. (2.21) and Eq. (2.22) we can obtain the magnitudes of forced vibrations in any interval of load action. For calculation of magnitudes of forced vibrations the different internal friction factor γ has been used. The values of internal friction factors are taken from [35]. In this case, it has been assumed that values of internal friction factors include losses of structural damping.

The calculation results for mass m_1 are depicted graphically in Figure 2.3 and Figure 2.4. The graphs of forced vibrations with different internal friction factor γ showed that due to damping the displacements become smaller. Such big influence of damping on the vibration displacements can be explained by the small duration Δt of the load in comparison with the time interval τ between repeating loading (Figure 2.2,a). In consequence, the system vibrates freely for the large part of time interval τ and due to presence of damping, the decaying of free vibrations occurs even faster. If the duration of loading $\Delta t > 2.5T_1$, where $T_1 = 2\pi/\omega_1$ - the period of the first frequency of structure, then calculation will be reduced to the static one with equivalent load μF_1 , where $\mu = 2$ for sudden loading and $\mu = 1$ in the case of sudden unloading.

However, if the duration of the loading $\Delta t < 0.1T_n$, where $T_n = 2\pi/\omega_n$ is the period of the highest frequency in the spectrum of natural frequencies (the first order harmonics), then calculation will be reduced to the calculation for the instant impulses. If the period between repeated loadings is $\tau > 2T_1/\gamma$, then calculation is for the single impulse. From this, we can conclude that when $0,1T_n \leq \Delta t \leq 2,5T_1$ and $\Delta t \leq \tau \leq 2T_1/\gamma$ the displacements under the action of repeating loading are determined by Eq. (2.3).

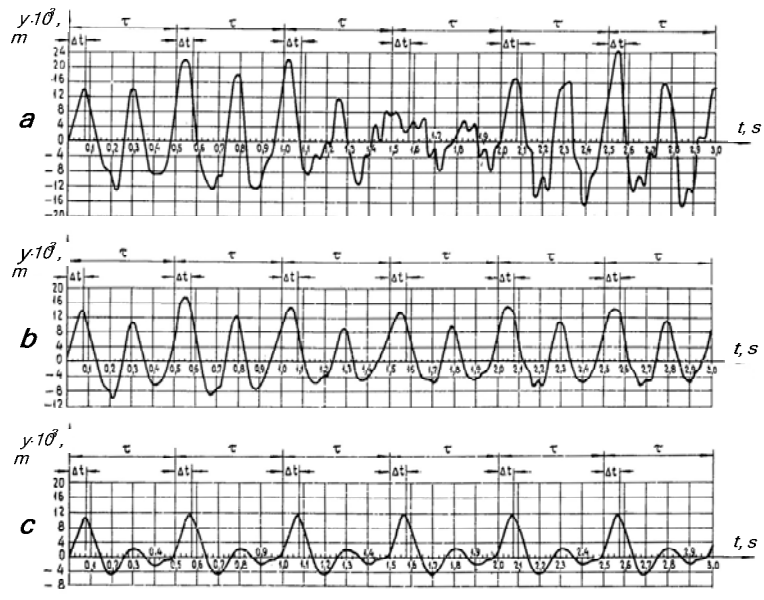


Figure 2.3. Forced vibrations of mass m_1 taking into account the all principal modes with different internal friction factors: a - $\gamma = 0$; b - $\gamma = 0.06$; c - $\gamma = 0.2$.

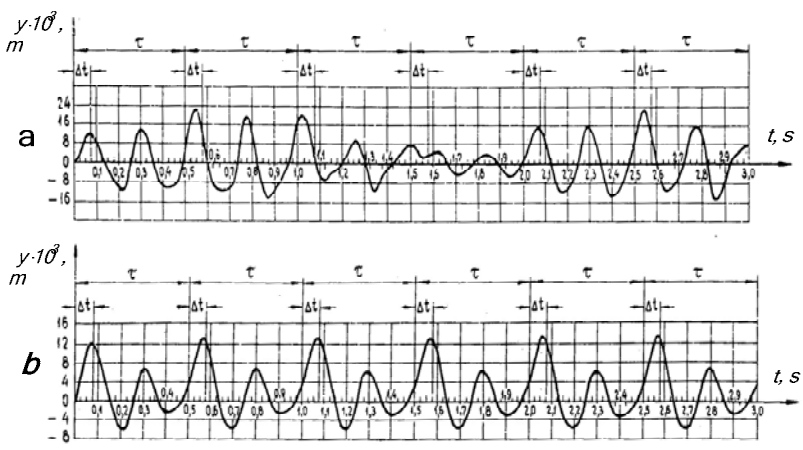


Figure 2.4. Forced vibration of mass m_1 taking into account different frictional factors of two principal modes

In order to find out how the highest modes influence the displacement magnitudes, calculation was carried out taking into account the first two modes only. The calculation results are given in Figure 2.4. It can be seen that these results are not much different from those on Figure 2.3, where all r normal modes of vibration were taken into account. However, in the case of resonance when the system has maximum displacements it is not enough to use the first two modes only. The necessity to take into account also the highest modes of vibrations is explained by the fact that the frequency spectrum of ladder frames is not continuous, but has isolated zones with highly packed frequencies. In addition, frequency values do not increase so quickly with the total number of frequencies. The absence of some these frequencies can lead to errors in calculations.

2.4 Steady-state forced vibration

It is seen from the graphs of the forced vibrations in Figure 2.4, that after some time stationary forced vibrations are established. Typically, the vibrations excited by suddenly applied periodic loading are not periodic. However, for simplification of solution the vibrations can be represented as a sum of periodical stationary vibrations with the period of exciting load τ and free vibrations. The free vibrations caused by the presence of the initial conditions and action of repeated loading take place only for the initial transitive period of movement. After some time vibrations were gradually damped out due to resisting forces and finally steady-state periodical vibrations were established. Such problem has already been discussed for systems with one and two degrees of freedom [3], [30], [32]. In this thesis, this problem was extended to the system with multiple degrees of freedom.

Taking into account the aforementioned simplifications and resolving the load into normal modes of vibration (the normal mode method), and then each mass displacement of the discrete scheme (Figure 2.1) in any interval τ of loading for each single mode of natural vibrations separately may be represented in the following form

$$y_{ki}(t) = \exp\left(-\frac{\gamma}{2}\omega_i t\right) \cdot \left(y_{ki}(0) \cos \omega_i t + \frac{y_{ki}(0) + \frac{\gamma}{2}\omega_i y_{ki}(0)}{\omega_i} \cdot \sin \omega_i t \right) + y_{ki}^*(t^*) \quad (2.23)$$

$(i, k = 1, 2, 3, \dots, r),$

where the first two terms of this solution represent free vibrations depending on the initial conditions, but the third term represents vibrations produced by loading in the given time interval $0 \leq t^* \leq \tau$. In order to ensure, that the steady-state forced

vibrations occur in each time interval, we compared the displacements and velocities of masses at the beginning and the end of the interval for the each single mode of natural vibrations separately $y_{ki}(0) = y_{ki}(\tau), \dot{y}_{ki}(0) = \dot{y}_{ki}(\tau), (i, k = 1, 2, 3, \dots, r)$. Then it is possible to form two equations for the each mode separately, from which the initial conditions of the periodical vibration were determined. The total displacements of system in any time interval taking into account all modes of vibrations are the following

$$y_k(t) = -\sum_{i=1}^r \exp\left(-\frac{\gamma}{2}\omega_i t\right) \cdot \left[y_{ki}(0) \cos \omega_i t + \frac{y_{ki}(0) + \frac{\gamma}{2}\omega_i \dot{y}_{ki}(0)}{\omega_i} \cdot \sin \omega_i t \right] + \sum_{i=1}^r \exp\left(-\frac{\gamma}{2}\omega_i t^*\right) \cdot \left[y_{ki}(0) \cos \omega_i t^* + \frac{y_{ki}(0) + \frac{\gamma}{2}\omega_i \dot{y}_{ki}(0)}{\omega_i} \cdot \sin \omega_i t^* \right] + \sum_{i=1}^r y_{ki}^*(t^*) \quad (2.24)$$

$(k = 1, 2, 3, \dots, r),$

where $y_{ki}(0), \dot{y}_{ki}(0)$ - the initial conditions of the steady-state forced vibrations.

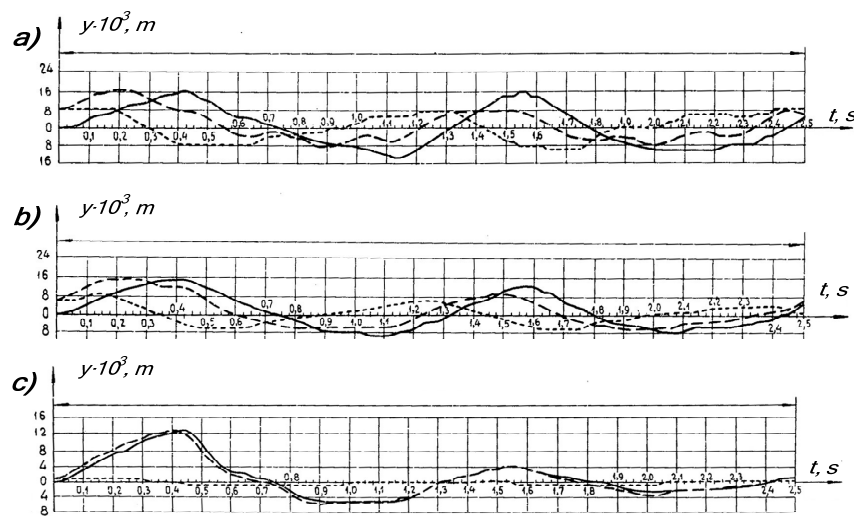


Figure 2.5. Steady-state forced vibrations with different internal friction

- factors γ : a) - $\gamma = 0$; b) - $\gamma = 0.06$; c) - $\gamma = 0.2$
- forced vibrations caused by action of repeated loading
 - - - steady-state forced vibrations
 - · · free vibrations depending on the initial conditions

The first two terms express free vibrations of system, the last one – the forced vibrations due to loading acting during time interval τ .

The calculation results of steady-state forced vibrations of ladder frame (Figure 2.1) are represented in Figure 2.5.

In comparison of calculated results, it is seen good correlation, especially in the case of large resistance. It is so because with increase of resistance the influence of free vibrations is decreased. These vibrations are determined by the first two terms in Eq. (2.27) for the total displacements.

2.5 Conclusion to the chapter

The discrete calculation scheme is given; it determines with a sufficient degree of accuracy the forced vibrations of ladder frames under the action of repeated interrupted loading. It is necessary to take into account resisting forces determined by internal friction factor γ independent of frequency of cyclical strains. The magnitude of the factor γ is common for the whole system. It was established that we can use generalized internal friction factor γ taking into account structural damping.

The expressions for determining steady-state periodical forced vibrations that allow considering only one time interval τ of loading has been devised. Such solution is especially convenient in the case of resonance when it is enough to take into account only one normal resonance mode. It has been shown that the frequency spectrum of such structure of ladder frames has zones, where frequency values are close to each other, but normal modes corresponding to them are different. Absence of some of these frequencies can lead to errors in calculations.

Previously developed theory is applicable to use for calculation of amplitudes of forced vibration in the field of naval engineering, civil engineering, vehicle engineering etc.

3 STUDY OF FREE VIBRATION OF LADDER FRAMES REINFORCED WITH PLATE

3.1 Background

Floor systems that consist of continuous steel or concrete panel and steel frame in plane to reinforce it are very widely used in industrial and civil buildings and vehicle industry. Examples of this kind of orthotropic system in the vehicles industry are floor systems of tipping bodies of trucks and trailers, where bottom of tipping bodies generally consists of high wear resistant cold rolled metal sheets in general and these are reinforced with steel frame. In the field of industry and civil buildings, concrete floor with reinforcing ribs can be considered as an orthotropic floor system. Most common structures of reinforcing steel frames are ladder frames consisting of uniform straight beams of massive and/or thin-walled structural shapes. Covering steel or concrete plates enlarge rigidity of reinforcing frames or vice versa and so alter vibrational characteristics of all design. Taking into account that reinforcing frames, which might consist of beams with different cross-sectional dimensions and can be in plane or one beam can be situated above one another, then analytical calculation of free vibrations of such floor design is a quite complex calculation problem.

In vibration analysis of stiffened plates, researchers have proposed many methods: orthotropic model [36], the grillage model [37], the Ritz or Rayleigh–Ritz method [38] and [39], the matrix method [40], the finite difference method [41], the finite element method [42], the differential quadrature method [43], mesh-free method [44], wave analysis [45] etc. Literature survey reveals that orthotropic plate model is still commonly used [46] due to its simple formulation [44]. According to the orthotropic plate model the structural behavior of stiffened plate is approximated by converting this system into a homogeneous plate of constant thickness using the stiffness properties of the beams (as additional layer) [47].

The orthotropic plate model does not represent real deformations of system [46], so calculated natural frequencies for orthotropic plate using this model differ from exact values within the range of 5% up to 70% [48].

In this thesis, a discrete model for calculation of natural frequencies of orthotropic floor systems is proposed. In case of the discrete model, an orthotropic floor system is replaced by a system of crossed beams (ladder frame) stiffened locally by plate and the last one as the continuous system is replaced by the discrete system of concentrated masses.

Calculations by an orthotropic plate models and equivalent discrete systems are executed on real industrial floor systems to compare calculation results with existing data. In this case, the orthotropic floor system consists of concrete plate with

reinforcing ribs. Discrete model of orthotropic floor design leads to calculation of ladder frames and the effect of the plate is taken account using T-beams instead of ribs. Rigidity of plate is represented by the top section of T-beam. Determination of the proper dimensions of this top section has not been solved up until today. To determine the size of the top section, consecutive approximations are necessary. To assess the accuracy of considered models, the displacement method (slope deflection method) for continuous system [49], [32] of floor design and ANSYS program is used. Although floor system are used as the example, which consist of concrete plates and reinforcing steel ribs, calculations by discrete scheme can be extended to orthotropic floor systems, which consist of steel plates and frames to reinforce them.

3.2 Basic concept of the discrete scheme

Equations of the free vibrations of a discrete system with n^{th} degrees of freedom have the form [48]

$$\sum m_i \delta_{ij} \ddot{y}_i(t) + \ddot{y}_i(t) = 0, (j=1,2, \dots, n) \quad (3.1)$$

where

m_i - value of i^{th} concentrated mass,

y_i - displacement of i^{th} concentrated mass,

δ_{ij} - unit displacements of system at the points of application of the concentrated masses.

The static calculation is performed on ANSYS program. Calculation of free vibrations was carried out for two models of the orthotropic floor system. In calculations by the orthotropic plate model the joint deformation work of the plate and beams were taken into account. In calculation by discrete scheme, a system of crossed beams is considered instead of an orthotropic plate. To determine values of moment of inertia of cross-sections of main and auxiliary beams, the influence of plate is represented as rectangular cross-section with proper dimensions. After calculation of the unit displacements δ_{ij} , the problem of calculation of natural frequencies and normal modes of the floor is reduced to a problem of eigenvalues and eigenvectors

$$(B - \lambda E) \bar{y} = 0 \quad (3.2)$$

where

\bar{y} - a column vector,

λ - frequency parameter,

B - square matrix, received as a result of multiplication of the matrix of unit displacements δ_{ij} with the matrix of concentrated masses m_i ,
 E - the unit matrix.

For the solution of Eq. (3.2), methods of simultaneous iteration or direct iteration and MatLab programs are used.

3.3 Calculation of rib floors as an orthotropic plate

Let us consider a simply supported concrete panel (floor) reinforced with parallel symmetrically placed five concrete ribs (Figure 3.1). The floor has the following characteristics: the modulus of elasticity of concrete $E_c=2,1 \cdot 10^9$ N/m², thickness of the panel $h = 0,1$ m, width of the panel $b = 5$ m, length of the panel $a = 10$ m, density of concrete $\gamma_c = 24$ kN/m³, cross section of the ribs $0,3 \times 0,5$ m²,

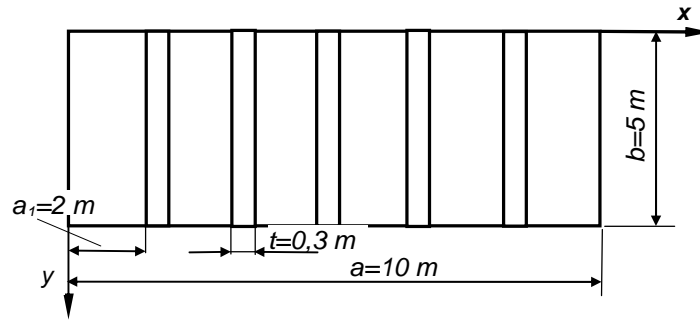


Figure 3.1. Panel reinforced with five ribs in one direction

Canceling the masses and stiffnesses of the ribs on the whole panel, we get an orthotropic plate, the natural frequencies ω_{ij} of which are determined by the formulas [47]

$$\omega_{ij} = \frac{\pi^2}{b^2} \sqrt{\frac{1}{m}} \cdot \sqrt{D_1 \left(\frac{i}{c}\right)^4 + 2D_3 j^2 \left(\frac{i}{c}\right)^2 + D_2 j^4} \quad (3.3)$$

where

D_1, D_2, D_3 - flexural and torsional rigidities of orthotropic plate,

m - mass per unit area,

a, b - the length and the width of the orthotropic plate respectively and $c = a/b$

ω_{ij} - frequency with i number of half sine waves in longitudinal direction and j is the number of half sine wave in transverse direction.

In the case of plate reinforced with symmetrically placed ribs according to Figure 3.1, the rigidities in Eq. (3.3) are as follows [47]

$$D_1 = \frac{E_c a_1 h^3}{12(a_1 - t + \alpha^3 t)}; \quad D_2 = \frac{E_r I}{a_1}; \quad D_3 = 0 \quad (3.4)$$

where

E_c - modulus of elasticity of plate,

E_r - modulus of elasticity of ribs,

a_1 - spacing between ribs,

t - width of the rib,

$\alpha = h/H$ - where h - height of the plate only and H - total height (plate and rib),

I - moment of inertia of equivalent T-beam with width of flange a_1 respect to its centroid

Same orthotropic floor system using discrete calculation scheme as system of the concentrated masses with ten degrees of freedom is given in Figure 3.2.

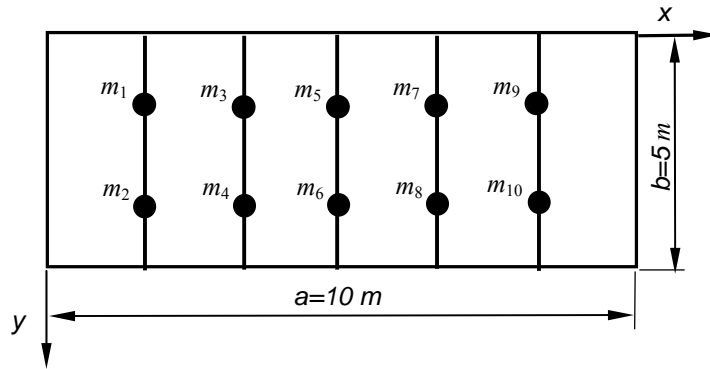


Figure 3.2. Discrete calculation scheme of panel with 10 degrees of freedom

The numerical results of the calculation are given in Table 3.1 and Figure 3.3, where the exact magnitudes [48] are given for comparison.

Table 3.1. Calculated natural frequencies of a panel reinforced with five ribs in rad/s

Nr. of frequency	On orthotropic plate	On discrete scheme	Solution given in [48]
1	61,1	119,2	118,1
2	123,8	126,3	124,9
3	198,6	142,4	139,6
4	224,4	176,4	168,1

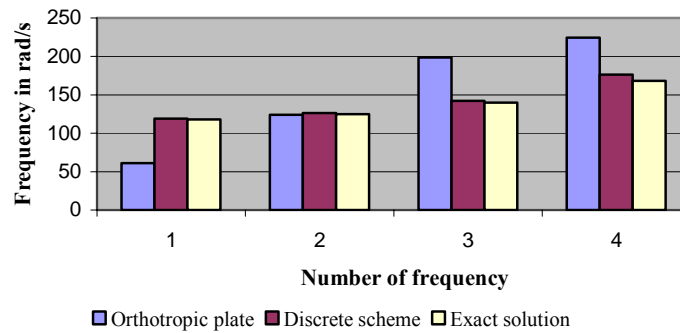


Figure 3.3. Natural frequencies of a panel reinforced with five ribs

It can be seen from Table 3.1 and Figure 3.3 that the calculation using the model of an orthotropic plate gives rather large differences especially for the first frequency. The explanation for this is that for a panel reinforced by ribs placed parallel to each other in one direction the model of an orthotropic plate does not represent the real deformation of such a type of panel.

Let to consider a concrete panel reinforced with four (auxiliary) secondary longitudinal and four main lateral (cross-girder) steel concrete beams given in Figure 3.4. The characteristics of the floor structure are the following: modulus of elasticity: concrete $E_c=2,1 \cdot 10^9$ N/m², reinforcing rod $E_r=200 \cdot 10^9$ N/m², thickness of the plate $h = 0,1$ m, width of the plate $b = 5$ m, length of the plate $a = 10$ m, cross-section of the beams $0,3 \times 0,5$ m².

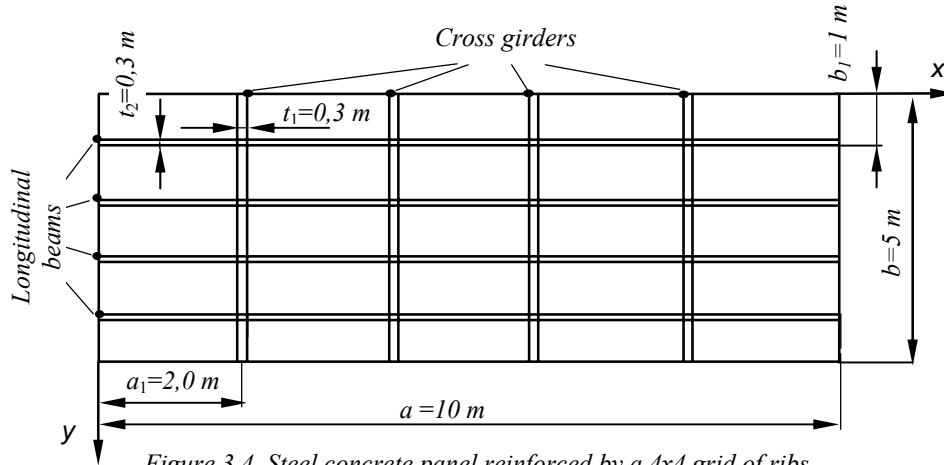


Figure 3.4. Steel concrete panel reinforced by a 4x4 grid of ribs

Canceling the masses and stiffness of the ribs of the whole panel, we get an orthotropic plate. The natural frequencies are calculated by use of Eq. (3.3). In the case of symmetrically placed main and auxiliary beams, the flexural and torsional rigidities in Eq. (3.3) are expressed as follows [47]

$$D_1 = \frac{E_c h^3}{12(1-\nu^2)} + \frac{E_r I_1}{a_1}; \quad D_2 = \frac{E_c h^3}{12(1-\nu^2)} + \frac{E_r I_2}{b_1}; \quad D_3 = \frac{E_c h^3}{12(1-\nu^2)} \quad (3.5)$$

where

I_1, I_2 - moment of inertia of main and auxiliary beams parallel to the x and y -axis respectively

b_1 - spacing of auxiliary beams,

ν - Poisson ratio of plate.

The discrete scheme with sixteen discrete masses concentrated at the nodes of intersection of the cross girders and longitudinal beams is given in the Figure 3.5.

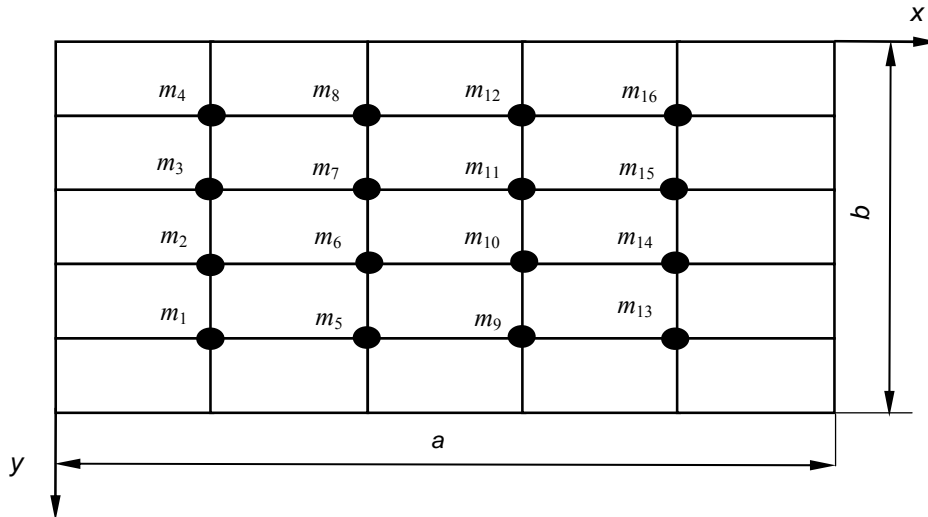


Figure 3.5. Discrete calculation scheme of panel with 16 degrees of freedom

Numerical results of the calculation of natural frequencies using the model of an orthotropic plate are given in Table 3.2 and Figure 3.6. In the same table, the results of the exact solution [48] as well as the results of calculation on the discrete scheme are given.

For notation of natural frequencies ω_{ij} the two-index, numbering is used. Here, the first index i means that a longitudinal beam vibrates in the principal or normal mode of vibration having $(i-1)$ nodes, the second index j means that a lateral (cross girder) beam vibrates in the normal mode with $(j-1)$ nodes. Use of such kind of indexing allows to represent normal modes of a beam supported at two ends as a system of plane lines, which are in sections parallel to the supported contour and create a complicated curved surface of bending with $[(i-1) + (j-1)]$ nodes corresponding to the natural frequency of crossed beams ω_{ij} .

From Table 3.2, we can see that the maximum difference in calculation of the frequencies by theory of an orthotropic plate does not exceed 15 %. This shows that in the case of a panel reinforced with a grid of ribs calculation by the scheme of an orthotropic plate is quite satisfactory.

Table 3.2. Natural frequencies of steel concrete panel reinforced with a 4x4 grid of ribs in rad/s

Nr. of frequency	Normal mode		On orthotropic plate [47]	On discrete scheme	Exact solution on [48]
	<i>i</i>	<i>j</i>			
1	1	1	160,1	154,3	151,3
2	2	1	172,5	171,3	169,8
3	3	1	211,9	220,4	226,6
4	4	1	289,6	322,4	330,4
5	1	2	637,1	615,8	599,7
6	2	2	640,2	627,4	606,1
7	3	2	651,9	639,4	628,2
8	4	2	681,1	691,2	679,3

From Table 3.2 and Figure 3.6, it is seen that the maximum difference in calculation of the frequencies by theory of an orthotropic plate does not exceed 15 %. This shows that in the case of a panel reinforced with a grid of ribs calculation by the scheme of an orthotropic plate is quite satisfactory.

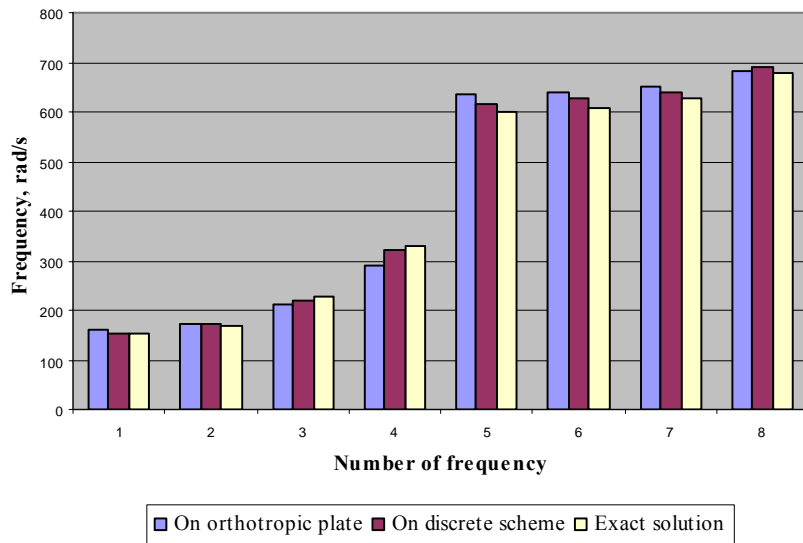


Figure 3.6. Natural frequencies of steel concrete panel reinforced with 4x4 grids of ribs

However, the discrete calculation scheme prescribed in Figure 3.5 in comparison with the model of an orthotropic plate gives results that are more exact. Though the ribs also render essential influence on the values of natural frequencies of the floor, this influence is much less significant, than it is in the case of static calculation of rib floors [47].

3.4 System of crossed beams (ladder frames)

Let us consider ladder frame, which are a widely used structure in the field of industrial and civil buildings, vehicle industry and ship hulls. As an example is represented a frame of 2x2 prescribed in Figure 3.7 with the following characteristics: $I_1=I_2=0,03125 \cdot 10^{-4} \text{m}^4$, $\bar{m}_1 = \bar{m}_2 = 1,1927 \text{ kg/m}$

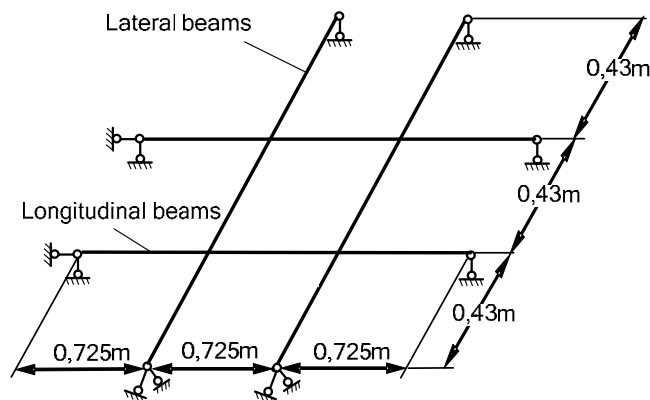


Figure 3.7. System of crossed beams (ladder frame) 2x2

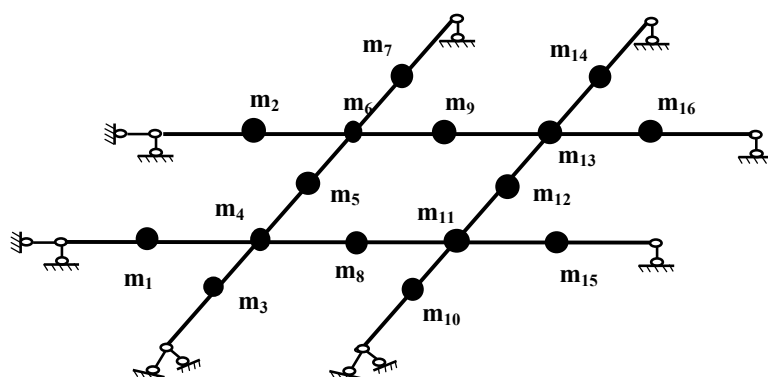


Figure 3.8. Discrete scheme of the 2x2 crossed beams with 16 degrees of freedom

The results of calculation on the scheme of an orthotropic plate are given in Table 3.3 and Figure 3.9. The results of calculation on the discrete scheme with sixteen degrees of freedom prescribed in Figure 3.8 and the so-called exact solution based on the method of dynamic slope and deflection developed in paper I are given as well.

The maximum calculated differences by the scheme of an orthotropic plate do not exceed 26 %. With the growth of frequency number the differences decrease. The exception is the second frequency, for which the difference is greater than for the first frequency. This instability of the calculation error is affected by approximation of the model considered as an orthotropic plate.

Table 3.3. Natural frequencies of crossed beams 2x2, rad/s

Number of frequency	Normal mode		On orthotropic plate [47]	On discrete scheme	On ANSYS	On displacement method Paper I
	<i>i</i>	<i>j</i>				
1	1	1	31,6	26,4	26,5	26,2
2	2	1	66,3	53,7	54,6	52,8
3	1	2	113,9	103,2	105,2	103,2
4	2	2	127,8	110,2	111,4	108,6

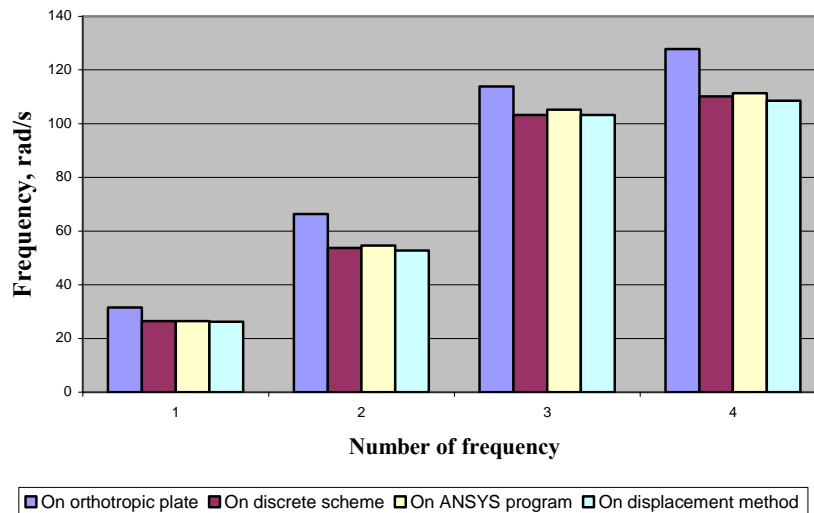


Figure 3.9. Natural frequencies of ladder frame of 2x2

3.5 Calculation of continuous reinforced concrete floor of an industrial building

Let us consider a real reinforced concrete floor designed for a churn machine. A churn machine supported with eight concrete columns and reinforced with six secondary longitudinal beams and four continuous cross girders. The initial data concerning the floor and churn machine is from [35]. The calculation scheme of the floor represents a discrete system of concentrated masses at the nodes of intersection of the longitudinal beams and cross girders and in the middle of spans of the secondary longitudinal beams. The discrete calculation scheme is presented in Figure 3.10.

The magnitudes of the concentrated masses according to a lever rule are from Figure 3.10

$$m_i = 130 \text{ kg}, i = 1 \dots 6, 13 \dots 18, 25 \dots 30, 37 \dots 42$$

$$m_k = 240 \text{ kg}, k = 7 \dots 12, 19 \dots 24, 31 \dots 36, 43 \dots 48.$$

Considering the weight of the churn machine, four additional masses $m_{55} = m_{56} = m_{57} = m_{58} = 81 \text{ kg}$ are located at support points on secondary longitudinal beams accordingly and represented in Figure 3.10. Magnitudes of these masses are not constant values. During the time, when a block butter falling inside the machine drum from height $H = 1,3 \text{ m}$ in $0,51 \text{ s}$, the weight of the churn machine decreases by the value of butter block $G' = 6 \text{ kN}$.

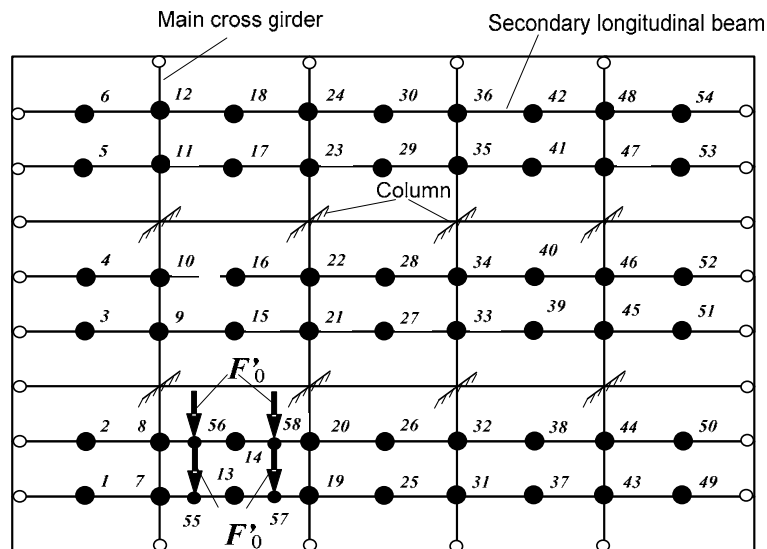


Figure 3.10. Discrete calculation scheme

The magnitudes of the concentrated masses will decrease accordingly and will become $m_{55} = m_{56} = m_{57} = m_{58} = 65,7$ kg, i.e. during vibrations, there is a mass jump of the system. It is known, that in this case, dynamic calculation becomes considerably more complicated. Usually, this requires the use of the approximated calculation, where the change of physical constants of the system happens according to the step law. According to such a method, the dynamic calculation should be carried out with two different spectra of natural frequencies of vibrations of the floor according to different values of the system mass. However, in comparison to the whole mass of the system, the butter block mass falling inside the drum is very small and is 1/150 of the whole mass of the floor. Therefore, the values of frequencies, taking into account the butter mass, will differ from the corresponding values without the account of the weight of the butter no more than 0,3-0,4 %. Therefore, we can presume that the values of additional masses are: $m_{55} = m_{56} = m_{57} = m_{58} = 81$ kg = *const.*

Table 3.4. Values of natural frequencies of reinforced concrete floor, rad/s

No. of frequency		On method [35]	On discrete scheme	Difference in %
Series of frequencies of the basic harmonics	1	24,92	25,09	0,7
	2	25,00	25,38	1,3
	3	-	26,37	0
	4	28,10	28,36	1,0
	5	31,89	32,18	2,5
	6	-	32,85	-
	7	-	33,15	-
	8	35,82	34,57	-2,8
	9	43,00	46,51	7,4
	10	46,13	46,73	1,3
	11	-	47,47	-
	12	53,02	48,60	-9,0
Series of frequencies of second order	13	94,50	96,50	2,1
	14	98,45	97,92	-0,5
	15	-	98,79	-
	16	100,01	99,27	-0,6
	17	106,05	106,85	0,7
	18	-	107,82	-
	19	110,27	108,32	-1,8
	20	120,11	122,33	1,8

The total number of the concentrated masses from Figure 3.10 is 58, i.e. we have the discrete calculation scheme as a system of the concentrated masses with 58 degrees of freedom.

The results of calculation are shown in Table 3.4. In addition, the results received from calculation by [35] are given in this table.

Table 3.4 shows that the values of natural frequencies of the floor calculated by method [35] and discrete calculation scheme are well in coherence. However, use of the discrete calculation scheme gives the more complete spectrum of the frequencies in comparison with the frequency spectrum received by method [35]. This especially concerns frequencies that are close in magnitude, parts of which are missed when calculation are performed by [35].

3.6 Conclusion to the chapter

For floors reinforced by ribs placed parallel to each other in one direction, the model of an orthotropic plate does not represent the real deformation of such type of floors. In the case of floors reinforced with a grid of ribs, the calculation results based on the scheme of an orthotropic plate are quite satisfactory. The discrete calculation scheme provides a more complete spectrum of frequencies in comparison to a spectrum of frequencies received according to [35]. This concerns especially frequencies that are close in magnitude. The study has been shown that using consecutive approximation for refining the width of the top section of the T-beams for determination of the moment of inertias of cross-sections of the beams of the ladder frames gives to the discrete model a satisfactory degree of accuracy.

GENERAL CONCLUSIONS

The generalized conclusions of the work are the following:

1. Coupled flexural-torsional free vibration of ladder frames

- 1.1. The governing differential equations of motion of massive-profiled and thin-walled beam elements with one axis of symmetry has been solved in closed form and nodal end forces and moments has been evaluated. The evaluated nodal end forces and moments were used for calculation of natural frequencies and corresponding mode shapes of ladder frames. In case of massive profiled beams, the effect of shearing force and rotatory inertia was taken into account in differential equation of motion.

- 1.2. It has been established that the value of natural frequencies depends on the position of thin-walled longitudinal and lateral members at the nodes. When shear centers of longitudinal and lateral members of ladder frames coincide (left part of Figure 1-8), then the one constraint on the warping by calculation of the displacement method must be imposed. When shear centers of longitudinal and lateral members of ladder frames are in different plane (right part of Figure 1-8), then two constraints on the warping must be applied. This conclusion is valid for beams with two axis of symmetry too.

- 1.3. It has been established that the values of natural frequencies depend on theory used for calculation of natural frequencies. The values of natural frequencies calculated by theory of massive-profiled beams have lower values compared to natural frequencies calculated by theory of thin-walled beams. The differences of values of natural frequencies grow with growth of the frequency numbers.

- 1.4. The evaluated nodal end moments and forces can be used for theoretical studies of free vibration of ladder frames and for practical calculation of natural frequencies and corresponding mode shapes of ladder frames, especially when higher frequencies are needed. The evaluated nodal end moments and forces can be used for validation of approximate methods of calculation of natural frequencies and mode shapes.

2. Forced vibration of ladder frames under the action of repeated loading.

2.1. An approach for determination of forced response of ladder frames to periodic interrupted loading in presence of hysteretic damping for practical use has been developed. The response of MDOF system to periodic interrupted loading with same sign and opposite sign was solved.

2.2. It has been shown, that by use of frequency independent equivalent viscous damping, it is possible to describe the equation of motion of the system by normal coordinates and to use normal mode method for calculation of forced response of the multi-degree-of-freedom systems to periodic interrupted rectangular loading.

2.3. The expression for determination of steady-state forced vibrations that allow considering only one time interval τ of loading has been devised. It is especially convenient in the case of resonance, when it is enough to take into account only one normal resonance mode.

2.4. The proposed approach can be used for calculation of forced response of ladder frames to periodic interrupted loading.

3. Study of free vibration of ladder frames.

3.1. It has been shown that use of discrete model for calculation of natural frequencies of ladder frames reinforced with plate gives more complete spectrum of frequencies compared to orthotropic plate model.

3.2. It has shown that rigidity of plate can be modeled as top section of T-beam.

3.3. The proposed alternative approach can be used for calculation of natural frequencies of ladder frames reinforced with plate for practical use.

KOKKUVÕTE

RISTTALADEST TASANDRAAMIDE VÕNKUMISED

Risttaladest tasandraamid on laialt levinud toetuskonstruktsioonid, mis võivad olla mingi osa ehitistest, sildadest, laevadest, suurte sõidukite raamidest jne. Paljudel juhtudel on nad koormatud vibratsioonide või siis võnkumisi tekitavate seadmetega või avaldavad neile mõju teised keskkonnategurid, nagu näiteks lained laevadele, liikuvad sõidukid sildadele, teede ebatasasusest tekitatud võnkumised sõiduki raamidele, ehitiste vastupidavus maavärinatele jne. Tunduvalt lihtsam on teostada selliste tasandraamide võnkumiste või vibratsiooni analüüsi nende projekteerimise käigus, kui muuta konstruktsiooni peale nende valmimist. Seetõttu on iseloomulik, et sund- ja vabavõnkumiste analüüs on selliste dünaamiliselt koormatud konstruktsioonide projekteerimise üks lahutamatu osa.

Tasandraamide võnkumiste korral üldistatuna eksisteerib kolm peamist faktorit, mida on võimalik projekteerimise käigus muuta või siis kontrollida ning mis kajastavad tasandraamide võnkumiste iseloomu. Need faktorid on risttalade massid, nende jäikused ja takistusjõudude suurused. Nad määravad ära tasandraamide omavõnkesagedused ja neile vastavad võnkevormid ning on eelkõige olulised resonantside vältimiseks.

Doktoritöö „Risttaladest tasandraamide võnkumised“ keskendub risttaladest koostatud tasandraamide sund- ja vabavõnkumiste erinevate dünaamiliste analüüsides väljatöötamisele.

Käesoleva töö esimeses osas keskendutakse ühe sümmeetriateljega ja jaotatud massiga risttaladest koostatud tasandraamide dünaamilise analüüsi väljatöötamisele massiivsete profiilide ja õhukeseseinaliste profiilide omavõnkesageduste ja neile vastavate võnkevormide arvutamiseks. Massiivsete profiilide võnkumise diferentsiaalvõrrandite lahendamisel on võetud arvesse lõikejõudude ja ristlõike pöörlemise inertsimõju, kuid jäetud arvestamata deplanatsiooni mõju, mille mõju massiivsete profiilide teooria alusel on hüljatavalt väike. Õhukeseseinaliste profiilide võnkumise diferentsiaalvõrrandite süsteemi lahendamisel on jäetud arvestamata risttala väändejäikuse ja sektorialse inertsijõu mõju, selleks et uurida deplanatsiooni mõju tasandraami omavõnkesagedustele risttalade omavahelise erinevates tasandites paiknemise korral.

Võrdluseks on välja toodud ka omavõnkesageduste väärtused arvutatuna õhukeseseinaliste profiilide teooria kohaselt.

Käesoleva töö teises osas keskendutakse mitme vabadusastmega tasandraamide sundvõnkumiste dünaamilise analüüsi väljatöötamisele perioodiliselt muutuva ristküliku kujulise sundkoormuse mõjul, võttes arvesse hüstereetilisi takistusjõudusid.

Töö kolmandas osas keskendutakse risttaladest koostatud ja plaadiga tugevdatud tasandraamide dünaamilise analüüsi väljatöötamisele diskreetsete mudelite alusel. Diskreetse mudeli alusel arvatud omavõnkesagedusi on võrreldud teiste kirjandusallikates avaldatud tulemustega.

Doktoritöö üldistatud järeldused on järgnevad:

1. Jaotatud massiga ja ühe sümmeetriateljega risttaladest moodustatud tasandraamide vabavõnkumised.
 - 1.1 Massiivsete ja õhukeseseinaliste profiilide võnkumiste diferentsiaalvõrrandid on lahendatud kinnisel kujul. Võnkumise diferentsiaalvõrrandi lahendite põhjal on avaldatud ühikpaigutistest põhjustatud kinnitusemomentid ja jõud varda otstes sõltuvalt rajatingimustest, mille põhjal on koostatud tasandraami sõlmede tasakaaluvõrrandid ning leitud omavõnkesagedused ja võnkevormid. Massiivsete profiilide võnkumiste diferentsiaalvõrrandi lahendamisel ja kinnitusemomentide leidmisel ühikpaigutistest on võetud arvesse põikjõu ja ristlõike pöördinertsijõu mõju.
 - 1.2. Uurimise tulemusel on kindlaks tehtud, et õhukeseseinaliste profiilide korral sõltuvad omavõnkesageduste väärtused talade omavahelisest paiknemisest sõlmedes. Kui õhukeseseinaliste profiilide lõikekeskmed paiknevad ühes tasapinnas, siis omavõnkesagedused omavad suuremaid väärtusi, võrreldes profiilidega, mille lõikekeskmed paiknevad erinevates tasandites samade kaalu- ja jäikusomaduste korral. Antud järeldus on kehtiv ka kahe sümmeetriateljega õhukeste profiilide korral.
 - 1.3. On kindlaks tehtud, et omavõnkesageduste väärtused erinevad nende arvutamiseks kasutatavate teooriate vahel. Massiivsete profiilide teooria põhjal arvatud omavõnkesagedused omavad madalamat väärtust kui omavõnkesageduste väärtused arvatuna õhukeseseinaliste profiilide teooria alusel. Erinevus võnkesageduste väärtuses kasvab võnkesageduse numbriga suurenedes.
 - 1.4. Arendatud meetodikat on võimalik kasutada sellise risttaladest moodustatud tasandraamide omavõnkespektri ja vastavate võnkevormide arvutamiseks, kus on nõutavad suuremad täpsused omavõnkesageduste kõrgematel väärtustel, ligilähedaste arvutusmeetodite kontrollarvutusteks, teoreetilisteks eesmärkideks ja praktilisteks arvutusteks. Omavõnkesageduste arvutamise meetodikat massiivsete profiilide teooria lausel on võimalik kasutada selliste risttaladest moodustatud tasandraamide korral, kus põikjõu mõju ei saa hüljata. Omavõnkesageduste arvutamise arendatud meetodikat on võimalik kasutada erinevas tasapinnas paiknevate risttalade omavõnkesageduste määramisel.
2. Risttaladest moodustatud tasandraamide sundvõnkumine perioodiliselt muutuva mitte pideva sundkoormuse mõjul.

2.1 On välja töötatud arvutusmetoodika risttaladest moodustatud tasandraamide sundvõnkumiste määramiseks perioodiliselt muutuva mittepideva ristkülikukujulise sundkoormuse mõjul, arvestades väikeste hüstereetiliste takistusjõududega mitme vabadusastmega süsteemide jaoks.

2.2 On näidatud, et sisemise hõõrdumise teguri asendamine võnkumiste sagedusest mittesõltuva ekvivalentse viskoossusteguriga väikeste hüstereetiliste takistusjõudude korral võimaldab kirjeldada süsteemi liikumisvõrrandeid normaalkoordinaatides ning kasutada modaalanalüüsi mitme vabadusastmega süsteemide sundvõnkumiste amplituudide arvutamiseks.

2.3 On välja toodud lahend mitme vabadusastmega süsteemide jaoks väljakujunenud sundvõnkumiste amplituudide arvutamiseks, arvestades ainult ühte sundkoormuse mõju perioodi ja võnkevormi resonantsile lähedaste sageduste korral.

2.4. Väljatöötatud diskreetseid skeeme on võimalik kasutada praktilisteks risttaladest moodustatud tasandraamide sundvõnkumiste amplituudide määramiseks: stantside ja hüdropresside aluskonstruktsioonid, laevade mootorite aluskonstruktsioonid, sõidukite sundvõnkumised auklikel teedel jne.

3. Plaatidega tugevdatud risttaladest moodustatud tasandraamide vabavõnkumised.

3.1. On näidatud, et diskreetsete mudelite kasutamine plaatidega tugevdatud tasandraamide korral laialdaselt kasutatava ortotroopse plaadi asemel annab täiuslikuma omavõnkesageduste spektri.

3.2. On näidatud, et plaadi mõju risttaladele võib asendada täiendava horisontaalse võõna, mille laiuse määramiseks kasutatakse järkjärgulise lähene-mise meetodit.

3.3 Ortotroopsete plaatide diskreetseid mudeleid on võimalik kasutada plaatidega tugevdatud tasandraamide omavõnkesageduste arvutamiseks praktilistel eesmärkidel.

Doktoritöö antud käsitluse keskseks teemaks on risttaladest moodustatud tasandraamide omavõnkesageduste ja omavõnkevormide määramine. Esimene osa võimaldab määrata tasandraamide omavõnkesageduste nn. „täpsustatud“ väärtusi, kuna need baseeruvad jaotatud massiga talade ristlõike liikumise diferentsiaalvõrrandite kinnistel lahendustel. Antud tulemused võimaldavad hinnata diskreetsetes mudelites kasutatavate diskreetsete masside arvu ja asukohtasid, mida kasutatakse antud doktoritöö teises ja kolmandas osas.

REFERENCES

- [1] Eslimy-Isfahany, S.H.R, Banerjee, J.R. 2000. Use of generalized mass in the interpretation of dynamic response of bending-torsion coupled beams. *J. of Sound and Vibration*, **238**(2), pp. 295-308. doi:10/1006 /jsvi.2000.3160.
- [2] Tseytlin, Y., M. 2006. *Structural Synthesis in Precision Elasticity*. Springer Science + Business Media, Inc. ISBN 10:0-387-25156-1.
- [3] Timoshenko, S., Young D., H. 1974. *Vibration Problems in Engineering. 4ed.* John Wiley & Sons. ISBN 0-471-87315-2.
- [4] Vlasov, V., Z. 1961. *Thin-walled Elastic Beams*. Israel Program of Scientific Translations Ltd. Published by ProQuest 2007.
- [5] Hallauer W.L., Liu R.Y. 1982. Beam bending-torsion dynamic stiffness method for calculation of exact vibration modes. *J. of Sound and Vibration*, **85**, pp. 105-113.
- [6] Friberg, P.O. 1983. Coupled vibration of beams - an exact dynamic element stiffness matrix. *Int. J. of Numerical Methods in Engineering*, **19**, pp. 479-493.
- [7] Dokumaci, E. 1987. An exact solution for coupled bending and torsion vibrations of uniform beams having single cross-sectional symmetry. *J. of Sound and Vibration*, **119**, pp. 443-459.
- [8] Bishop, R.E, Cannon, S.M, Miao S. 1989. On coupled bending and torsional vibration of uniform beams. *J. of Sound and Vibration*, **131**, pp. 457-464.
- [9] Friberg, P.O. 1985. Beam element matrices derived from Vlasov's theory of open thin-walled elastic beams. *Int. J. of Numerical Methods in Engineering*, **21**, pp. 1205-1228.
- [10] Leung, A.Y. 1992. Dynamic stiffness analysis of thin-walled structures. *Thin-walled Structures*, **14**, pp. 209-222.
- [11] Banerjee, J. R., William, F. W. 1994. An exact dynamic stiffness matrix for coupled extensional-torsional vibration of structural members, *Computers and Structures*, **50**, pp. 161-66.

- [12] Banerjee, J. R., William, F. W. 1994. Coupled bending-torsional dynamic stiffness matrix for an axially loaded Timoshenko beam element. *Int. J. of Solid and Structures*, **31**, pp. 749–762.
- [13] Wittrick WH, Williams FW. 1971. A general algorithm for computing natural frequencies of elastic structures. *The Quarterly J. of Mech. and Applied Math.*, **24(3)**, pp. 263-284; doi:10.1093/qjmam/24.3.263.
- [14] Banerjee, J.R. 1999. Explicit frequency equation and mode shapes of cantilever beam coupled in bending and torsion. *J. of Sound and Vibration*, **224(2)**, pp. 267-281.
- [15] Li J., Shen R., Hua H., Jin X. 2003. Coupled bending and torsional vibration of axially loaded Bernoulli-Euler beams including warping effect. *Applied Acoustics*, **65**, pp. 153-170. doi: 10.1016/j.apacoust. 2003.07.06.
- [16] Li J., Shen R., Hua H., Jin X. 2004. Coupled bending and torsional vibration of axially loaded thin-walled Timoshenko beams. *Int. J. of Mechanical Science*, **46**, pp. 299-320. doi:10.1016/j.ijmecsci.2004. 02.009.
- [17] Senjanovich, I., Catipovich, I., Tomaševich, S. 2007. Coupled flexural and torsional vibrations of ship-like girders. *Thin-Walled Structures*, **45**, pp. 1002-1021. Elsevier,doi:10.1016/j.tws. 2007.07.013.
- [18] Megson, T., H., G. 1974. *Linear Analysis of Thin-Walled Elastic Structures*. Halsted Press, A division of John Wiley & Sons. ISBNB 0-470-59035-1.
- [19] Han S., M, Benaroya H., Wei, T. 1999. Dynamics of transversely vibrating beams using four engineering theories. *J. of Sound and Vibration*, **225(5)**, pp. 935-988.
- [20] Mendez-Sanchez R., A., Morales A. 2005. Flores J. Experimental check on the accuracy of Timoshenko's beam theory. *J. of Sound and Vibration*, **279**, pp. 508–512. doi:10.1016/j.jsv.2004.01.050.
- [21] Stephen N., G., Puchegger S. 2006. On the valid frequency range of Timoshenko beam theory. *J. of Sound and Vibration*, **297**, pp. 1082–1087. doi:10.1016/j.jsv.2006.04.020.

- [22] Senjanovich, I., Catipovich, I., Tomaševich, S. 2008. Coupled horizontal and torsional vibrations of flexible barge. *J. of Engineering Structures*, **30**, pp. 93-109. doi:10.1016/j.engstruct.2007.03.08.
- [23] Kelly G., S. 1993. *Fundamentals of Mechanical Vibrations*. McGraw-Hill, Inc. ISBN 0-07-911533-0.
- [24] Beards C., F. 1997. *Structural Vibration*. John Wiley & Sons. ISBN-0-470-23586-1.
- [25] Muravskii, G. B. 2004. On frequency independent damping. *J. of Sound and Vibration*, **274**, pp. 653–668. doi:10.1016/j.jsv.2003.05.012.
- [26] Gounaris, G., D., Antonakakis, E., Papadopoulos, E., A. 2007. Hysteretic damping of structures vibrating at resonance. *J. of Computers and Structures*, **85**, pp. 1858–1868. doi:10.1016/j.compstruc.2007.02.026.
- [27] Chen, K., F., Zhang, S., W. 2008. On the impulse response precursor of an ideal linear hysteretic damper. *J. of Sound and Vibration*, **312**, pp. 576–583. doi:10.1016/j.jsv.2007.07.091.
- [28] Henwood, D.J. 2002. Approximating the hysteretic damping matrix by viscous matrix for modeling in the time domain. *J. of Sound and Vibration*, **254(3)**, pp. 575-593. doi:10.1006/jsvi.2001.4136.
- [29] Tsai, H., C., Lee, T., C. 2002. Dynamic analysis of linear and bilinear oscillators with rate-independent damping. *J. of Computers and Structures*, **80**, pp. 155–164.
- [30] Harris, C., M. *Shock and Vibration Handbook*. 1993. McCraw-Hill Publishing Company, New York. ISBN-0070268010.
- [31] Zienkiewicz, O.C., Taylor, R.C. 2005. *Finite Element Method for Solid and Structural Mechanics*, 6th Ed. Butterworth-Heinemann. ISBN 0750663219.
- [32] Koloushek, V. 1973. *Dynamics of Engineering Structures*. Butter-worths, London. ISBN-0408701609.

- [33] Aryassov, G. 1995. Discrete models for the dynamic analysis for constructions of particular type. *Proc. of Int. Symp. of Modern Problems of Dynamics and Seismology of Structures*, pp. 14-15.
- [34] Meirovitch, L. 1967. *Analytical Methods in Vibrations*. Prentice Hall, ISBN 0-02-380140-9.
- [35] Sorokin E.S. 1966. *Instruction for Calculation of Floors Under Action of Impulse*. Stroizdat, Moscow.
- [36] Nei, S., F., G.G. Kulkarni, G., G. 1972. On the transverse free vibration of beam-slab type highway bridges. *J. of Sound and Vibration*, **21**, pp. 249–261.
- [37] Balendra, T., Shanmugam, N., E. 1985. Free vibration of plated structures by grillage method. *J. of Sound and Vibration*, **99**, pp. 333-350.
- [38] Liew, K.M., Wang, C.M. 1993. Rayleigh–Ritz method for general plate analysis. *Engineering Structures*, **15 (1)**, pp. 55–60.
- [39] Xiang, Y., Wang, C.M., Kitipornchai, S., Liew, K.M. 1994. Buckling of triangular Mindlin plates under isotropic inplane compression. *Acta Mechanica*, **102 (1–4)**, pp. 123–135.
- [40] Long, B.R. 1971. A stiffness-type analysis of the vibration of a class of stiffened plates, *J. of Sound and Vibration*, **16**, pp. 323–335.
- [41] Aksu, G., Ali, R. 1976. Free vibration analysis of stiffened plates using finite difference method, *J. of Sound and Vibration*, **48**, pp. 15–25.
- [42] Mukherjee, A., Mukhopadhyay, 1988. M. Finite element free vibration of eccentrically stiffened plates, *J. of Computers and Structures*, **30 (6)**, pp. 1303–1317.
- [43] Zeng, H., Bert, C.W. 2005. A differential quadrature analysis of vibration for rectangular stiffened plates. *J. of Sound and Vibration*, **241**, pp. 247–252. doi:10.1006/jsvi.2000.3295.
- [44] Peng, L.X., Liew, K.M, Kitipornchai; S. 2006. Buckling and free vibration analyses of stiffened plates using the FSDT mesh-free method. *J. of Sound and Vibration*, **289**, pp. 421–449, doi:10.1016/j.jsv. 2005.02.023.

- [45] Grice, R.M., Pinnington, R.J. 2000. A method for vibration analysis of built-up structures. Part 1. *J. of Sound and Vibration*, **230(4)**, pp. 825-849. doi: 10.1006/jsvi.1999.2657.
- [46] Sapountzakis, E.J., Katsikadelis, J.T. 2000. Elastic deformation of ribbed plates under static, transverse and inplane loading. *J. of Computers and Structures*, **74**, pp. 571-581.
- [47] Vainberg, D., Vainberg, E., D. 1970. *Calculation of plates*. Budivelnic, Kiev.
- [48] Filippov, A., P. 1970. *Vibrations of Deformed Systems*, Machinostroenie, Moscow.
- [49] Engelbrecht, J., Henrych, I. 1971. The Calculation of Natural Frequencies of Circular Grillages with Straight Bars. Transactions of the Slovenia Academy of Sciences, No. 7, pp. 519-546.
- [50] Aryassov, G. 1997. *Consideration of Resisting Forces in Vibration of Mechanical Systems*. Tallinn, TUT Press.
- [51] Gounaris G., D, Anifantis N., K. 1999. Structural damping determination by finite element approach. *J. of Computers and Structures*, **73**, pp. 445-452.

Paper I

Aryassov, G., Petritshenko, A. 2007. Advanced dynamic models for analysis of ladder frames. *Annals of DAAAM for 2007 & Proceedings of the 18th International DAAAM Symposium*, Editor B. Katalinic, Published by DAAAM International, Vienna, Austria, pp. 565-566. ISBN 3-901509-58-5, ISSN 1726-9679.

ADVANCED DYNAMIC MODELS FOR ANALYSIS OF LADDER FRAMES

PETRITSHENKO, A[ndres] & ARYASSOV, G[ennadi]*

Abstract: The aim of this paper is to introduce an alternative method for calculating free vibration of ladder frame construction. Ladder frame constructions are widely used in trailers industry and are used especially as floor structures of trailers. Prediction of vibration behaviour of ladder frames of trailers provides valuable information in evaluating durability or reliability quantities in design process of trailers.

Key words: Bending – Torsion Vibrations, Trailers Floor Construction, Displacement method

1. INTRODUCTION

One of the most common structures in design of ladder frames are orthogonal grillages (systems of crossed beams attached at the nodes) consisting of uniform straight beams of both massive and thin-walled structural shapes. The system considered in this paper is made up of two orthogonal sets of beams strongly attached to each other at the nodes so that bending and torsion moments are transmitted from one set to the other. This system then can be considered as a 3D model for studying bending-torsion vibration of grillages.

This paper studies the bending-torsion vibrations of orthogonal grillages consisting of uniform straight beams of both massive and thin-walled structural shapes. The free vibration analysis of grillages as a continuous system is carried out by the displacement method (Filippov 1970), (Koloushek 1967).

Depending on the required precision, effect of shearing force and rotatory inertia on the free vibrations of grillages can either be excluded or included in the composition of the canonical equations that arise with this displacement method. Symmetry in the plane of the grillages is taken into account, as long as the system is made up of two orthogonal sets of beams. Symmetry allows us to represent a determinant of the displacement method equations as a product of four determinants and to obtain four independent frequency equations.

2. BASIC CALCULATION PARAMETERS

2.1 Massive cross-section beam

The differential equations of bending - torsion vibrations of a straight uniform beam (Fig.1) having one axis of symmetry are decomposed to two independent systems (Vlasov 1957), one of which

$$EI_x \frac{\partial^4 \eta(z,t)}{\partial z^4} + \frac{\gamma A}{g} \frac{\partial^2 \eta(z,t)}{\partial t^2} - \left(\frac{\gamma I_x}{g} + \frac{EI_x \gamma}{gk'_x G} \right) \frac{\partial^4 \eta(z,t)}{\partial z^2 \partial t^2} + \frac{\gamma^2 I_x}{g^2 k'_x G} \frac{\partial \eta(z,t)}{\partial t^4} = 0 \quad (1)$$

describes the transverse bending vibrations in the plane of symmetry and another one

$$EI_y \frac{\partial^4 \xi(z,t)}{\partial z^4} - \left(\frac{\gamma I_y}{g} + \frac{EI_y \gamma}{gk'_y G} \right) \frac{\partial^2 \xi(z,t)}{\partial z^2 \partial t^2} + \frac{\gamma A}{g} \frac{\partial^2 \xi(z,t)}{\partial t^2} + \frac{\gamma^2 I_y}{g^2 k'_y G} \frac{\partial^4 \xi(z,t)}{\partial t^4} + a_y \frac{\gamma A}{g} \frac{\partial^2 \theta(z,t)}{\partial t^2} = 0 \quad (2)$$

$$a_y \frac{\gamma A}{g} \frac{\partial^2 \xi(z,t)}{\partial t^2} + EI_\phi \frac{\partial^4 \theta(z,t)}{\partial z^4} - GI_d \frac{\partial^2 \theta(z,t)}{\partial z^2} - \frac{\gamma I_\phi}{g} \frac{\partial^4 \theta(z,t)}{\partial z^2 \partial t^2} + r^2 \frac{\gamma A}{g} \frac{\partial^2 \theta(z,t)}{\partial t^2} = 0$$

determines the bending-torsion vibrations, where $\xi(z, t)$ and $\eta(z, t)$ are deflections of the beam in the horizontal and vertical planes accordingly, $\theta(z, t)$ is a angle of rotation, EI_x and EI_y are flexural rigidity, γ is a material specific weight, a_y is a coordinate of bending centre, GI_d is a torsion rigidity, k'_x and k'_y are coefficients of cross section form for shearing force, A is a cross-sectional area; I_ϕ is a geometrical characteristic (bimoment of inertia), r is a geometrical parameter, EI_ϕ is a sectorial rigidity [6]. The solutions of Eq. (2) are

$$\xi(z) = C_1 \sinh \lambda_{1\xi} \frac{z}{l} + C_2 \cosh \lambda_{1\xi} \frac{z}{l} + C_3 \sin \lambda_{2\xi} \frac{z}{l} + C_4 \cos \lambda_{2\xi} \frac{z}{l} + C_5 \sin \lambda_{3\xi} \frac{z}{l} + C_6 \cos \lambda_{3\xi} \frac{z}{l} \quad (3)$$

$$\xi(z) = C_1 \rho_1 \sinh \lambda_{1\xi} \frac{z}{l} + C_2 \rho_1 \cosh \lambda_{1\xi} \frac{z}{l} + C_3 \rho_2 \sin \lambda_{2\xi} \frac{z}{l} + C_4 \rho_2 \cos \lambda_{2\xi} \frac{z}{l} + C_5 \rho_3 \sin \lambda_{3\xi} \frac{z}{l} + C_6 \rho_3 \cos \lambda_{3\xi} \frac{z}{l}, \quad (4)$$

$$\text{where } \rho_i = a_y \omega^2 \gamma A / g \left(GI_d \frac{\lambda_{i\eta}^2}{l^2} + \frac{r^2 \gamma \omega^2}{g} \right), \quad (i=1, 2, 3)$$

are characteristics of principal modes of vibration. Referring to Eq. (3,4) the basic parameters of the slope deflection method can be easily derived.

2.2 Thin-walled cross-section

The differential equations of bending-torsional vibrations of thin-walled beam having one axis of symmetry (Fig.2) can be obtained from Eq. (1) and Eq. (2) by substituting I_ϕ for I_ω (Vlasov 1957). Here I_ω is the sectorial moment of inertia. One of these equations determines the bending vibration in the plane of symmetry, solution of which is analogous to the solution of Eq. (1). The system describes the joint bending-torsional vibrations under the conditions of constrained warping of cross section. Following a well-known procedure, we write $\xi(z,t) = \xi(z) \sin \omega t$, $\theta(z,t) = \theta(z) \sin \omega t$, where $\xi(z)$ and $\theta(z)$ are amplitudes of assumed harmonic vibration. Hence

$$\begin{aligned}
& EI_y \frac{d^4 \xi(z)}{dz^4} - \frac{\gamma A \omega^2}{g} \xi(z) + \frac{\gamma I_y}{g} \omega^2 \frac{d^2 \xi(z)}{dz^2} - \\
& - \frac{a_y \gamma A}{g} \omega^2 \theta(z) = 0, \\
& EI_\omega \frac{d^4 \theta(z)}{dz^4} - GI_d \frac{d^2 \theta(z)}{dz^2} + \frac{\gamma I_\omega}{g} \omega^2 \frac{d^2 \theta(z)}{dz^2} - \\
& - \frac{r^2 \gamma A \omega^2}{g} \theta(z) - \frac{d_y \gamma A \omega^2}{g} \xi(z) = 0
\end{aligned} \tag{5}$$

Neglecting torsional stiffness GI_d and rotatory inertia (Aryassov 1995), the solutions of Eq. (5) has the form

$$\begin{aligned}
\xi(z) &= C_1^* \cos \lambda_1^* \frac{z}{l} + C_2^* \sin \lambda_1^* \frac{z}{l} + C_3^* \cosh \lambda_1^* \frac{z}{l} + C_4^* \sinh \lambda_1^* \frac{z}{l} + \\
&+ C_5^* \cos \lambda_2^* \frac{z}{l} + C_6^* \sin \lambda_2^* \frac{z}{l} + C_7^* \cosh \lambda_2^* \frac{z}{l} + C_8^* \sinh \lambda_2^* \frac{z}{l}, \\
\theta(z) &= C_1^* \rho_1^* \cos \lambda_1^* \frac{z}{l} + C_2^* \rho_1^* \sin \lambda_1^* \frac{z}{l} + C_3^* \rho_1^* \cosh \lambda_1^* \frac{z}{l} + \\
&+ C_4^* \rho_1^* \sinh \lambda_1^* \frac{z}{l} + C_5^* \rho_2^* \cos \lambda_2^* \frac{z}{l} + C_6^* \rho_2^* \sin \lambda_2^* \frac{z}{l} + \\
&+ C_7^* \rho_2^* \cosh \lambda_2^* \frac{z}{l} + C_8^* \rho_2^* \sinh \lambda_2^* \frac{z}{l}
\end{aligned} \tag{6}$$

Referring to Eq. (3), (4) and (5), below we can obtain the nodal forces of the slope deflection method: the bending moment M , the shearing force Q , the bending-torsional bimoment B , and the general moment L .

3. CALCULATION OF GRILLAGES BY DISPLACEMENT METHOD

3.1 Case of massive-profiled beam

According to the displacement method we can compose for each node (z, x) of a grillage three equations of equilibrium of bending moments and shearing forces

$$\sum_{i,j} M_{ij}^x = 0, \quad \sum_{i,j} M_{ij}^z = 0, \quad \sum_{i,j} Q_{ij} = 0 \tag{7}$$

Effect of shearing force and rotatory inertia are included and aft excluded in the composition of the canonical equations. In the last case the nodal forces will be functions of one frequency parameter. When effect of shearing force and rotatory inertia are included in the composition of the canonical equations, the nodal end-forces will be functions of two frequency parameters λ_1 and λ_2 . Equalizing the determinant of homogeneous equations of displacement method to zero we obtain a frequency equation, from which can be determined the frequency spectrum of required length.

3.2 Case of thin-walled beams

In the case of thin-walled beams there exists the deflection in the plane of symmetry, transverse deflection and the warping of nodes. As the conditions of conjunction according to the warping at the nodes there are two not well-defined antipodal cases are considered: (I) cross-sections of beams adjoining to the nodes are being warping equally and (II) cross-sections of beams adjoining to the nodes are being warping independently to each other and have different mode.

In the first case the warping of node can be determined by one unknown. For each node (z, x) of a grillage can be obtained four equations of equilibrium

$$\sum_{i,j} M_{ij}^x = 0, \quad \sum_{i,j} M_{ij}^z = 0, \quad \sum_{i,j} Q_{ij} = 0, \quad \sum_{i,j} B_{ij} = 0 \tag{8}$$

In the second case the warping of the nodes can be determined by two unknowns. Then for each node (z, x) of a grillage can be obtained five equations of equilibrium

$$\sum_{i,j} M_{ij}^x = 0, \quad \sum_{i,j} M_{ij}^z = 0, \quad \sum_{i,j} Q_{ij} = 0, \quad \sum_{i,j} B_{ij}^x = 0, \quad \sum_{i,j} B_{ij}^z = 0 \tag{9}$$

These equations are correct either for beams having one axis of symmetry and for beams having two axes of symmetry.

4. CONCLUSION

The analysis has been shown that natural frequencies of vibration of the grillage consisting of thin-walled beams essentially differ from appropriate frequencies of the system with massive-profiled beams at identical bending and torsion characteristics of cross-section. The maximum difference of the values of frequencies takes place, when calculations by the theory of thin-walled beams have been executed taking into account of one constraint imposed on the warping of a node. The greater bending stiffness of the beams gives the greater difference between the values of natural frequencies, but it concerns of grillages consisting of thin-walled beams of channel section having one plane of symmetry, when two constraints on the warping of a node are imposed. It was defined that with the growth of frequency number the difference of the values of frequencies is increased and can achieve 12...16 per cent.

Investigation of the free vibrations of the systems consisting of thin-walled beams has shown that for nodal conjunctions where longitudinal and cross girders are in the same plane of the system, therefore on the calculation by the displacement method on the warping one constraint must be imposed. However in the case of nodal conjunctions, when beams are in different planes of the system, two constraints must be applied. Results are obtained in previous analysis give the possibility to estimate accuracy of approximate calculations (Aryassov et al., 1999), (Aryassov 1995) and (Engelbrecht & Henrych 1971). The results of theoretical investigations can be used for design of road train trailers with floor structures consisting of uniform straight beams of massive and thin-walled structural shapes both.

5. REFERENCES

- Aryassov, G., Pappel, T. and Teder, L. *Theoretical Experimental Investigation of Grillages Vibration under the Action of Repeated Loading*, OST 99 Symp. On Machine Design, Stockholm, 1999, pp.165-174.
- Aryassov, G. *Discrete Models for the Dynamic Analysis for Constructions of Particular Type*, Proceeding of Intern. Symp. Of Modern Problems of Dynamics and Seismology of Structures, St. Petersburg, 1995, pp. 14-15.
- Engelbrecht, I. and Henrych, J. *The Calculation of Natural Frequencies of Circular Grillages with Straight Bars*, Transactions of the Slovenia Academy of Sciences, Bratislava, 1971, nr.7, pp. 519-546.
- Filippov, A.P. (1970). *Vibrations of deformed systems*, 712 p., Machinostroenie, Moscow, (in Russian).
- Koloushek, V. *Dynamic of Civil Engineering*, SVTL, 650 p., Bratislava, 1967.
- Vlasov, V.Z. *Thin-walled elastic beams*. Publisher of physics and mathematics, Moscow, 1957, 566 p. (in Russian).

Paper II

Aryassov, G., Petritshenko, A. 2008. Forced vibration of ladder frames under the action of repeated loading. *Proceedings of 6th International Conference of DAAAM Baltic INDUSTRIAL ENGINEERING*, Ed. R. Kyttner, 24-26 April 2008, Tallinn, Estonia, pp. 25-30

FORCED VIBRATION OF LADDER FRAMES UNDER THE ACTION OF REPEATED LOADING

Aryassov, G; Petritshenko, A

Abstract: *In this paper, the forced vibration of ladder frames under the action of repeated interrupted loading are studied. This problem has not been yet considered in sufficient detail and width in technical and scientific literature. Often vibration of ladder frames under the action of instant impulses or periodical harmonic force has been considered. To solve a problem, a discrete scheme of concentrated masses with multi-degrees of freedom is proposed. More complex calculation schemes can lead to significant errors in the calculation; therefore, simplified discrete schemes based on experimental tests are used.*

Key words: Vibration, Discrete Scheme, Grillages, Repeating Loading, Experiment.

1. INTRODUCTION

In this paper, a discrete scheme of concentrated masses with multi-degrees of freedom is considered. The solution of problem is given via formulas applicable for computer calculation. The dynamic lateral deflections of grillages in any interval of loading and pure forced periodical displacements, which are repeated in every time interval, are determined. The problem is solved with and without taking into account the resisting forces. A survey of the experimental investigation of free and forced vibrations of grillages is given as well. A description of experimental mounting allowing receiving repeated loading of final duration is presented. The experimental results are in good agreement

with the theoretical values taking into account the discrete scheme.

2. FORCED VIBRATION

Discrete scheme of grillages is represented in (Fig. 1) and it consists for simplicity of system with four masses concentrated at the nodes of lateral and longitudinal crossing beams with $r = n \cdot m$ degrees of freedom, where n – number of lateral beams, m – number of longitudinal beams. From Fig. 1, $n = m = 2$.

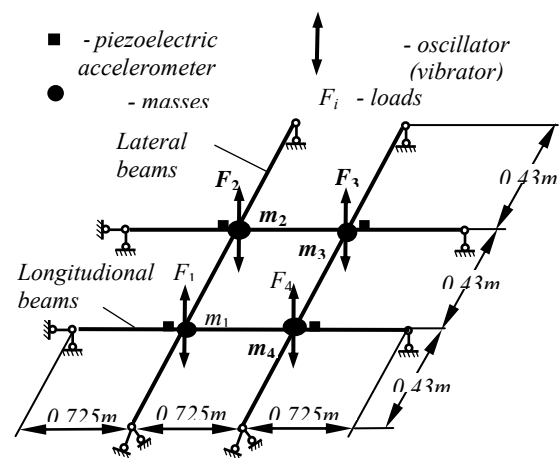


Fig. 1. Scheme of loading of grillages in general

It is assumed that loads are applied to these concentrated masses. Such formulation of the problem does not change a general solution, because any load can be reduced to the points of concentration of the masses [3, 4]. Latest holds even in conditions, when real disturbing forces are absent and support excitations occur. Structural damping and internal friction due to imperfect elasticity of vibrating bodies are

the main factors of damping in the grillages. In general, structural damping depends on the definite type of construction and must be determined for every case separately. In this paper, it is assumed that structural damping and internal friction due the imperfect elasticity are linear. Therefore, for simplification of calculations it is accepted that the viscous damping factor γ is independent of frequency of cyclical strains, and includes the losses of structural damping.

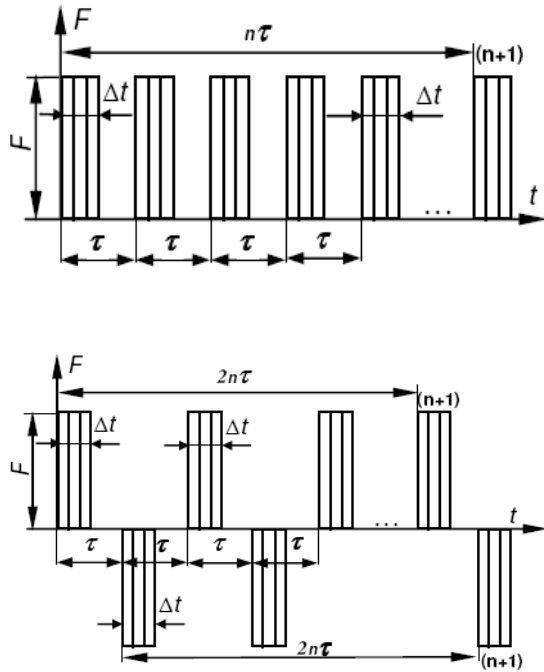


Fig. 3. Periodical repeated loading of the opposite sign

Differential equations of forced vibrations taking into account resisting forces according to Sorokin's complex internal friction theory [3] are

$$m_k \ddot{y}_k^*(t) + (u + iv) \sum_{j=1}^r C_{kj} y_j^*(t) = F_k \quad (1)$$

$(k=1, 2, 3, \dots, r)$

where

$$u = \frac{1 - \gamma^2/4}{1 + \gamma^2/4}, \quad v = \frac{\gamma}{1 + \gamma^2/4} \quad (2)$$

y_k^* – complex displacement of k^{th} mass,
 C_{kj} – stiffness coefficient of system, γ – internal friction factor.

In practical problems, it can be assumed with sufficient accuracy that small resisting forces do not affect the frequencies and the modes of vibration. In this case, the load can be resolved into components of normal modes of vibrations (normal mode method) [2]. Thus by use of normal modes we reduced the coupled equations of forced vibrations of a multi-degrees of freedom to a set of uncoupled equations, each involving just a single degree of freedom. Moreover, for sufficiently small damping and the region far from resonance we can neglect the phase difference between the separate vibrating masses of system and their normal modes. Such an approach gives the possibility to get convenient expressions for computer calculation.

By integration of Eq.1 and taking into account, that initial conditions (displacements and velocities) are null, we obtain the expression for determining the displacements after $(n+1)^{\text{th}}$ load application

$$y_k(t) = u \sum_{i=1}^r \left[\frac{y_{ki} \sum_{j=1}^r F_j y_{ji}}{\omega_i^2 \sum_{j=1}^r m_j y_{ji}^2} (A_i^* - B_i^*) \right] \quad (3)$$

where A_i^* and B_i^* – trigonometrical functions

$$A_i^* = \sum_{v=0}^n \exp \left[-\frac{\gamma}{2} \omega_i (t - v\tau - \Delta t) \right] (-1)^v \cdot \left\{ \cos \omega_i (t - v\tau - \Delta t) + \frac{\gamma}{2} \sin \omega_i (t - v\tau - \Delta t) \right\} \quad (4)$$

$$B_i^* = \sum_{v=0}^n \exp \left[-\frac{\gamma}{2} \omega_i (t - v\tau) \right] (-1)^{v+1} \cdot \left[\cos \omega_i (t - v\tau) + \frac{\gamma}{2} \sin \omega_i (t - v\tau) \right]$$

keeping in mind that the multipliers $(-1)^v$ and $(-1)^{v+1}$ in A_i^* and B_i^* in case of the repeated loading of the same sign are always equal to one.

3. CALCULATION EXAMPLE

Consider the calculation example of the grillages 2x2 given in Fig.1, where force F_1 is applied to mass m_1 only. The masses of longitudinal and lateral beams per unit length are $\bar{m}_x = \bar{m}_y = 1.1927$ kg/m, moments of inertia of the beams are $I_x = I_y = 0.03125 \cdot 10^{-8}$ m⁴, four equal masses $m_1 = m_2 = m_3 = m_4 = 1.3775$ kg, concentrated in the crossing nodes of the beams. The periodical repeated load $F_1=29.7$ N was applied to mass m_1 (Fig.1), the duration of loading was $\Delta t = 0.08$ s, the interval between the repeated loading was $\tau = 0.5$ s. The normal mode method requires the natural frequencies and modes of free vibrations to be known.

Taking into consideration the discrete scheme with four degrees of freedom, we received the following natural frequencies of the grillages: $\omega_1 = 28.6$ s⁻¹, $\omega_2 = 53.3$ s⁻¹, $\omega_3 = 104.0$ s⁻¹, $\omega_4 = 112.0$ s⁻¹ and normal mode characteristics of vibrations

Table 1. Normal mode characteristics of vibrations

$y_{11} = 1$	$y_{21} = 1$	$y_{31} = 1$	$y_{41} = 1$
$y_{12} = 1$	$y_{22} = 1$	$y_{32} = -1$	$y_{42} = -1$
$y_{13} = 1$	$y_{23} = -1$	$y_{33} = 1$	$y_{43} = -1$
$y_{14} = 1$	$y_{24} = -1$	$y_{34} = -1$	$y_{44} = 1$

Substituting these values into the Eq. 4, we can obtain the magnitudes of forces vibrations in any interval of load action.

The calculation results for mass m_1 are depicted graphically in Figs. 4 and 5.

The graphs of forced vibrations with different internal friction factor γ showed that due to damping the displacements become smaller.

Such big influence of damping on the vibration displacements can be explained by the small duration Δt of the load in comparison with the time interval τ between repeating loading (Fig. 2). In consequence, the system vibrates freely for the large part of time interval τ and due to

presence of damping, the decaying of free vibrations occurs even faster.

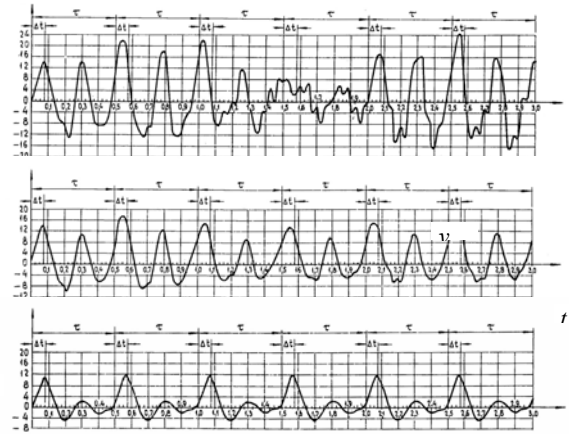


Fig. 4. Forced vibrations of mass m_1 taking into account the all principal modes with different internal friction factory: a - $\gamma = 0$; b - $\gamma = 0.06$; c - $\gamma = 0.2$.

If the duration of loading $\Delta t > 2.5T_1$, where $T_1 = 2\pi/\omega_1$ - the period of the first frequency of structure, then calculation will be reduced to the static one with equivalent load μF_1 , where $\mu = 2$ for sudden loading and $\mu = 1$ in the case of sudden unloading. However, if the duration of the loading $\Delta t < 0.1T_n$, where $T_n = 2\pi/\omega_n$ is the period of the highest frequency in spectrum of natural frequencies (the first order harmonics), then calculation will be reduced to the calculation for the instant impulses. If the period between repeated loadings is $\tau > 2T_1/\gamma$, then calculation is for the single impulse. From this, we can conclude that when $0.1T_n \leq \Delta t \leq 2.5T_1$ and $\Delta t \leq \tau \leq 2T_1/\gamma$ the displacements under the action of repeating loading are determined by Eq. 3.

In order to find out how the highest modes (the second order harmonics) influence the displacement magnitudes, calculation was carried out taking account the first two modes only. The calculation results are given in Fig.5. It can be seen that these results are not up to much differ from those

on Fig.4, where all r normal modes of vibration were taken into account.

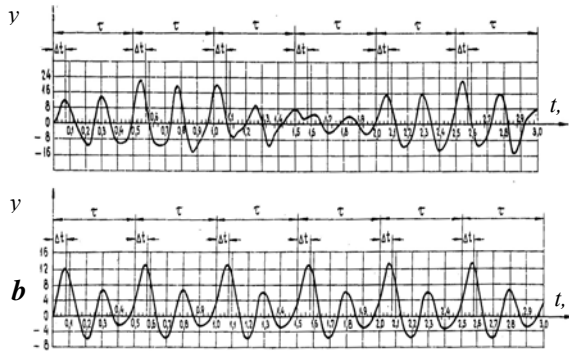


Fig. 5. Forced vibration of mass m_1 taking into account different frictional factors of two principal modes

However, in the case of resonance when the system has maximum displacements it is not enough to use the first two modes only. The necessity to take into account also the highest modes of vibrations is explained by the fact that frequency spectrum of grillages is not continuous, but has isolated zones with highly packed frequencies [3, 4]. In addition, frequency values do not increase so quickly with the total number of frequencies. Absent of some these frequencies can lead to errors in calculations.

4. PURE PERIODICAL FORCED VIBRATION

It is seen from the graphs of the forced vibrations in Fig. 5, that after some time stationary forced vibrations are established. In typical case, the vibrations excited by suddenly applied periodical loading are not periodical.

However, for simplification of solution the vibrations can be represented as a sum of periodical stationary vibrations with the period of exciting load τ and free vibrations. The free vibrations caused by the presence of the initial conditions and action of repeated loading take place only for the initial transitive period of movement. After some time vibrations were gradually damped out due to resisting

forces and finally pure force periodical vibrations were established. Such problem has already been discussed for systems with one and two degrees of freedom [1-3]. In this paper, this problem was extended to the system with multiple degrees of freedom.

Taking into account fore mentioned simplifications and resolving the load into normal modes of vibration (the normal mode method), and then each mass displacement of the discrete scheme (Fig.1) in any interval τ of loading for each single mode of natural vibrations separately may be represented in the following form

$$y_{ki}(t) = \exp\left(-\frac{\gamma}{2}\omega_i t\right) \cdot \left[y_{ki}(0) \cos \omega_i t + \frac{\gamma}{2} \frac{\omega_i y_{ki}(0)}{\omega_i} \cdot \sin \omega_i t \right] + (5) + y_{ki}^*(t^*)$$

$(i, k = 1, 2, 3, \dots, r),$

where the first two terms of this solution represent free vibrations depending on the initial conditions, but the third term represents vibrations produced by loading in the given time interval $0 \leq t^* \leq \tau$.

In order to ensure, that the pure periodical repeated vibrations occur in each time interval, we compared the displacements and velocities of masses at the beginning and the end of the interval for the each single mode of natural vibrations separately $y_{ki}(0) = y_{ki}(\tau)$,

$\dot{y}_{ki}(0) = \dot{y}_{ki}(\tau)$, $(i, k = 1, 2, 3, \dots, r)$. Then it is possible to form two equations for the each mode separately, from which the initial conditions of the periodical vibration were determined. The total displacements of system in any time interval taking into account all modes of vibrations with zero initial conditions are following

$$\begin{aligned}
y_k(t) = & -\sum_{i=1}^r \exp\left(-\frac{\gamma}{2}\omega_i t\right) \\
& \left[y_{ki}(0)\cos\omega_i t + \frac{y_{ki}(0) + \frac{\gamma}{2}\omega_i \dot{y}_{ki}(0)}{\omega_i} \cdot \sin\omega_i t \right] + \\
& + \sum_{i=1}^r \exp\left(-\frac{\gamma}{2}\omega_i t^*\right) \\
& \left[y_{ki}(0)\cos\omega_i t^* + \frac{y_{ki}(0) + \frac{\gamma}{2}\omega_i \dot{y}_{ki}(0)}{\omega_i} \cdot \sin\omega_i t^* \right] + \sum_{i=1}^r y_{ki}^*(t^*) \\
& (k = 1, 2, 3, \dots, r),
\end{aligned} \tag{6}$$

where $y_{ki}(0)$, $\dot{y}_{ki}(0)$ - the initial conditions of the pure periodical vibrations the first two terms express free vibrations of system, the last three – the pure periodical vibrations.

In the case of loading with different sign (Fig.3), the problem was solved by means of summing up the two solutions in the Eq. 5), but with the second solution evaluated by replacing t by $(t - \tau)$.

Comparing calculation results, it is seen good correlation, especially in the case of large resistance. It is so because with increasing of resistance the influence of free vibrations is decreased. These vibrations are determined by the first two terms in Eq. 5 for the total displacements.

5. DESCRIPTION OF THE EXPERIMENTAL MOUNTING AND MEASURING METHOD

The experimental mounting represents the system of crossed beams (grillages) the scheme and the sizes of which are given on Figure 1.

The beams are made of steel bars of mark S235 in accordance with the standard EN-10025 with rectangular cross-section 3x0.5 cm and having at the ends cylindrical hinges. Bolts the tension of which can be regulated connect the lateral and longitudinal beams to each other. The support designs were made The beams are hinged at their ends to a massive rectangular frame of standard I beams IPE20 with precision providing minimum friction and excluding vibration and appearance of axial forces in the beams.

For exciting vibration of grillages, two types of equipment were used. One of them creates a harmonic force produced by misbalanced rotor and was used in determination of frequencies of free vibration only and to ensure reliable results. The second type of the exciter is a permanent electromagnet creating of repeated interrupted loading. The operation of the electromagnet was carried out with help of an electronic relay, which allowed adjusting the duration of loading Δt from 0.01 up to 0.16 s and period between the repeated loadings from 0.05 up to infinity. Four piezoelectric accelerometers were used (Fig. 1).

The vibration analyzer SigLab 20.22A was used for measurements with special software in MATLAB, designed for multi-channel investigations of vibroacoustic signals in the frequency band from 2 Hz to 50 kHz.

6. TEST RESULTS

Free vibration. For determination of natural frequencies and modes of vibrations, the resonant method was used. The vibration of grillages was excited by harmonic and repeated interrupted loading. The experimental results for repeated interrupted loading are submitted in table 2 where for comparisons are given results of the theoretical study, which has been carried out with the different calculation schemes.

Table 2. Natural frequencies of the grillages 2x2 [s^{-1}].

N of frequency	Experiment	On discrete scheme	Exact solution
1	25.4	28.6	26.2
2	53.8	53.3	52.8
3	102.8	104.0	102.4
4	109.6	112.0	108.6

The results of theoretical calculation carried out with taking into account the discrete scheme with four degrees of

freedom (Fig.1) are in good correlation with the experimental results and with results of exact solution which is based on the method of slopes and deflections [4], [5]. The generalized internal friction factor γ also was determined. Its magnitude for the given design was within the range 0.06 - 0.11.

Forced vibration. The amplitudes of forced vibrations were measured with the help of the optical instruments, the state-pencils and piezoelectric accelerometers and the oscillograph, which records electrical vibrations on a film. A system factor was determined for decoding the oscillograms of vibrations taking into account sensitivity of all elements of the vibration measurement apparatus. On Fig.6 are shown the results of experiments and theoretical calculation for forced vibrations of mass m_1 . There is good correlation of the experimental and theoretical results.

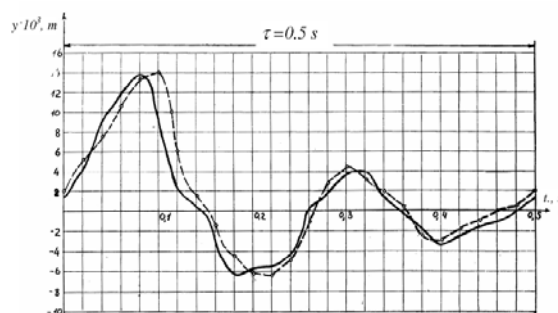


Fig. 6. Experimental and theoretical displacements of mass m_1 in interval τ

7. CONCLUSION

The discrete calculation scheme is given which determines with a sufficient degree of accuracy the forced vibrations of grillages under the action of repeated interrupted loading. It is necessary to take into account resisting forces determined by internal friction factor γ independent of frequency of cyclical strains. The magnitude of the factor γ is common for the whole system and was accepted according to the first mode of vibrations.

We devised the expressions for determining pure periodical forced

vibrations that allow considering only one time interval τ of loading. Such solution is especially convenient in the case of resonance when it was enough to take into account only one normal resonance mode. Experimentally and theoretically has been shown that the frequency spectrum of such structure of grillages has zones, where frequency values are close to each other, but normal modes corresponding to them are different. Absent of some these frequencies can lead to errors in calculations.

The experimental mounting and method for experimental investigations of vibrations of grillages was worked out. The comparison of experimental data with results of theoretical investigation shows their good correlation.

It was established that we can use generalized internal friction factor γ taking into account structural damping. Obtained experimental magnitude of the generalized factor γ was within 0.06-0.11 that correlate with magnitudes used in theoretical calculation.

8. REFERENCES

1. Timoshenko, S. *Vibration Problems in Engineering*. Princeton 1975.
2. Shock and Vibration Handbook edited by CYRIL M.Harris, 3d ed., Mc Craw-Hill Book Company, 1312 p., New York, 1993.
3. Koloushek, V. *Dynamic of Civil Engineering*, Bratislava, 1967.
4. Aryassov, G. Discrete Models for the Dynamic Analysis for Constructions of Particular Type, Proc. of Int. Symp. of Modern Problems of Dynamics and Seismology of Structures. 1995, 14-15.
5. Engelbrecht, I., Henrych, J. The Calculation of Natural Frequencies of Circular Grillages with Straight Bars. Transactions of the Slovenia Academy of Sciences, 1985, 7, 519-546.

Paper III

Aryassov, G., Petritshenko, A. 2009. Study of free Vibration of Ladder Frames Reinforced with Plate. *Solid State Phenomena*, **147-149**, pp. 368-373. doi: 10.4208/www.scientific.net/ SSP.147-149.368.

Study of Free Vibration of Ladder Frames Reinforced with Plate

Gennadi Aryassov^{1, a}, Andres Petritshenko^{1, b}

¹Ehitajate tee 5; Tallinn, 19086, Estonia

^agarjasov@staff.ttu.ee, ^bpetritsenko@hotmail.com

Keywords: free vibration, ladder frames, orthotropic system, discrete schemes, displacement method

Abstract. The aim of this paper is to develop a simplified method for analysis of free vibration of floor system consisting of continuous steel plate and steel frame in plane to reinforce it. The study of such orthotropic system is of practical interest and aimed at small businesses, which are not able to obtain expensive programs for performing such calculations.

Introduction

Floor systems that consist of continuous steel or concrete panel and steel frame in plane to reinforce it are very widely used in industrial and civil buildings and the vehicle industry. Examples of this kind of orthotropic system in vehicles industry are floor systems of tipping bodies of trucks and trailers, where bottom of tipping bodies consists of high wear resistant cold rolled metal sheets in general and these are reinforced with steel frame. In the field of industry and civil buildings, concrete floor with reinforcing ribs can be considered as orthotropic floor system. Most common structures of reinforcing steel frames are orthogonal grillages consisting of uniform straight beams of massive and/or thin-walled structural shapes. Covering steel or concrete plates enlarge rigidity of reinforcing frames or vice versa and so alter vibrational characteristics of all design. Taking into account that reinforcing frames, which might consist of beams with different cross-sectional dimensions and can be in plane or one beam can be situated above another, then analytical calculation of free vibrations of such floor design is a quite complex calculation problem.

In most cases, calculations of free vibration are performed using the model of orthotropic plate. It leads to canceling out reinforcing frames and to the problem of calculation of stiffened plate [1]. Model of orthotropic plate does not represent real deformations of system, so calculated natural frequencies for orthotropic plate using this model differ from exact values within the range of 5% up to 70%.

In this paper, a discrete model for calculation of natural frequencies of orthotropic floor systems is proposed. In case of discrete model, orthotropic floor system is replaced by system of crossed beams (grillages) stiffened locally by plate and the last one as continuous system is replaced by the discrete system of concentrated masses.

Calculations by fore aft mentioned models are executed on real industrial floor systems to compare calculation results with existing data. In this case, orthotropic floor system consists of concrete plate with reinforcing ribs. Discrete model of orthotropic floor design leads to calculation of grillages and effect of the plate is taken account using T-beams instead of ribs. Rigidity of plate is represented by top section of T-beam. Determination of the proper dimensions of this top section has not been solved up today. For determination the size of top section, consecutive approximations are necessary. For assessing the accuracy of considered models, the displacement method (slope deflection method) for continuous system [2, 3] of floor design and ANSYS program is used. Although for examples are used floor system, which consist of concrete plates and reinforcing steel ribs, calculations by discrete scheme can be extended to orthotropic floor systems, which consist of steel plates and frames to reinforce them.

Basic concept of discrete scheme

Equations of the free vibrations of a discrete system with n^{th} degrees of freedom have the form [4]

$$\sum m_i \delta_{ij} \ddot{y}_i(t) + \ddot{y}_i(t) = 0, \quad (j=1,2, \dots, n). \quad (1)$$

where

m_i - value of i^{th} concentrated mass,

y_i - displacement of i^{th} concentrated mass,

δ_{ij} - unit displacements of system at the points of application of the concentrated masses.

The static calculation is performed on ANSYS program. Calculation of free vibrations was carried out for two models of the orthotropic floor system. In calculation by model of orthotropic plate the joint deformation work of the plate and beams were taken into account. In calculation by discrete scheme instead of orthotropic plate a system of crossed beams is considered. To determine values of moment of inertia of cross-sections of main and auxiliary beams, the influence of plate is represented as rectangular cross-section with proper dimensions. After calculation of the unit displacements δ_{ij} , the problem of calculation of natural frequencies and normal modes of the floor is reduced to a problem of eigenvalues and eigenvectors

$$(B - \lambda E) \bar{y} = 0. \quad (2)$$

where

\bar{y} - a column vector,

λ - frequency parameter,

B - square matrix, received as a result of multiplication of the matrix of unit displacements δ_{ij} with the matrix of concentrated masses m_i ,

E - the unit matrix.

For the solution of Eq. 2, a method of simultaneous iteration or direct iteration [4] and MatLab, MathWorks programs are used.

Calculation of rib floors as an orthotropic plate

Let us consider a simply supported concrete panel (floor) reinforced with five ribs. The floor has the following characteristics: the module of elasticity of concrete $E_c = 2.1 \cdot 10^9 \text{ N/m}^2$, thickness of the panel $h = 0.1 \text{ m}$, width of the panel $b = 5 \text{ m}$, length of the panel $a = 10 \text{ m}$, density of concrete $\gamma_c = 24 \text{ kN/m}^3$, cross section of the ribs $0.3 \times 0.5 \text{ m}^2$. Dimensions of floor are given in Fig. 1.

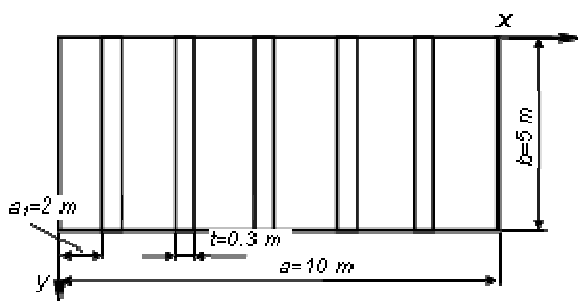


Fig. 1. Panel reinforced with five ribs in one direction

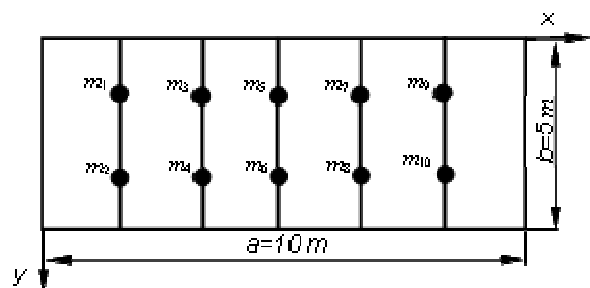


Fig. 2. Discrete calculation scheme of panel with 10 degrees of freedom

Canceling the masses and stiffnesses of the ribs on the whole panel, we get an orthotropic plate, the natural frequencies ω_{ij} of which are determined by the formulas [1]. Same orthotropic floor

system using discrete calculation scheme as system of the concentrated masses with ten degrees of freedom is given in Fig. 2.

The numerical results of the calculation are given in Table 1, where the exact magnitudes [4] are given for comparison.

N of frequency	On orthotropic plate	On discrete scheme	Exact solution on [5]
1	61.1	119.2	118.1
2	123.8	126.3	124.9
3	198.6	142.4	139.6
4	224.4	176.4	168.1

Table 1. Calculated natural frequencies of a panel reinforced with five ribs [s⁻¹]

It can be seen from Table 1 that the calculation using the model of an orthotropic plate gives rather large errors especially for the first frequency. The explanation for this is that for a panel reinforced by ribs placed parallel to each other in one direction the model of an orthotropic plate does not represent the real deformation of such a type of panel.

Let us consider a concrete panel reinforced with four (auxiliary) secondary longitudinal and four main lateral (cross-girder) steel concrete beams given in Fig. 3. Characteristics of floor structure are following: modulus of elasticity: concrete $E_c=21 \cdot 10^9$ N/m², reinforcing rod $E_r=200 \cdot 10^9$ N/m², thickness of the plate $h = 0,1$ m, width of the plate $b = 5$ m, length of the plate $a = 10$ m, cross-section of the beams 0.3×0.5 m².

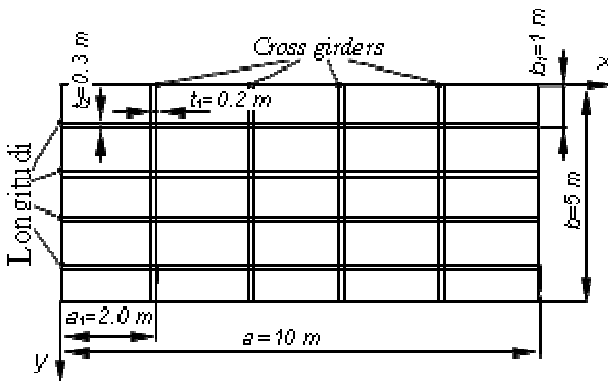


Fig. 3. Steel concrete panel reinforced by a 4x4 grid of ribs

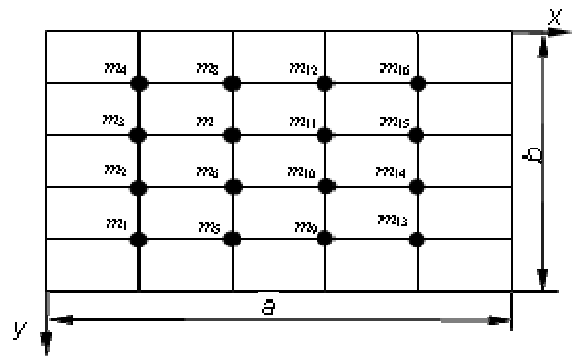


Fig. 4. Discrete calculation scheme of panel with 16 degrees of freedom

Canceling the masses and stiffness of the ribs of the whole panel, we get an orthotropic plate. The discrete scheme with sixteen discrete masses concentrated at the nodes of intersection of the cross girders and longitudinal beams is given on Fig. 4. Numerical results of the calculation of natural frequencies using the model of an orthotropic plate are given in Table 2. In the same table, the results of exact solution [4] as well as the results of calculation on the discrete scheme are given. For notation of natural frequencies ω_{ij} the two-index, numbering is used. Here first index i means that a longitudinal beam vibrates in the principal or normal mode of vibration having $(i-1)$ nodes, the second index j means that a lateral (cross girder) beam vibrates in the normal mode with $(j-1)$ nodes. Use of such kind of indexing allows to represent normal modes of a beam supported at two ends as system of plane lines, which are in sections parallel to the supported contour and create a complicated curved surface of bending with $[(i-1) + (j-1)]$ nodes corresponding to the natural frequency of crossed beams ω_{ij} .

From Table 2, we can see that the maximum error in calculation of the frequencies by theory of an orthotropic plate does not exceed 15 %. This shows that in the case of a panel reinforced with a grid of ribs calculation by the scheme of an orthotropic plate is quite satisfactory.

N of frequency	Normal mode		On orthotropic plate	On discrete scheme	Exact solution on [5]
	<i>i</i>	<i>j</i>			
1	1	1	160.1	154.3	151.3
2	2	1	172.5	171.3	169.8
3	3	1	211.9	220.4	226.6
4	4	1	289.6	322.4	330.4
5	1	2	637.1	615.8	599.7
6	2	2	640.2	627.4	606.1
7	3	2	651.9	639.4	628.2
8	4	2	681.1	691.2	679.3

Table 2. Natural frequencies of steel concrete panel reinforced with a 4x4 grid of ribs [s^{-1}]

From Table 2, we can see that the maximum error in calculation of the frequencies by theory of an orthotropic plate does not exceed 15 %. This shows that in the case of a panel reinforced with a grid of ribs calculation by the scheme of an orthotropic plate is quite satisfactory.

However, the discrete calculation scheme prescribed in Fig. 4 in comparison with the model of an orthotropic plate gives results that are more exact. Though the ribs also render essential influence on the values of natural frequencies of the floor, this influence is much less significant, than it is in the case of static calculation of rib floors [1].

System of crossed beams

Let us consider a ladder frame, which is common structure in design of tipper and trailer's floor systems. For example is represented a system of crossed beams 2x2 prescribed in Fig.5 with the following characteristics [5]:

$$I_1=I_2=0.03125 \cdot 10^{-4} \text{m}^4, \bar{m}_1 = \bar{m}_2 = 1.1927 \text{ kg/m}$$

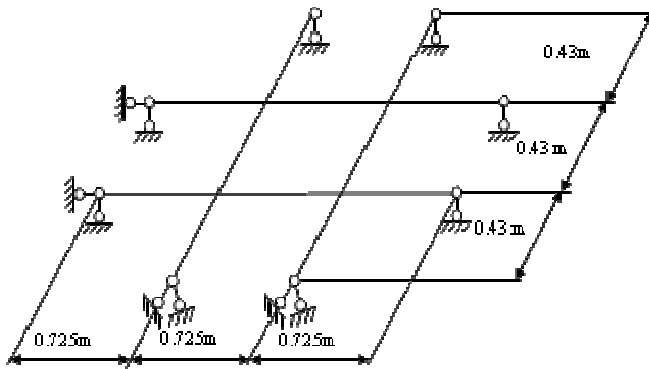


Fig. 5. System of crossed beams 2x2

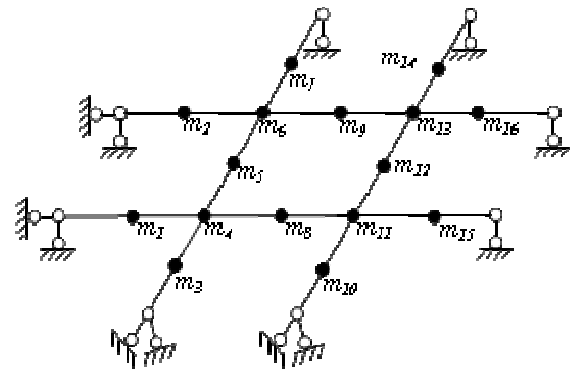


Fig. 6. Discrete scheme of the 2x2 crossed beams with 16 degrees of freedom

The results of calculation on the scheme of an orthotropic plate are given in Table 3. The results of calculation on the discrete scheme with sixteen degrees of freedom prescribed in Fig. 6 and the exact solution based on the method of dynamic slope and deflection [3] are given as well.

The maximum calculation error by the scheme of an orthotropic plate does not exceed 26 percent. With the growth of frequency number the calculation error decreases. The exception is the second frequency, for which the calculation error is greater than the calculation error for the first frequency. This instability of the calculation error is affected by approximation of the model considered as an orthotropic plate.

Number of frequency	Normal mode		On orthotropic plate	On discrete scheme	On ANSYS	On displacement method [2,3]
	i	j				
1	1	1	31.6	26.4	26.5	26.2
2	2	1	66.3	53.7	54.6	52.8
3	1	2	113.9	103.2	105.2	103.2
4	2	2	127.8	110.2	111.4	108.6

Table 3. Natural frequencies of system of crossed beams 2x2 [s⁻¹]

Calculation of continuous reinforced concrete floor of an industrial building

Let us consider a real reinforced concrete floor designed for a churn machine. Churn machine supported with eight concrete columns and reinforced with six secondary longitudinal beams and four continuous cross girders. The initial data concerning the floor and churn machine is from [6]. The calculation scheme of the floor represents a discrete system of concentrated masses at the nodes of intersection of the longitudinal beams and cross girders and in the middle of spans of the secondary longitudinal beams. Discrete calculation scheme is presented in Fig. 7.

The magnitudes of the concentrated masses according to a lever rule are from Fig. 7

$$m_i = 130 \text{ kg}, i=1\dots6, 13\dots18, 25\dots30, 37\dots42$$

$$m_k = 240 \text{ kg}, k=7\dots12, 19\dots24, 31\dots36, 43\dots48.$$

Considering the weight of the churn machine, four additional masses $m_{55} = m_{56} = m_{57} = m_{58} = 81$ kg are located at support points on secondary longitudinal beams accordingly and represented in Fig. 7. Magnitudes of these masses are not constant values. During the time, when a block butter falling inside the machine drum from height $H = 1.3$ m in 0.51 s, the weight of churn machine decreases by the value of butter block $G'=6$ kN. The magnitudes of the concentrated masses will accordingly decrease and will become $m_{55} = m_{56} = m_{57} = m_{58} = 65.7$ kg, i.e. during vibrations, there is a mass jump of the system. It is known, that in this case, dynamic calculation becomes considerably more complicated. Usually, this requires the use of the approximated calculation, where the change of physical constants of the system happens according to the step law. According to such method, the dynamic calculation should be carried out with two different spectra of natural frequencies of vibrations of the floor according to different values of the system mass. However, in comparison to the whole mass of the system, the butter block mass falling inside the drum is very small and is 1/150 of the whole mass of the floor. Therefore, the values of frequencies, taking into account the butter mass, will differ from the corresponding values without the account of the weight of the butter no more than 0.3-0.4 %. Therefore, we can presume that the values of additional masses are: $m_{55} = m_{56} = m_{57} = m_{58} = 81 \text{ kg} = \text{const}$.

The total number of the concentrated masses from Fig. 7 is 58, i.e. we have the discrete calculation scheme as a system of the concentrated masses with 58 degrees of freedom. The results of calculation are shown in Table 4. In addition, results received from calculation by [6] are given in this table. The comparisons of the natural frequencies, which have been determined by these two methods, are shown.

Table 4 shows that the values of natural frequencies of the floor calculated by method [6] and discrete calculation scheme are well in coherence. However, use of discrete calculation scheme gives the more complete spectrum of the frequencies in comparison with the frequency spectrum received by method [6]. This especially concerns frequencies that are too close in magnitude, part of which is missed when calculating by [6].

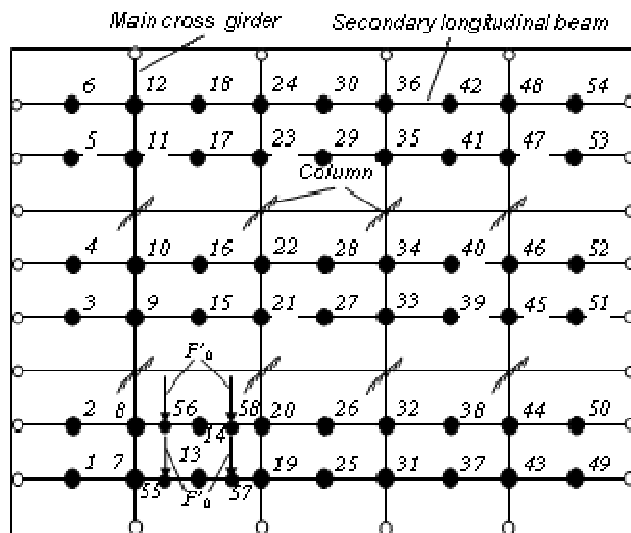


Fig. 7. Discrete calculation scheme of floor

No. of frequency	On method [6]	On discrete scheme	Error in %	
Series of frequencies of the basic harmonics	1	24.92	25.09	0.7
	2	25.00	25.38	1.3
	3	-	26.37	0
	4	28.10	28.36	1.0
	5	31.89	32.18	2.5
	6	-	32.85	-
	7	-	33.15	-
	8	35.82	34.57	-2.8
	9	43.00	46.51	7.4
	10	46.13	46.73	1.3
	11	-	47.47	-
	12	53.02	48.60	-9.0
Series of frequencies of second order	13	94.50	96.50	2.1
	14	98.45	97.92	-0.5
	15	-	98.79	-
	16	100.01	99.27	-0.6
	17	106.05	106.85	0.7
	18	-	107.82	-
	19	110.27	108.32	-1.8
	20	120.11	122.33	1.8

Table 4. Values of natural frequencies of reinforced concrete floor [s^{-1}]

Conclusion

For floors reinforced by ribs placed parallel to each other in one direction, the model of an orthotropic plate does not represent the real deformation of such type of floors. In the case of floors reinforced with a grid of ribs calculation results on the scheme of an orthotropic plate is quite satisfactory. However, the discrete calculation scheme gives results that are more exact. On the discrete calculation scheme, we receive a more complete spectrum of frequencies in comparison with a spectrum of frequencies received according to [6] and even in calculations performed by ANSYS program. This concerns especially frequencies that are too close in magnitude. The study has been shown that using consecutive approximation for refining the width of the top section of the T-beams for determination of the moment of inertias of cross-sections of the beams of the grillages gives to discrete model satisfactory degree of accuracy. Results of theoretical study by discrete method will be proved in future by experiments.

References

- [1] D. V. Vainberg, E. D. Vainberg: *Calculation of plates*. Budivelnic, Kiev,(1970).
- [2] G. Aryassov, A.Petritshenko: *Advanced Dynamic Models for Analysis of Ladder Frames*, Ann. DAAAM Proc. Int. DAAAM Symp, Vol 18, No 1 (2007), pp. 565-566
- [3] I. Engelbrecht, J. Henrych: *The Calculation of Natural Frequencies of Circular Grillages with Straight Bars*. Transactions of the Slovenia Academy of Sciences, nr.7, pp. 519-546, Bratislava.(1971)
- [4] A. P. Filippov: *Vibrations of deformed systems*, 712 p., Machinostroenie, Moscow, (1970).
- [5] G. Aryassov, T. Pappel and L. Teder: *Theoretical Experimental Investigation of Grillages Vibration under the Action of Repeated Loading*, OST 99 Symp. On Machine Design, Stockholm, pp.165-174. (1999)
- [6] Sorokin E.S.: *Instruction for calculation of floors under action of impulse*. Stroizdat, Moscow, (1966).

ELULOOKIRJELDUS (CV)

1. Isikuandmed

Ees- ja perekonnanimi	Andres Petritšenko
Sünniaeg ja -koht	02.08.1969 Tallinn
Kodakondsus	Eesti
Perekonnaseis	Abielus
Lapsed	Kätlin (sünd. 1993), Katrin (sünd. 1996)

2. Kontaktandmed

Aadress	Puhangu 59-7, Tallinn, 10316
Telefon	50 76 055
E-posti aadress	petritsenko@hotmail.com

3. Hariduskäik

<i>Õppeasutus</i>	<i>Lõpetamise aeg</i>	<i>Haridus</i>
Tallinna Tehnikaülikool	1993	Autod ja autondus/diplomeeritud mehaanikainsener
Tallinna Ehitus- ja Mehaanikatehnikum	1988	Autode hooldus ja remont/ tehnik-mehaanik
Tallinna 24. Keskkool	1988	Algharidus

4. Keelteoskus

Eesti	Kõrgtase
Vene	Keskase
Inglise	Keskase
Soome	Keskase

5. Teadustöö põhisuunad

Sund- ja vabavõnkumised metallkonstruktsioonides

CURRICULUM VITAE

1. Personal data

Name	Andres Petritšenko
Date and place of birth	02.08.1969 Tallinn
Citizenship	Eesti
Family status	Married
Children	Kätlin (born 1993), Katrin (born 1996)

2. Contact

Address	Puhangu 59-7, Tallinn, 10316
Phone	+ 372 50 76 055
E-mail	petritsenko@hotmail.com

3. Education

<i>Educational institution</i>	<i>Graduated</i>	<i>Speciality</i>
Tallinn University of Technology	1993	Diploma engineer
Tallinn Technical High School	1988	Mechanical engineer
Tallinna 24. Keskkool	1988	Elementary education

4. Language skills

Estonian	Advanced
Russian	Intermediate
English	Intermediate
Finnish	Intermediate

5. Main research interest

Free and forced vibration of planar frames

**DISSERTATIONS DEFENDED AT
TALLINN UNIVERSITY OF TECHNOLOGY ON
*MECHANICAL AND INSTRUMENTAL ENGINEERING***

1. **Jakob Kübarsepp**. Steel-bonded hardmetals. 1992.
2. **Jakub Kõo**. Determination of residual stresses in coatings & coated parts. 1994.
3. **Mart Tamre**. Tribocharacteristics of journal bearings unlocated axis. 1995.
4. **Paul Kallas**. Abrasive erosion of powder materials. 1996.
5. **Jüri Pirso**. Titanium and chromium carbide based cermets. 1996.
6. **Heinrich Reshetnyak**. Hard metals serviceability in sheet metal forming operations. 1996.
7. **Arvi Kruusing**. Magnetic microdevices and their fabrication methods. 1997.
8. **Roberto Carmona Davila**. Some contributions to the quality control in motor car industry. 1999.
9. **Harri Annuka**. Characterization and application of TiC-based iron alloys bonded cermets. 1999.
10. **Irina Hussainova**. Investigation of particle-wall collision and erosion prediction. 1999.
11. **Edi Kulderknup**. Reliability and uncertainty of quality measurement. 2000.
12. **Vitali Podgurski**. Laser ablation and thermal evaporation of thin films and structures. 2001.
13. **Igor Penkov**. Strength investigation of threaded joints under static and dynamic loading. 2001.
14. **Martin Eerme**. Structural modelling of engineering products and realisation of computer-based environment for product development. 2001.
15. **Toivo Tähemaa**. Assurance of synergy and competitive dependability at non-safety-critical mechatronics systems design. 2002.
16. **Jüri Resev**. Virtual differential as torque distribution control unit in automotive propulsion systems. 2002.
17. **Toomas Pihl**. Powder coatings for abrasive wear. 2002.
18. **Sergei Letunovitš**. Tribology of fine-grained cermets. 2003.
19. **Tatyana Karaulova**. Development of the modelling tool for the analysis of the production process and its entities for the SME. 2004.
20. **Grigori Nekrassov**. Development of an intelligent integrated environment for computer. 2004.
21. **Sergei Zimakov**. Novel wear resistant WC-based thermal sprayed coatings. 2004.
22. **Irina Preis**. Fatigue performance and mechanical reliability of cemented carbides. 2004.
23. **Medhat Hussainov**. Effect of solid particles on turbulence of gas in two-phase flows. 2005.

24. **Frid Kaljas**. Synergy-based approach to design of the interdisciplinary systems. 2005.
25. **Dmitri Neshumayev**. Experimental and numerical investigation of combined heat transfer enhancement technique in gas-heated channels. 2005.
26. **Renno Veinthal**. Characterization and modelling of erosion wear of powder composite materials and coatings. 2005.
27. **Sergei Tisler**. Deposition of solid particles from aerosol flow in laminar flat-plate boundary layer. 2006.
28. **Tauno Otto**. Models for monitoring of technological processes and production systems. 2006.
29. **Maksim Antonov**. Assessment of cermets performance in aggressive media. 2006.
30. **Tatjana Barashkova**. Research of the effect of correlation at the measurement of alternating voltage. 2006.
31. **Jaan Kers**. Recycling of composite plastics. 2006.
32. **Raivo Sell**. Model based mechatronic systems modeling methodology in conceptual design stage. 2007.
33. **Hans Rämmal**. Experimental methods for sound propagation studies in automotive duct systems. 2007.
34. **Meelis Pohlak**. Rapid prototyping of sheet metal components with incremental sheet forming technology. 2007.
35. **Priidu Peetsalu**. Microstructural aspects of thermal sprayed WC-Co coatings and Ni-Cr coated steels. 2007.
36. **Lauri Kollo**. Sinter/HIP technology of TiC-based cermets. 2007.
37. **Andrei Dedov**. Assessment of metal condition and remaining life of in-service power plant components operating at high temperature. 2007.
38. **Fjodor Sergejev**. Investigation of the fatigue mechanics aspects of PM hardmetals and cermets. 2007.
39. **Eduard Ševtšenko**. Intelligent decision support system for the network of collaborative SME-s. 2007.
40. **Rünno Lumiste**. Networks and innovation in machinery and electronics industry and enterprises (Estonian case studies). 2008.
41. **Kristo Karjust**. Integrated product development and production technology of large composite plastic products. 2008.
42. **Mart Saarna**. Fatigue characteristics of PM steels. 2008.
43. **Eduard Kimmari**. Exothermically synthesized B₄C-Al composites for dry sliding. 2008.
44. **Indrek Abiline**. Calibration methods of coating thickness gauges. 2008.
45. **Tiit Hindreus**. Synergy-based approach to quality assurance. 2009.
46. **Karl Raba**. Uncertainty focused product improvement models. 2009.

47. **Riho Tarbe**. Abrasive impact wear: tester, wear and grindability studies. 2009.
48. **Kristjan Juhani**. Reactive sintered chromium and titanium carbide- based cermets. 2009.
49. **Nadežda Dementjeva**. Energy planning model analysis and their adaptability for Estonian energy sector. 2009.
50. **Igor Krupenski**. Numerical simulation of two-phase turbulent flows in ash circulating fluidized bed. 2010.